Relative Motion Calculator

Eirik Berg

MASTER THESIS IN MARINE TECHNOLOGY

SPRING 2012

FOR

STUD. TECHN. EIRIK BERG

CALCULATION OF RELATIVE MOTION BETWEEN OFFSHORE WIND TURBINE AND A SERVICE VESSEL

Offshore wind energy appears to be promising for alternative energy. Both bottom fixed wind turbines and floating wind turbines are being investigated. In particular, for floating wind turbines it is essential to make reliable assessments of marine operations regarding the relative motion between the wind turbine and a service vessel.

The purpose of this study is to develop a relative motion calculator for the relative motion between a floating offshore wind turbine and a service vessel.

The student shall:
1. Describe different concepts of offshore wind turbines and relevant marine operations for support and maintenance.
2. Perform calculations including a parameter study for a simplified system: fixed wind turbine and a service vessel in heave, sway and roll motion in long-crested beam seas. The parameters shall be chosen based on operational criteria, i.e. distance, velocity and acceleration.
3. Perform similar simulations as in Part 2 for a fixed wind turbine and a vessel with 6 degrees of freedom of motion.
4. Perform similar simulations as in Part 3 for short-crested waves.
5. In all cases the parameters shall be chosen based on discussion with the advisors. Test cases and validation studies shall also be included as part of the thesis.

In the thesis the candidate shall present his personal contribution to the resolution of problem within the scope of the thesis work.

Theories and conclusions should be based on mathematical derivations and/or logic reasoning identifying the various steps in the deduction.

The candidate should utilize the existing possibilities for obtaining relevant literature.

The thesis should be organized in a rational manner to give a clear exposition of results, assessments, and conclusions. The text should be brief and to the point, with a clear language. Telegraphic language should be avoided.

The thesis shall contain the following elements: A text defining the scope, preface, list of contents, summary, main body of thesis, conclusions with recommendations for further work, list of symbols and acronyms, reference and (optional) appendices. All figures, tables and equations shall be numerated.

The supervisor may require that the candidate, in an early stage of the work, present a written plan for the completion of the work. The plan should include a budget for the use of computer and laboratory resources that will be charged to the department. Overruns shall be reported to the supervisor.

The original contribution of the candidate and material taken from other sources shall be clearly defined. Work from other sources shall be properly referenced using an acknowledged referencing system.

The thesis shall be submitted in two copies:

- Signed by the candidate
- The text defining the scope included
- In bound volume(s)
- Drawings and/or computer prints that cannot be bound should be organized in a separate folder.
- The bound volume shall be accompanied by a CD or DVD containing the written thesis in Word or PDF format. In case computer programs have been made as part of the thesis work, the source code shall be included. In case of experimental work, the experimental results shall be included in a suitable electronic format.

Contact person at Statoil   : Dr. Rune Yttervik
Advisors   : Professor Bernt J. Leira
                   Professor Dag Myrhaug

Deadline   : 10.06.2012

Dag Myrhaug
Supervisor

Abstract

The wind power business has in recent times changed its focus from land-based installations to offshore installations. This has presented challenges both technological and financial, mainly related to construction and maintenance. To optimize the availability of the offshore wind turbines it is important to have support vessels and boarding systems that can handle as rough sea conditions as possible, and the relative motions between these vessels and the wind turbines become increasingly important to predict, as the offshore wind business expands.

For this purpose, a need has been expressed for a simple tool for quick estimation of such motions. In this thesis, a MATLAB program has been developed for this purpose. It takes various input from the user, such as information on the sea state and the physical situation to be considered, as well as limiting criteria. The program provides the user with information on the local vessel motions and the relative motions between a point on the vessel and a fixed point on the wind turbine, and then compares it to the given criteria. It also gives out various plots to illustrate the motions and the relevant transfer functions.

The final version of Relative Motion Calculator, RMC 2.3, features the following options:

- Two types of wave spectra
- Arbitrary placement of the moving coordinate system
- Arbitrary placement of the considered points
- Long- or short-crested wave theory

RMC 2.3 has undergone thorough testing to prove its validity, and all test results are reasonable and according to expectation. Although the program is a bit difficult to use, it can be used as intended, for calculating relative motions between a moving point on a vessel and a fixed point. Furthermore, the program might provide a good platform for further development.

Preface

This thesis is submitted as the finishing piece of work for the Master's degree in Marine Technology at NTNU. It has been worked out during the spring of 2012, and it has succeeded the initial project thesis which was started in the fall of 2011. The thesis has been the entire workload of 30 credits in the tenth semester of the Marine Technology Master programme.

The project thesis was suggested by Dr. Rune Yttervik at Statoil in august 2011, after I had expressed a desire to write a thesis about marine operations to Mr. Sigmund Lunde, also at Statoil. The assignment was approved by my supervisors at NTNU, but the problem was modified somewhat to first give a reasonable project assignment, and then elaborated further to give the final master thesis. The thesis has been written individually.

The deadline of the thesis was originally set to June 10th 2012. However, bad luck struck me as I was exercising, and I had an accident where I broke a finger on my right hand. This happened three weeks before the thesis was due, and I went through casting of my right arm, and later two operations with following medication. The deadline was therefore postponed three weeks to July 2nd.

First of all, I would like to thank my two supervisors at NTNU, Professors Dag Myrhaug and Bernt Leira. Their guidance and support has been invaluable, and I would not have been able to complete the thesis without them. Furthermore, I would like to give thanks to my supervisor at Statoil, Dr. Rune Yttervik, for support and for providing necessary information. At last, I would like to thank Mr. Sigmund Lunde for connecting me to the right people, and for guiding me in connection to the marine operations related to offshore wind turbines.

Oslo, July 1st 2012

Eirik Berg

Table of contents

Figure list

Table list

List of symbols

L	Length	ok
B	Breadth	ok
T	Draught	ok
g	Gravitational acceleration	
T_R	Reference period	
T_{POP}	Estimated operation time	
T_C	Contingency time	
OP_{LIM}	Limiting operational environmental criterion	
OP_{WF}	Required weather window	
α	Factor for determining weather window	
H_s	Significant wave height	
T_p	Peak period	
V	Velocity vector	
∇	Gradient operator	
ϕ	Velocity potential	
i, j, k	Unit vectors	
u, v, w	velocity components in x, y and z-direction	
a	Acceleration vector	
p	pressure	
ρ	Fluid density	
p_a	Atmospheric pressure	
F	Force	
S	Wet surface	
n	Normal vector	
ϕ_I	Incident wave potential	
ϕ_D	Diffraction potential	

ϕ_R	Radiation potential
ζ	Wave elevation
ζ_a	Wave amplitude
ω	Wave circular frequency
t	Time variable
k	Wave number
λ	Wave length
h	Water depth
ε_n	Random phase angle for wave component n
E_n	Energy per area for linear waves
N	Number of wave components
$S(\omega)$	Wave spectrum as a function of circular frequency
σ^2	Spectrum variance
$S(f)$	Wave spectrum as a function of frequency
α	Spectrum parameter
γ	Spectrum parameter
f_p	Peak frequency
ω_p	Peak circular frequency
$S_T(\omega)$	Torsethaugen spectrum
$S_{J,i}(\omega)$	JONSWAP spectrum which constitutes the Torsethaugen spectrum
a_f	Fetch length factor
T_f	Distinction period between wind and swell dominated ranges
$S_{sc}(\omega, \vartheta)$	Short-crested wave spectrum
$S_{lc}(\omega)$	Arbitrary long-crested wave spectrum
$D(\omega, \vartheta)$	Directional distribution
ϑ	Spreading angle variable

K_{2s}	Directional distribution factor
s	Wave spreading parameter
$x(t)$	Input signal
x_0	Input signal amplitude
$y(t)$	Output signal
y_0	Output signal amplitude
φ	Phase difference
$H(\omega)$	Transfer function
$A(\omega)$	Real part of the transfer function
$B(\omega)$	Imaginary part of the transfer function
η_{1-6}	Ship motions in 6 degrees of freedom
η_a	Motion amplitude
$S_x(\omega)$	General response spectrum
$S_y(\omega)$	Input spectrum
s	Displacement vector
r_3	Relative total point motion in z-direction
$R_{r_3 r_3}(\tau)$	Autocorrelation function for total z-motion
$S_{r_3 r_3}(\omega)$	Total response spectrum for z-motion
θ	Angle between considered points in the horizontal plane
ϕ	Angle between considered points in the vertical plane
$F_H(h)$	Rayleigh cumulative distribution function
$f_H(h)$	Probability density function
m_n	Spectral moments
T_z	Mean wave zero crossing period
N	Total number of waves in a sea state
D	Sea state duration
$F_y(y)$	Gumbel distribution

μ_y	Mean value for a Gumbel distribution
σ_y	Standard deviation for a Gumbel distribution
$E[H_{max}]$	Expected maximum wave height
γ	Vessel heading in global coordinate system
β	Wave propagation direction in global coordinate system
δ	Wave propagation direction relative to the local vessel coordinate system
α	Wave attack angle measured from ship bow
P1	Considered point on the vessel
P2	Considered point on the fixed wind turbine
ψ	Angle of the vector pointing from P1 to P2
λ	Angle between considered points in global coordinates
$\overline{H}(\omega)$	Mean transfer function for short-crested waves

List of abbreviations and acronyms

EWEA	European Wind Energy Association
TLP	Tension-Leg Platform
RAO	Response Amplitude Operator
GRP	Glass Reinforced Plastics
SWATH	Small Waterplane Area Twin Hull
SES	Surface Effect Ship
FRP	Fiber Reinforced Plastics
ACC	Air Cushioned Catamaran
DNV	Det Norske Veritas
IMO	International Maritime Organization
NORSOK	Norsk sokkels konkurranseposisjon
JONSWAP	JOint North Sea WAve Project
WAFO	Wave Analysis for Fatigue and Oceanography
GUI	Graphical User Interface
Dof	Degree of Freedom

1. Introduction

In the recent years, concerns about climate change and an energy crisis has led to increased interest in renewable energy sources. One of the fastest growing ones of these is wind power, which is a field that is experiencing great changes as of recent. The vast land areas required for land-based wind turbines, along with large environmental impact in the form of visual and noise pollution has driven the wind power business offshore. The huge areas suitable for deployment, and the stronger and more stable winds, are obvious advantages, but technical and financial challenges must be overcome for wind power to truly become the renewable energy source for the future.

One such technical difficulty is related to the marine operations required for safely and effectively constructing and maintaining offshore wind turbines. Particularly the maintenance operations make use of small craft for accessing the turbines, and they are thus sensitive to wave motions, even for rather benign sea states. Therefore there is a need for easy and quick assessment of relative motions between the support vessel and the wind turbine.

In this thesis, the development of a MATLAB tool which computes these relative motions is described. First backgrounds on offshore wind, marine operations and operational criteria are provided to put the MATLAB program into context. Then the theory on which the program is based is described, followed by a detailed description of the program itself. Finally, the program is put through various tests and parameter studies, to attempt to document its validity as thoroughly as possible.

The program, which is christened Relative Motion Calculator, takes various inputs from the user, to provide information on the motions as output. The final version of the program includes options on which wave spectrum to use, if long- or short-crested wave theory should be considered, as well as arbitrary geometry of the situation to be examined. Wave heading and vessel heading is also arbitrary. However, the program only considers one moving system (the vessel) relative to a fixed point (the wind turbine), even though the plan initially was to include two moving systems. After advice from my two advisors at NTNU, emphasis was shifted to other aspects of the program. Finally, the program requires a version of MATLAB to be installed on the computer in order to function.

1   Background

1.1   The offshore wind power market

As the technology enabling us to put wind turbines offshore is quite new, the history of offshore wind power is a rather short one. It started off the coast of Nogersund, Sweden in 1990 with a 220 kW test turbine located about 250 meters offshore (1). The world's first offshore wind farm, was commissioned a year later, in 1991, near the village of Vindeby in Denmark. Since the beginning, Europe has maintained its position as world leader in offshore wind energy.

Today, numerous offshore wind farms are operational in the waters off of Belgium, Denmark, Finland, Germany, Ireland, the Netherlands, Norway, Sweden, and the United Kingdom (2). In Europe as a whole, as of 30 June 2011, there are 1247 offshore wind turbines fully grid connected with a total capacity of 3,294 MW in 49 wind farms spread over 9 countries (3). Furthermore, this number is rising at a very quick rate, as is shown in Figure 1.1. The European Wind Energy Association (EWEA) predicts between 20 and 40 GW of installed offshore wind power by 2020 (4).

The rapid development of offshore wind power in Europe is mainly propelled by the EU's renewable energy and climate goals, as well as individual nation's legislations.

Development installed offshore wind power capacity in Megawatt (MW)
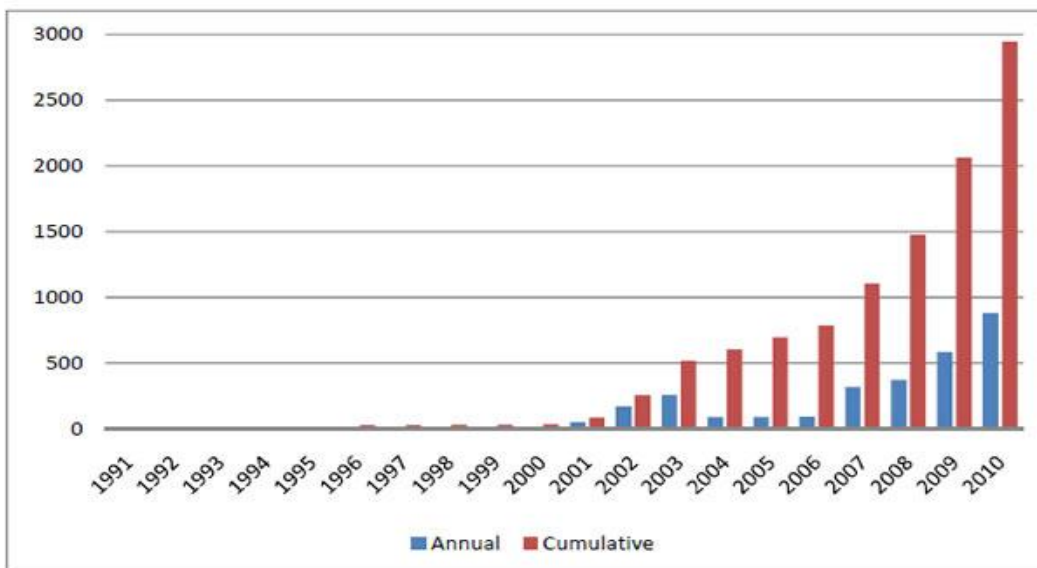
Source: EWEA

Figure 1.1 - Development of installed wind power in Europe (5)

Most of today's offshore wind farms mainly utilize bottom fixed wind turbines, as their concepts are more similar to the well-known onshore concepts. They range from mono piles, deployed in the shallowest waters (<30m), to different solutions for deeper waters (20m-60m)

(2). For larger water depths, floating concepts should be applied, and in the recent years, we have seen different concepts being developed.

The main advantage of floating wind turbines is that these types of turbines are not limited to shallow water depths. Accordingly, these types of wind turbines can in theory be placed along almost any coastline around the world, which would make this an extremely flexible concept for deploying wind power without excessive environmental intervention. Another advantage is that wind conditions are usually even steadier and stronger further out in the ocean, one of the important reasons for taking wind power offshore in the first place. However, this technology is still being developed, and challenges arise in technical as well as in economical fields. To overcome the technical difficulties, will probably prove feasible, but to do so in a profitable manner, might prove an even greater task. At this point, the development of floating wind turbines is therefore very much considered research more than business.

1.2   Fixed offshore wind concepts

Support structures for offshore wind turbines are highly dynamic, and have to cope with both dynamic wave and wind loads, as well as complex dynamic behavior from the wind turbine. Several factors influence the choice of solution for the support structure. Main factors include long- and short-term weather conditions, as well as geophysical conditions. There are four concepts which are commonly utilized in wind farms today (6).

1.2.1   Mono pile

This consists of a single pile which is driven 10-20 meters into the sea bed, to which a transition piece with a slightly larger diameter is welded The concept is shown in Figure 2.3. The structure is typically made of steel tube with a diameter of 4-6 meters. The concept is widely used for small to medium water depths.

1.2.2   Gravity based structure

The gravity based structure, as the name implies, relies on weight as the stabilization factor. Extra ballast might be added in the base of the structure, as shown in Figure 2.2. It is made from steel or concrete. The seabed will often need somewhat careful preparation prior to installation, and problems with scouring and undermining may occur. These structures are used in small to medium water depths.

1.2.3   Tripod structure

This structure is made from steel tubes that are welded together, typically with diameters from 1-5 meters. The structure is illustrated in Figure 2.5. A transition piece is incorporated onto

the center column. It is anchored by piles with diameters from 0.8-2.5 meters. This concept is deployed in medium to deep water depths.

1.2.4 Jacket structure

This concept is based on the widely-used jacket as the support structure, as shown in Figure 2.4. The jacket is made from steel tubes that are welded together, with typical diameters of 0.5-1.5 meters. It is commonly anchored by four piles with diameters from 0.8-2.5 meters. This concept is deployed in medium to deep water depths.
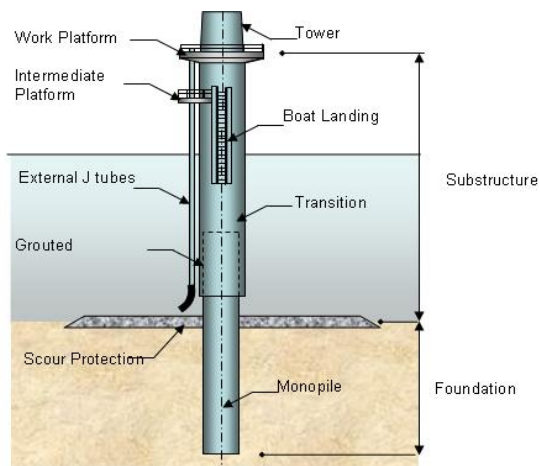
Figure 1.3 - Mono pile (6)
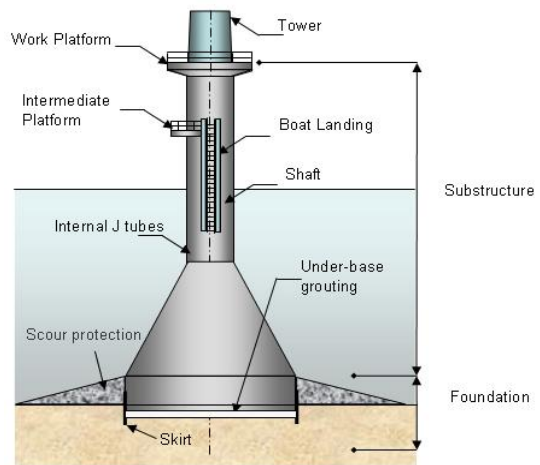
Figure 1.2 - Gravity based structure (6)
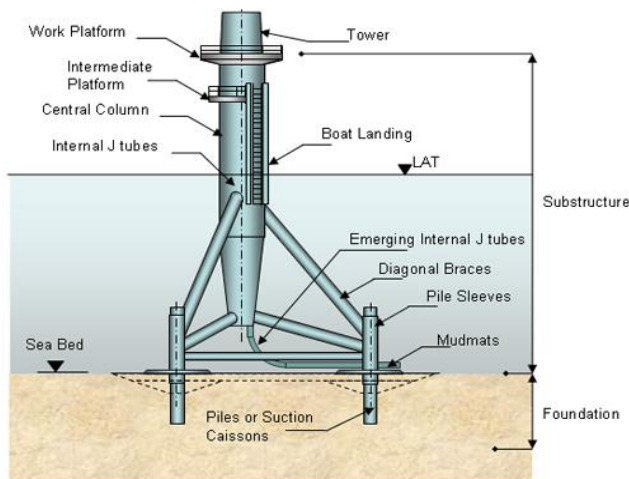
Figure 1.5 - Tripod structure (6)
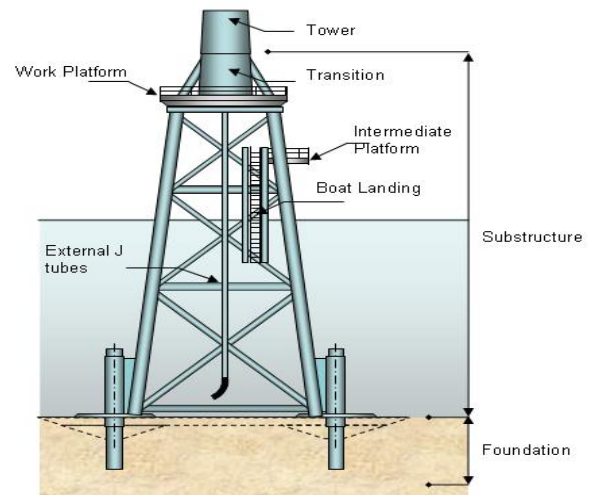
Figure 1.4 - Jacket structure (6)

1.3   Floating offshore wind concepts

Compared to the fixed concepts, the floating wind turbines have to face several technical difficulties. First of all, the floating platforms to which the towers are installed are free in all six degrees of freedom. This particularly makes marine operations related to installation and maintenance challenging. Furthermore, some of them might have to withstand heavier wind and sea loads because of rougher environment, and all floating concepts will be subject to dynamic load problems such as fatigue. Long subsea power cables will also be necessary in potential future deep water offshore wind farms.

In this section, the three most relevant concepts for floating concepts have been investigated. The three are a ballast stabilized spar buoy, a buoyancy stabilized semi-submersible, and a mooring-line stabilized tension leg platform, as shown on Figure 2.6.
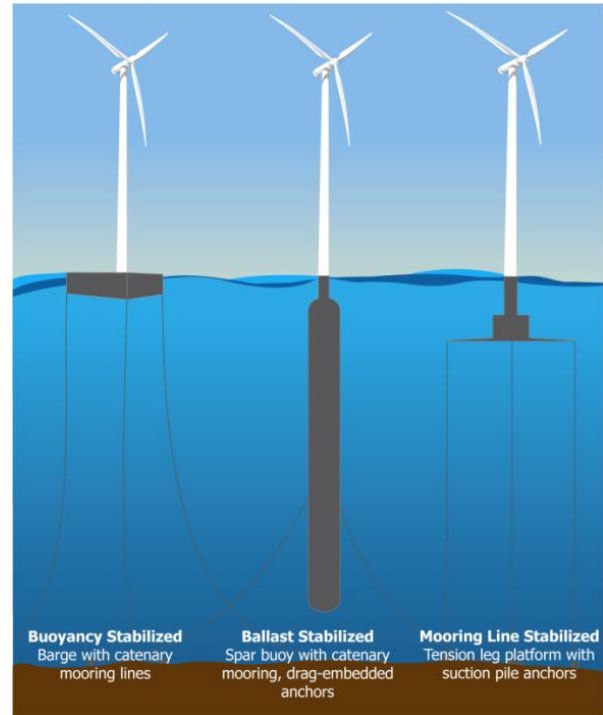
Figure 1.6 - Floating concepts (28)

1.3.1   Spar buoy platform

Statoil's Hywind project is the world's first full scale floating wind turbine. It was towed out to site near Karmøy, Norway in October 2009. It was to be in operation for two years, to gain knowledge about sea loads and motions on the system. It is, however, still functional on its third year, and the results so far look very promising. A visualization of the concept is given in Figure 2.7.

The tower is installed on top of a spar buoy platform, with a diameter of 8.3 m submerged, and 6 m at the sea surface, and a draught of 100 m (7). The buoy is mainly stabilized by ballast in the form of water and rocks. It is anchored by three catenary lines, which also contribute to the stability. This stability system gives the Hywind especially large inertia moments in roll and pitch, compared to the other concepts, the natural periods are large in almost all degrees of freedom (8). The exception is yaw, where the natural period is the smallest

Figure 1.7 – Hywind concept (26)

of the three concepts investigated. This could present problems related to marine operations, at least in theory, but one might argue that the system will probably not be subjected to any great yaw exciting moments.

1.3.2 Semi-submersible

WindFloat is a concept designed by American company Principle Power. It is, as of this autumn, being tested at Aguçadoura, off the coast of Portugal (9). It is designed for somewhat smaller turbines and water depths than the Hywind.

As is shown in Figure 2.8, the semi-submersible platform is based on a tri-column design, where the tower is installed on one of the columns. It seeks to improve the dynamic stability properties by dampening wave and turbine induced motions (10). It is moored by four anchor lines, of which two are fitted to the column holding the tower, creating an asymmetric mooring system for increased stability and reduced motions. The platform has natural periods in the same order of magnitude as the spar buoy, and also for the yaw motion, the natural period is quite large (8). It experiences small movements in most degrees of freedom. However, in spite of heave-damping flaps under each column, the platform experiences rather large responses in heave, which may complicate marine operations.

Figure 1.8 - Windfloat concept (10)

1.3.3 Tension-leg platform (TLP)

British offshore wind company Blue H is based on a TLP-concept developed in the Netherlands . In the summer of 2008 they installed a 75% size prototype off the coast of Puglia, Italy. They are currently building a full-scale model, which is to be completed and installed by 2012 (11).

The TLP-concept is basically a platform which is fully stabilized by mooring. It has relatively shallow draught, and the subsea structure includes a hexagonal frame, to which the six mooring lines are attached. These mooring lines are in tension, balanced by the substructure's buoyancy, limiting the amplitudes of the platform's movements. This system has natural periods below those of most waves in relevant sea states, thus avoiding resonance (8). It will, however, because of the small natural periods, experience faster movements in heave, roll and pitch. Second-order wave forces may lead to springing response, but under normal conditions the amplitudes will typically be small.

Figure 1.9 - Tension-leg platform (27)

2   Marine operations

2.1   General

The most common marine operations with regard to offshore wind turbines are either related to installation or maintenance operations. Operations related to installation include assembly, construction, towing and/or anchor handling operations. Maintenance operations typically include boarding and/or light crane lift operations. Assembly and construction operations are normally performed by jack-up vessels for bottom fixed turbines, while floating concepts are either finished on shore and towed out on site, or they are finished by very large vessels and in calm weather.

Since towing and anchor handling operations would have to focus on other parameters than those of relative motions, they are not considered in this thesis. We will place our focus mainly on the two types of maintenance operations which can be performed by the reference vessel. Because the program, given the proper transfer functions, could also be used to calculate motions on a large vessel during assembly of a wind turbine, a brief description is also given.

2.2   Reference support vessel

During the programming of the program, emphasis has been placed on making it as usable and flexible as possible. Therefore, the program is capable of reading any RAO-file of the same format, with arbitrary numbers of headings and frequencies. The vessel that has been used while testing the program, and while computing results, is not necessarily representable for typical marine operations on an offshore wind installation. Still, it is used for testing the functions of the program throughout this thesis, so a brief description has been given.

The reference vessel is a tug boat with a displacement of 160 tons and a length between perpendiculars of about 35 meters[1]. A tug boat has been chosen because it has so far been commonly used for operations in connection with Statoil's Hywind concept. However, a tug boat would probably not be the optimal choice of support vessel for a commercial offshore wind farm. It can be assumed that Statoil is deploying this type of vessel because of convenience, keeping in mind the fact that the Hywind concept is still a pilot project. For the various marine operations related to commercial offshore wind farms, more specialized vessels are deployed, and under development, as we will come back to shortly.

---

[1] Information about the boat is provided by Dr. Rune Yttervik at Statoil.

The tug boat's natural periods in heave and roll are 3.5 seconds and 3.0 seconds, respectively. These rather small periods are usually below the dominating frequencies in most sea states, resulting in the boat's motions following those of the waves, thus avoiding resonance. For lower sea states however, especially in developing waves, the dominating frequencies will be lower, and resonance may become more of a problem. The wave amplitudes in these low sea states will of course be lower, but as most marine operations are done in benign sea states, the issue should at least be addressed. Obvious solutions are larger boats for crane operations, and safer boarding systems for boarding operations.

Regardless of the wind turbine concept we consider, it is quite obvious that the motions on this tugboat (and most other types of support vessels) are much larger in magnitude[2], and much more frequent, than any motions we will observe from the wind turbines described. The vessel motions will thus constitute a very large part of the combined relative motions, and the platform motions can, for simplicity, be considered as stationary. The relative motions examined throughout this study are therefore the motions between a moving point on a vessel, and a fixed point on a platform. This will be elaborated later on.

2.3 Boarding operations

A major issue related to efficiently operating offshore wind parks, is that of accessing the turbines for routine servicing and emergency maintenance. Harsh weather conditions such as strong wind, rough sea and limited visibility can make such operations difficult or impossible (12). The traditional way to transport personnel and equipment and personnel out on site, is obviously by boat. Although this is a cost efficient and well known method, it is limited by quite small wave heights. Significant wave heights of more than 1-1.5 meters are generally not advisable for performing a safe boarding operation with traditional monohull service boats. Since acceptable motions for equipment handling are usually a bit larger, the boarding operations often become the limiting factor in maintenance operations. On this issue, the seasons play an important part, and this will be addressed later in this thesis.

For this reason, alternative ways of gaining access to the turbines have been considered. An example taken from the offshore industry is deploying helicopters (12). Although this eliminates the issue of sea states, the method is both expensive and cumbersome, as the wind turbine must be shut down and locked during boarding. Also, it is sensitive to wind conditions and visibility conditions. Other solutions that have been proposed for fixed turbines are underwater tunnels and small jack-up vessels. These solutions are also expensive and difficult

---

[2] Assuming there is no second-order force. In the opposite case, we might have motions which are quite large in magnitude. However, these motions would have very large periods, and therefore be of limited significance to a fastened vessel. For a dynamically positioned vessel, this could prove a challenge.

to implement, and emphasis has changed somewhat in recent years. Presently better concepts for both boats and access systems have emerged, and are constantly being developed. Boarding turbines by boat also works regardless of sea bed conditions and water depth.

2.3.1 Boarding vessels

The boarding of an offshore wind turbine has typically been done by having the boat approach the boarding platform on the turbine, bow first. The boarding boat will then have fenders in the contact area, as will possibly the platform. When contact is reached, the boat will thrust into the platform, thus avoiding air gaps. In this state boarding is then performed, as is shown in Figure 3.1. Obviously, this

Figure 2.1 - The service vessel "Buddy" in a boarding operation at Hywind. (29)

method presents risks to boarding crew if the boat motions become too large. Especially for monohulls, the motions become too large already for benign sea states, so development of boats with diminished response to waves is addressing this problem.

Another desired attribute of an offshore wind support vessel is speed. Due to limited weather windows, personnel and equipment must often be transported from shore as quickly as possible, and also between turbines in an offshore wind park. Thus, it seems that the ideal offshore boarding vessel should be both fast, and with as small response to waves as possible. Several new concepts are currently being deployed or are under development.

2.3.2 FOB Trim

Built in 2007 at Hvide Sande shipyard in Denmark, this trimaran is custom made for transporting personnel and equipment to offshore wind parks (13). It features a large operating deck with a small 1800 kg crane, and has room for 12 people. The vessel is shown in Figure 3.2. Its main dimensions are 24m x 7.4m x 1.95m (LxBxT), and it has a displacement of 76 tons. Its main engine delivers 969 kW to a large pitch propeller,

Figure 2.2 - FOB Trim (34)

giving a max speed of 21 knots. The hull shape and modest waterplane area makes the ship fairly resistant to heave and roll motions, and to further reduce roll, anti-roll tanks have been installed. It is allegedly safe for turbine boarding in significant wave heights up to 1.5 meters.

2.3.3 FOB SWATH 1

This offshore support boat was built at Måløy shipyard in Norway in February 2011. It is a twin hull boat built from light GRP (Glass Reinforced Plastic) sandwich material, and it functions in two modes; catamaran mode and SWATH mode (Small Waterplane Area Twin Hull). The vessel and the two modes are shown in Figure 3.3. Its main dimensions are 27.2m x 10.6m x 1.15m/2.75m (LxBxT) (14), and it can carry a deadweight of 70 tons. It is equipped with a light crane of 2000 kg, and has a 36 person passenger capacity. It can totally generate about 1600 kW of power, providing an operating speed of about 25 knots in catamaran mode.
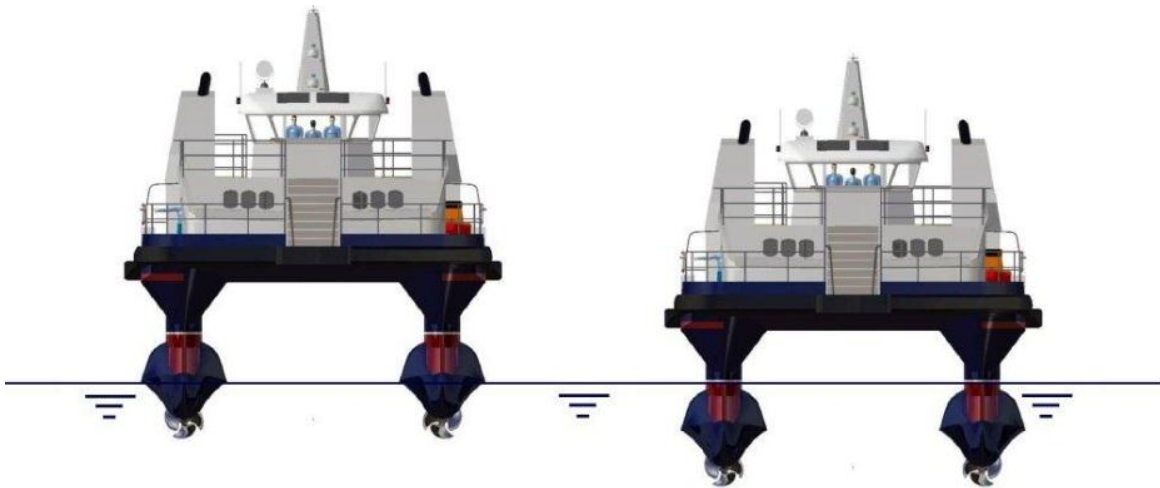
Figure 2.3 - FOB Swath. Left: Catamaran mode. Right: SWATH mode. (30)

It features some highly advanced technological solutions. The unique crossover between the two concepts makes it able to move as fast a catamaran vessel, while keeping the excellent stability of a SWATH vessel. It changes from catamaran mode to SWATH mode by filling four ballast tanks in the two hulls, while keeping the right trim using a patented system. The tanks can be operated even while operating the ship and filling or emptying the tanks takes about six minutes. To further reduce the boat motions, a roll suppressing system is installed, reducing roll by 40-50% (14). Furthermore, the boat features a docking system designed by Norwegian manufacturer Undertun. This is a bridge with a gripping arm for holding on to the turbine, which can then move dynamically with the ship motions, providing safe access for the crew even at larger waves. Docking operations can be performed with the FOB SWATH in significant wave heights up to 2.5-3 meters.

2.3.4   SES offshore vessel

The SES offshore vessel (Surface Effect Ship) is a concept being developed by Norwegian shipyard Umoe Mandal. They are currently a global market leader in the segment of technologically advanced surface effect ships. They are widely acknowledged for their

expertise in using FRP (Fiber Reinforced Plastics) materials in light-weight ships. They built and developed six SES coastal corvettes for the Royal Norwegian Navy between 1998 and 2009, called the "Skjold"-class. This project proved extremely expensive and technologically challenging, but did spawn some of the most advanced naval war ships ever, and definitely the quickest, reaching up to 60 knots.

Figure 2.4 - SES offshore concept by Umoe Mandal (31)

The SES offshore vessel will utilize the same ACC (Air Cushioned Catamaran) concept as the "Skjold"-class, providing the same basic benefits of an ACC. This concept is basically a catamaran with heavy rubber covers in the front and aft, constituting an air tight space between the two hulls. Heavy fans increase the air pressure, and the hulls are partially elevated out of the water, thus reducing draught, displacement and wet surface. These characteristics then make the vessel both fast and very resistant to wave motions. The ACC concept is a quite new technology, and requires advanced control and monitoring systems to work, and the light-weight FRP hulls are expensive to manufacture. However, with the experience gained from the "Skjold"-project, this concept might very well prove feasible, both economically and practically. If so, the result might be the fastest and most stable of all offshore support vessels.

2.4   Crane operations

In the field of marine operations, it is common to distinguish between two types of crane operations; light crane operations and heavy crane operations (15). In light crane operations, the weight of the lifted object is small compared to the crane vessel, the object weights typically ranging up to a few hundred tons. The vessel motions are thus not affected much by the object's weight. The most frequent crane operations regarding support and maintenance fall under this category. Heavy crane operations are typically related to construction and/or assembly of marine structures. The lifted objects constitute a larger part of the crane vessel's total weight, and the response dynamics and stability of the system is changed significantly.

2.4.1 Heavy crane operations

Offshore wind turbines are typically assembled either by jack-up construction vessels, for bottom fixed concepts, or inshore and in very calm weather and then towed out on site, for floating concepts. If provided with the proper RAOs for the relevant crane vessel/lifted object-system, the Relative Motion Calculator can be used to calculate relative motions of the rigid system (but not the free hanging object), if the assembled turbine is fixed. If it is floating, the program should not be used because it computes with only one moving system. Both systems' motions should be considered because the orders of magnitude of the motion periods are closer when both systems are of large size. However, heavy crane operations were not an aim during development of the program, which was made primarily with boarding operations and light crane operations in mind.

2.4.2 Light crane operations

When performing a light crane operation, there are both larger and quicker motions to be considered than those of heavy crane operations. When lifting a light object onto the turbine, one should be aware of the placements of the mooring lines attached to the buoy bottom. In case the object should accidentally be dropped from the crane, it must be made sure that this does not happen directly over a mooring line, to prevent damage. The vessel should be positioned with regard to this. Other factors affecting the choice of vessel placement, are current, waves and wind. If there are significant current conditions, the vessel is usually positioned with the bow against the current direction. Often vessel movement is minimized if facing the wave propagation, somewhat depending on the type of vessel, so these factors may have to be assessed against each other.

Figure 2.5 - Light crane operation on an offshore wind turbine (32)

We assume that the weight of the lifted object is small enough so that the strength of the crane wire is not a limiting factor due to added loading from accelerations. However, one should avoid snap loads, as they drastically increase impulse loads, resulting in possible damages.

Snap loads may occur if the vertical acceleration of the crane tip exceed that of the gravitational acceleration g. In this regard, this should be a natural criterion. Furthermore, when we assume that the object weight is small compared to the vessel's weight, we can thus regard the vessel/object-system as equal to the vessel system only. The crane tip can be considered a rigid body, and the motions of the crane tip can be calculated from the ordinary equation of motion for a floating body (See eq. (4.53)). This is what the program does, and in this manner the crane tip's relative motions are sufficiently modeled. For the motions of the hanging objects, however, the program lacks equations including the pendulum motions of the hanging object. It should not be used directly for assessing the motions of a hanging object, but rather by analyzing the motions at the crane tip. Including motions of a hanging object is a good idea for further work on the Relative Motion Calculator.

Depending on the location of the crane in the vessel system, different degrees of freedom have different impacts on the crane tip motions, but one can generally say that the rotations on the ship may cause large amplitudes of motions on the crane tip. Of course, the further the considered point is from the origin of the vessel system, the larger the motions become. An interesting aspect of the computations is the counter-effect of different degrees of freedom on each other. Particularly, we can often see a rotation working against a translation, such as roll versus sway. The resultant motions can in this manner become quite small, an effect that might be exploited when performing marine operations.

3   Operational Criteria

3.1 General

When planning a general marine operation, it is necessary to establish some limiting criteria to ensure safe and properly executed operations. The program calculates motions (distances, velocities and accelerations) in different degrees of freedom, and checks these against user provided motion criteria. The user must also provide weather data such as significant wave height, top period of the wave spectrum, type of wave spectrum as well as duration of operation. It is essential to the acquisition of valid results that the user provides the program with good input such as criteria. However, in addition to stating whether the criteria have been fulfilled or not, the program does indeed print out the expected maxima of the motions, for the user to interpret.

3.2 Motion criteria

The limiting criteria taken by the program are given as minimum and maximum values for distance between a given point on the vessel, and a given point on the fixed platform. Furthermore, maximum velocity and acceleration for the point on the vessel is examined. Specific restricting values regarding this have not been found from DNV rules and regulations, neither from IMO rules. It seems there are no rules limiting these values in relation to marine operations. Rather, it is necessary to consider these values for each specific marine operation, which will have its own special considerations to be made. For the program to be useful, it is therefore vital that it is made as flexible and general as possible, for the user to get the answers he needs for his exact case. Consequently, no restrictions are put on the user for which points can be considered, or on the provided geometry such as placement and heading of vessel coordinate system.

The program automatically computes the values linearly between the two points considered. This direction is arbitrary in the 3D-space, as is elaborated further in section 5.3.3.3. Along with motions along this line, the program writes out the local x-, y- and z-motions for the considered point in the vessel coordinate system. The geometry and the assumptions made in the calculations will be addressed further later in this thesis.

Some motion criteria that would be natural to provide, could be:

- Maximum vertical acceleration equal to the gravitational acceleration to avoid snapping loads
- Distance between points never becomes zero or lower, avoiding collision
- Distance between the points never exceeds the length of the boarding bridge in the case of such an operation.

If the user wants to check distance or other motions along other directions, this can be done by altering the examined point on the platform.

3.3   Weather restrictions

Some criteria related to marine operations are subject to rules and regulations. In Norway, regulations regarding transportation and transfer of installations, as well as safety on sea, are covered by the Norwegian Maritime Directorate (16). NORSOK is a group that was founded to ensure cooperation between different parties operating on the Norwegian Continental Shelf. They have worked out some common requirement standards for marine operations, which have been agreed upon by the Norwegian industry.

The standards describe, among other things, how an operation should be planned, and include a checklist for the planning of some non-routine marine operations. It also states that "Risk evaluations/analyses shall be carried out when specified or required by recognized authority" (17). In Norway, one such authority is the Norwegian Veritas (DNV), which has composed a vast number of rules, regulations and recommended practices. These are widely recognized and utilized, both nationally and internationally, and are commonly considered the standard regarding marine operations on the Norwegian Continental Shelf.

One important standard establishes a method of determining which weather criteria to use for the relevant operation. From this DNV standard (18), it is found that marine operations can be classified as either weather restricted or unrestricted. The difference is that the weather restricted operations have a limited duration, while the unrestricted operations have much longer duration, and therefore must pay attention to long-term wave statistics. An operation is considered restricted if it has a reference period[3] shorter than 96 hours, and a planned operation time of less than 72 hours, assuming reliable weather forecasts are available. In this thesis, we will consider weather restricted operations only, because of the nature of the relevant marine operations.

3.3.1   Weather window

As we see from Figure 4.1, the reference period T_R is the sum of the estimated operation time T_{POP} and the contingency time T_C (> 6 hours). These values must be assessed and estimated for each specific case. The limiting operational environmental criterion OP_{LIM} shall be established and clearly described in the marine operations manual. Now, to find the required weather window OP_{WF} we need to find the right α-value. This is depends on both the

---

[3] The reference period is the sum of the planned operation time and a safety period for unexpected delays.
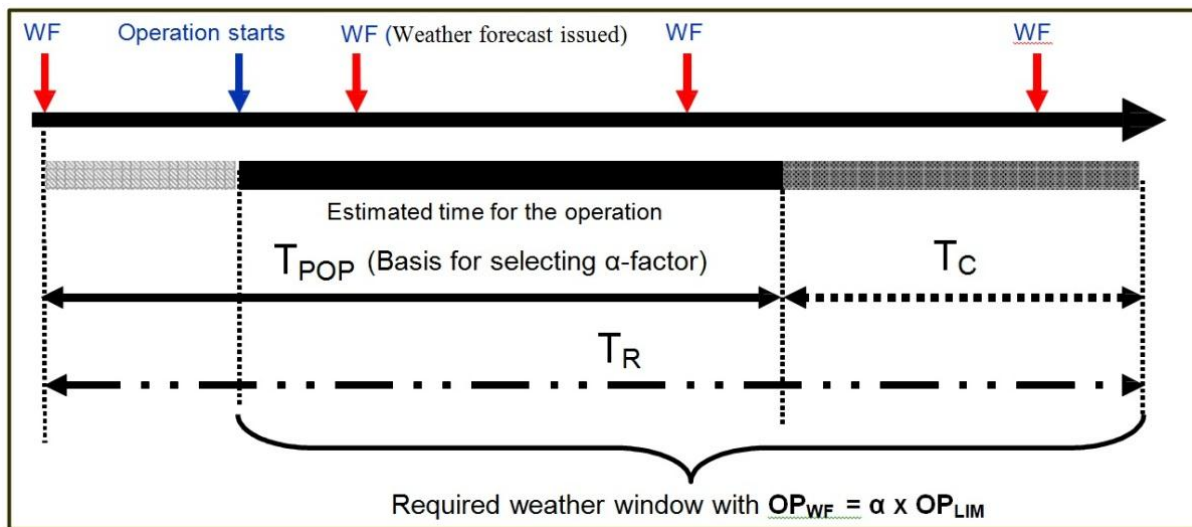
Figure 3.1 - Weather window for a weather restricted marine operation (18)

significant wave height and the duration of the sea state. The values for α also vary with different types of weather forecasts. An example of α-values is provided in table 1. For example, for an operation of less than 48 hours, with an H_S of 1 meter, the required weather window will be 60% of the original limiting operational environmental criterion stated in the operation manual. The α-factor reflects the uncertainties related to both weather forecasts and monitoring of environmental conditions. Note that the given α-values reflect increased uncertainty for longer operational periods, and the fact that forecasts for lower wave heights are more sensitive than those for higher wave heights. The marine operations which are considered in this report, are typically of very short length such as 3 hours or less, and can only be performed in quite limited wave heights.

Table 3.1- Example of alpha-factor table (18)

Table 4-1 α-factor for waves, base case							
Operational Period [h]	Design Wave Height [m]						
	$H_s = 1$	$1 < H_s < 2$	$H_s = 2 = 2$	$2 < H_s < 4$	$H_s = 4$	$4 < H_s < 6$	$H_s \geq 6$
$T_{POP} \leq 12$	0.65	Linear Interpolation	0.76	Linear Interpolation	0.79	Linear Interpolation	0.80
$T_{POP} \leq 24$	0.63		0.73		0.76		0.78
$T_{POP} \leq 36$	0.62		0.71		0.73		0.76
$T_{POP} \leq 48$	0.60		0.68		0.71		0.74
$T_{POP} \leq 72$	0.55		0.63		0.68		0.72

3.4   Availability

An offshore wind park, as any kind of offshore installation, needs to be periodically followed up, inspected and maintained by qualified personnel. In the planning of these activities, it is vital to assess the long-term weather statistics related to the relevant area.

These long-term statistics are produced from on-site measurements which are typically presented in so-called scatter diagrams, which consist of measured sea states ordered by

significant wave heights H_s and peak periods T_p. Significant wave height, H_s, is a measure frequently used in marine statistics, and represent the top 1/3 of wave heights in a sea state. The top period T_p, is a measure for the period corresponding to the frequency where a sea spectrum has its peak, thus it is a dominating period in the sea state. These values will be discussed more later on.
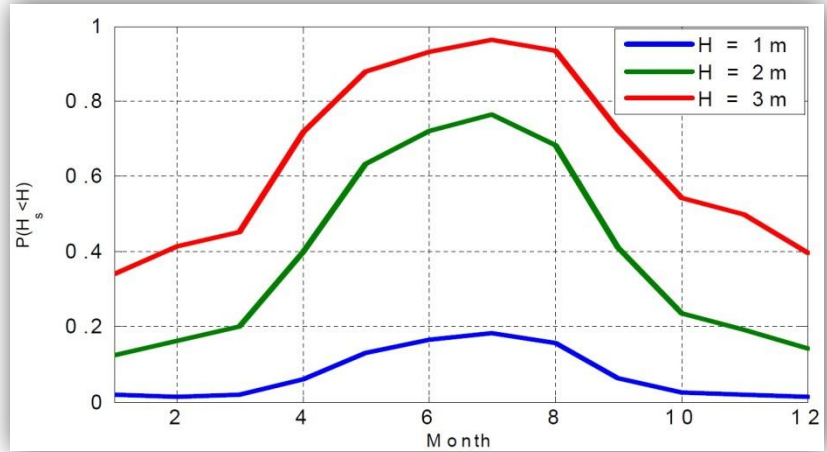
Figure 3.2 - Example of seasonal variations in sea states (33)

An example of a scatter diagram taken from the northern part of the North Sea is given in appendix A. These numbers are provided by my supervisor from Statoil, Dr. Rune Yttervik. The data is produced from observations in the northern North Sea made every 10 minutes throughout a full year, and can therefore not represent seasonal variations, which are of major importance. Figure 4.2 gives an example of the significance of seasonal variations. The numbers are unrelated to the scatter diagram, and only illustrate the difference in weather conditions throughout a year. Note that for restricting H_s of 1 meter, which has earlier been used as a criterion when boarding wind turbines, weather windows may be quite rare even in the summer season. In the winter season, opportunities are even scarcer, making even operations of short duration hard to execute. Conditions improve dramatically when the limiting criteria become less strict. The figure gives a good indication of the importance of enhancing wind turbine support vessels and boarding systems.

When we look at data from the scatter diagram, as plotted in Figure 4.3, we quickly realize that benign sea states are quite rare over the course of a year. The probability that a sea state will have an H_s of under 2.0 meters is about 50%, and this number is obviously much lower in the winter season. If we look at a benign sea state of 1.0 meter significant wave height, the probability sinks to about 20%, considering the whole year.
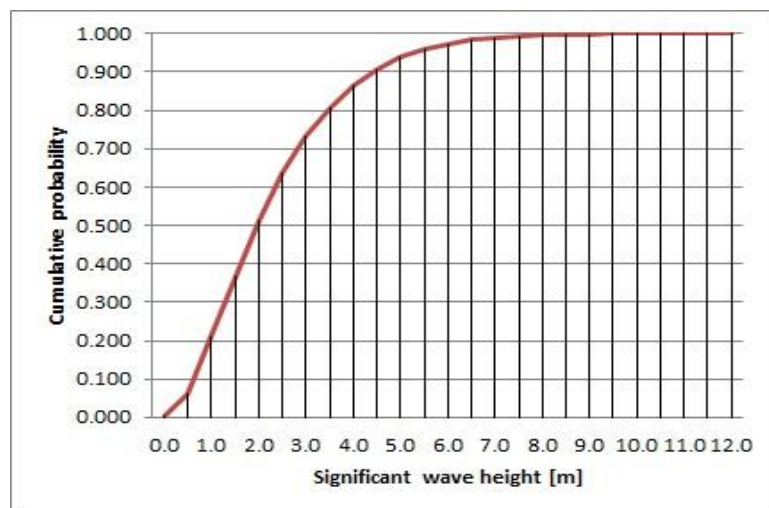
Figure 3.3 - Cumulative probability for exceeding significant wave height

Figure 4.4 shows the distributions of top periods for some rather easy sea states. We see that the bulk of top periods are between 7 and 10 seconds, with few sea states beneath 5 and above 13 seconds T_p. The small periods represent quick, small waves, typical for developing sea. On the contrary, the long periods are typical for swell and old waves.

It would be interesting to examine the effects of different periods as well as different significant wave heights when the program is to be deployed for analyses with the given reference vessel. The three types of sea states, namely developing sea, mixed sea and swell, should each be represented by a top period. Different significant wave heights should of course also be looked into.
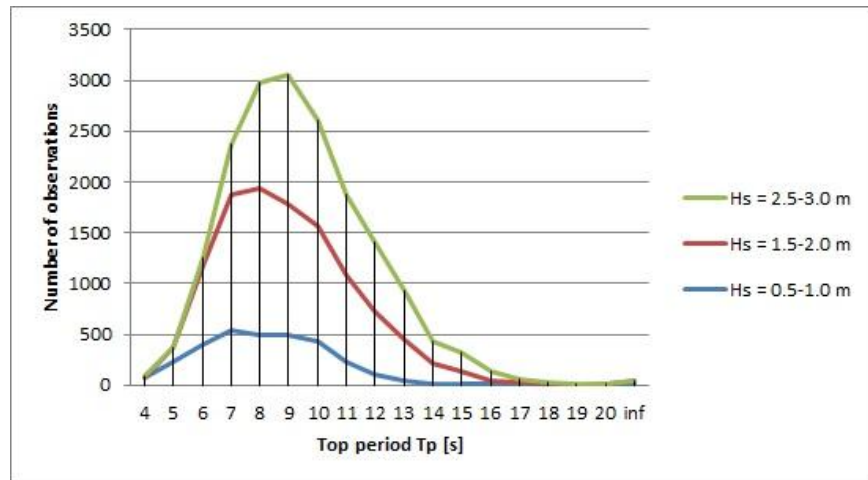
Figure 3.4 - Distribution of top periods for northern North Sea over a year

4 Background theory

4.1 General

The analysis of the vessel motions in our program is based on the given transfer functions. To use the transfer functions in our calculations, we need to make some assumptions:

- Linear potential theory. We neglect higher order terms in the Bernoulli equation (4.3).
- No hydrodynamic interaction. The effects from the turbine tower changing the waves are not considered. This will cause inaccuracies when the two systems are close.
- No wind loads or current loads are included.
- Large water depth.
- Small vessel motions.
- Slender ship hull (linear sea keeping).

The physical problem that we are investigating is in principle quite complex, from a hydrodynamic point of view. However, because all the information regarding the vessel's response to the sea, is given from the transfer functions, the focus in this assignment is more on the transformation of wave motions into vessel motions and the statistics connected to this, than on the sea loads causing these movements. Nonetheless, a description of the basic theory behind the transfer functions is provided.

4.2 Potential theory

When doing calculations related to fluid behavior, it is common to use potential theory. This theory describes a fluid by applying a velocity potential and adding certain boundary conditions (19). From this the fluid particle movements such as velocities and accelerations can be obtained, and hence also the fluid pressure. In potential theory, the following assumptions have to be made:

- Incompressible fluid (constant density)
- Inviscid (No viscosity)
- Irrotational flow

For most cases, these assumptions do not cause large errors. However, for some cases the ignored effects play an important part and have to be corrected to give decent results. An example of this is the flow around a cylinder, where both viscosity and vortex generation occur. To include these effects, Morrison's equation is commonly utilized.

4.2.1 Velocity potential

The fluid velocity vector in a potential flow field is expressed by:

$$\boldsymbol{V} = \nabla\phi = \boldsymbol{i}\frac{\partial\phi}{\partial x} + \boldsymbol{j}\frac{\partial\phi}{\partial y} + \boldsymbol{k}\frac{\partial\phi}{\partial z} = \boldsymbol{i}u + \boldsymbol{j}v + \boldsymbol{k}w \tag{4.1}$$

where ∇ denotes the gradient, $\boldsymbol{i}, \boldsymbol{j}$ and $\boldsymbol{k}$ are the unit vectors, and u, v and w are the velocity components in x, y and z-directions respectively. The accelerations can be found by differentiating this velocity vector with respect to time:

$$\boldsymbol{a} = \frac{\partial}{\partial t}(\nabla\phi) \tag{4.2}$$

To find the pressure, we introduce the Bernoulli equation:

$$p = -\rho\left(\frac{\partial\phi}{\partial t} + \frac{1}{2}|\boldsymbol{V}|^2 + gz\right) + p_a \tag{4.3}$$

Where ρ is the fluid density, z is the mean distance under the free surface, and p_a is the atmospheric pressure. Since we are interested in the wave loads, and because we assume linear theory, we can neglect the terms except for the dynamic pressure. The pressure can thus be expressed as:

$$p = -\rho\frac{\partial\phi}{\partial t} \tag{4.4}$$

If we now have a floating object for which we want to find the wave loads, this can be done by integrating the pressure over the wet surface of the floating object:

$$F = -\iint\limits_{S} p\boldsymbol{n}dS \tag{4.5}$$

Here F is the wave force, $\boldsymbol{n}$ is the normal vector pointing out from the object surface, and S is the wet surface of the object. Our problem now, is to make the velocity potential resemble and behave like a floating object in an ocean environment. To accomplish this, first we add together the different velocity potentials, namely the incident wave potential ϕ_I, the diffraction potential ϕ_D and the radiation potentials associated with the rigid body motions, ϕ_R. The total velocity potential is then written as

$$\phi = \phi_I + \phi_D + \phi_R \tag{4.6}$$

4.2.1.1 Wave potential

The wave potential ϕ_I describes how the waves move in a 2D-plane, as a function of space and time. We can describe a wave elevation on a free surface, moving along the positive x-axis, as (20):

$$\zeta = \zeta_a \sin(\omega t - kx) \tag{4.7}$$

21

where ζ_a is the wave amplitude, ω is the wave angular frequency, t is the time variable, and k is the wave number related to the wave length λ by

$$k = \frac{2\pi}{\lambda} \tag{4.8}$$

Then we get the following general expression for the wave potential for this 2D wave:

$$\phi_I = \frac{g\zeta_A \cosh(kh + hz)}{\omega \cosh(kh)} \cos(\omega t - kx) \tag{4.9}$$

where h is the water depth and g is the gravitational constant. However, in our case we assume deep water, so the wave potential becomes

$$\phi_I = \frac{g\zeta_A}{\omega} e^{kz} \cos(\omega t - kx) \tag{4.10}$$

which is associated with the dispersion relationship for deep water

$$\omega^2 = kg \tag{4.11}$$

4.2.1.2 Diffraction potential

The diffraction potential basically describes how the incoming waves are being changed by the presence of the floating object, or in other words it is the potential due to the diffracted waves. The diffraction potential needs to satisfy the following conditions:

- Laplace equation or continuity equation:

$$\nabla^2 \phi = 0 \tag{4.12}$$

- Free surface condition:

$$\frac{\partial^2 \phi}{\partial t^2} + g \frac{\partial \phi}{\partial z} = 0 \quad on \quad z = 0 \tag{4.13}$$

This condition has two parts, namely the dynamic boundary condition and the kinematic boundary condition. The dynamic boundary condition is a result from the Bernoulli equation, and states that the pressure on the free-surface must be equal to the atmospheric pressure. The second part, the kinematic boundary condition, states that a fluid particle on the free-surface will remain on the free-surface.

- Body boundary condition:

$$\frac{\partial \phi_D}{\partial n} = 0 \tag{4.14}$$

This conditions states that there can be no water flow through the hull.

- Sea bottom boundary condition:

$$\frac{\partial \phi_D}{\partial z} = 0 \quad for \quad z = -h \tag{4.15}$$

Where h is the water depth. This condition states that there can be no fluid flow through the seabed. This condition obviously also applies to the wave potential.

4.2.1.3 Radiation potentials

The radiation potentials for the six degrees of freedom are found by solving a differential equation in a similar manner as the diffraction potential. The difference is the body boundary condition. When finding the radiation potentials, one imagines the floating object to be oscillating with the wave frequency ω in still water. The fluid around the hull is now set in motion, and this is the motion we want to describe with the radiation potential. The body boundary condition therefore has to be equal to the velocity of the motion:

$$\frac{\partial \phi_R}{\partial n} = \boldsymbol{V} \cdot \boldsymbol{n} \tag{4.16}$$

where $\boldsymbol{V}$ is the body velocity vector and $\boldsymbol{n}$ is the normal vector to the hull.

4.2.2 Irregular waves

When we made the wave potential, we assumed the wave elevation in 2D was given by eq. (4.7). This describes a regular sinusoidal wave with amplitude ζ_a which propagates in the positive x-direction. But a real ocean environment never behaves like a regular sinusoidal wave. Therefore, we have to expand our model to make the waves resemble a real sea state. A real sea state can be thought of as composed of a large number of individual waves with different heights, periods and directions. We can thus model a real sea state by superpositioning a large (or infinite) number of regular waves, and in this way create an irregular wave condition. The parameters such as the amplitudes, phases and frequencies, will be governed by stochastic processes.

Let us first confine our example to 2D, i.e. we consider long crested waves, moving in positive x-direction. The wave elevations are constant along the y-direction, thus the wave is infinitely broad. Then the wave elevations can be written as (21)

$$\zeta(x,t) = \sum_{n=1}^{N} \zeta_{An} \cos(\omega_n t - k_n x + \varepsilon_n) \tag{4.17}$$

where ζ_{An} is the wave amplitude, ω_n the wave frequency, k_n is the wave number and ε_n is the random phase angle for each wave component n. The energy per area for a regular linear wave is given as

$$E_n = \frac{1}{2}\rho g \zeta_{An}^2 \tag{4.18}$$

To get the total energy in a sea state, we sum up the energy from all the wave components:

$$\frac{E}{\rho g} = \sum_{n=1}^{N} \frac{1}{2}\zeta_{An}^2 \tag{4.19}$$

Now we can define the spectrum $S(\omega)$ related to the total wave elevation $\zeta(t)$ as

$$\frac{1}{2}\zeta_{An}^2 = S(\omega_n)\Delta\omega \tag{4.20}$$

such that the area within the frequency interval $\Delta\omega$ equals the total energy of the wave components within this interval. Then, as illustrated in Figure 5.1, we can write the total energy as:

$$\frac{E}{\rho g} = \sum_{n=1}^{N} \frac{1}{2}\zeta_{An}^2 = \sum_{n=1}^{N} S(\omega_n)\Delta\omega \tag{4.21}$$

If we let $N \to \infty$ such that $\omega \to 0$, the expression finally becomes

$$\frac{E}{\rho g} = \frac{1}{2}\zeta_A^2 = \int_0^\infty S(\omega)d\omega \tag{4.22}$$

For the sea state that this spectrum describes, we have made the following assumptions:

- It is stationary, i.e. within a short time interval (20 minutes – 3 hours) the mean value and variance will be constant.
- The wave elevation is normally distributed with a mean value of zero and a variance of σ^2.
- The process is ergodic, i.e. a single time series is representative of the whole process.
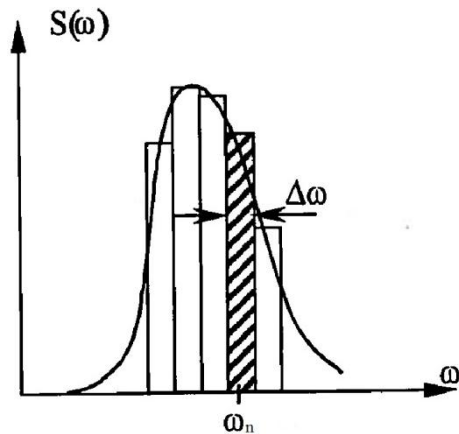
Figure 4.1 - Example of spectrum integration (20)

Finally, the variance of the wave elevation is given by

$$\sigma^2 = \int_0^\infty S(\omega)d\omega \tag{4.23}$$

4.3   Wave spectra

From long periods of observations, various wave spectra have been constructed to reflect these wave data. These spectra can then, by adding the correct parameters, reproduce a sea state for the user to deploy in his calculations. Many models have been developed, dependent on different locations and measurements, and with different input parameters. Since our analysis primarily includes the North Atlantic Ocean, it is convenient to start with the JONSWAP spectrum, which is custom made for these conditions. However, the JONSWAP spectrum only works in a limited H_s/T_p-range, so to be able to look outside this range the Torsethaugen spectrum has also been used.

These two wave spectra are imported into the MATLAB program using an external toolbox called WAFO (Wave Analysis for Fatigue and Oceanography) (22). This toolbox has been developed at the University of Lund in Sweden, and apart from sea modeling, additionally includes fatigue analysis, statistics and numerics. The WAFO package is thus quite extensive, though in this thesis, it has only been used for reproducing wave spectra.

4.3.1   JONSWAP spectrum

The JONSWAP (JOint North Sea WAve Project) spectrum was the result of a multinational measuring project from the south-eastern parts of the North Sea in 1969-1969 (21). It is derived from the more general Pierson-Moskowitz wave spectrum. The JONSWAP spectrum is valid for not fully developed sea states, but it is also used to represent fully developed sea states. It is particularly well suited to characterize wind generated sea in the so-called JONSWAP-range, i.e. when

$$3.6\sqrt{H_s} < T_p < 5\sqrt{H_s} \tag{4.24}$$

The spectrum should be used with care outside this range. The JONSWAP spectrum is given on the following form, as presented in Marin Dynamikk by Myrhaug (21):

$$S(f) = \alpha g^2 (2\pi)^{-4} f^{-5} \exp[-\frac{5}{4}(\frac{f}{f_p})^{-4}] \gamma^{\exp\{-\frac{\left(\frac{f}{f_p}-1\right)^2}{2\sigma^2}\}} \tag{4.25}$$

where α is a parameter describing the form of the spectrum in the high frequency range, f_p is the top frequency corresponding to ω_p, γ is a parameter describing the maximum of the spectrum in relation to the maximum of a corresponding Pierson-Moskowitz spectrum, and σ is the spectral width parameter, given as

$$\sigma = \sigma_a \text{ for } \omega \leq \omega_p$$

$$\sigma = \sigma_b \text{ for } \omega > \omega_p \tag{4.26}$$

By using the relations

$$f = \frac{\omega}{2\pi} \tag{4.27}$$

and

$$S(f) = 2\pi S(\omega) \tag{4.28}$$

we transform the spectrum into angular frequency:

$$S(\omega) = \alpha g^2 \omega^{-5} \exp[-\frac{5}{4}(\frac{\omega}{\omega_p})^{-4}] \gamma^{\exp\{-\frac{\left(\frac{\omega}{\omega_p}-1\right)^2}{2\sigma^2}\}} \tag{4.29}$$

Average values for the JONSWAP experiment data are $\gamma = 3.3$, $\sigma_a = 0.07$ and $\sigma_b = 0.09$. γ typically varies between 1 and 7, and for $\gamma = 1$ the JONSWAP spectrum reduces to the Pierson-Moskovitz spectrum. The two spectrum types are illustrated in Figure 5.2.

This makes it a three parameter spectrum with the input parameters α, γ and ω_p. ω_p is the singular frequency corresponding to the top of the spectrum, in our case given by the user input T_p.
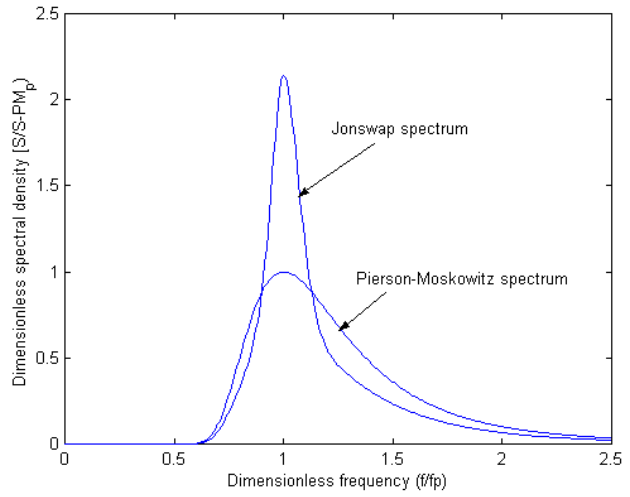
Figure 4.2 - JONSWAP spectrum related to a regular Pierson-Moskowitz spectrum

By using a parameterization (21), we can express the parameters α and γ by the more commonly used H_s and T_p, thus making it a two parameter spectrum. The parameters are expressed as

$$\alpha = 0.036 - 0.0056 \frac{T_p}{\sqrt{H_s}} \tag{4.30}$$

and

$$\gamma = \exp[3.484 \left(1 - 0.1975\alpha \frac{T_p^4}{H_s^2}\right)] \tag{4.31}$$

H_s and T_p are taken as user input in the program, creating the relevant sea state.

4.3.2 Torsethaugen spectrum

The Torsethaugen spectrum is a double peak spectral model developed based on measured spectra for Norwegian waters (Haltenbanken and Statfjord). It is basically put together by two JONSWAP added together, where one represent a wind-dominated sea state, and the other one represents a swell-dominated sea state. Each of these sea systems is defined by distinctive parameters, which are in turn parameterized in terms of the sea state significant wave height and spectral peak period. The Torsethaugen spectrum can thus be expressed as:

$$S_T(\omega) = \sum_{i=1}^{2} S_{J,i}(\omega) \tag{4.32}$$

Where $S_{J,i}$ denotes the JONSWAP spectra of which the Torsethaugen spectrum is composed. The distinction between the wind dominated and the swell dominated sea states is defined by the fully developed sea state, for which

$$T_f = a_f \sqrt[3]{H_s} \tag{4.33}$$

Then $T_p < T_f$ is the wind dominated range and $T_p > T_f$ is the swell dominated range. The factor a_f depends on fetch length, with $a_f = 6.6$ corresponding to a fetch length of 370 km, and $a_f = 5.3$ corresponding to a fetch length of 100 km (23).

The complete buildup of the spectrum is quite complex, and is derived in DNV-RP-C205. In the program, giving H_s and T_p as input produces a unique Torsethaugen spectrum from the WAFO toolbox, as shown in Figure 5.3.
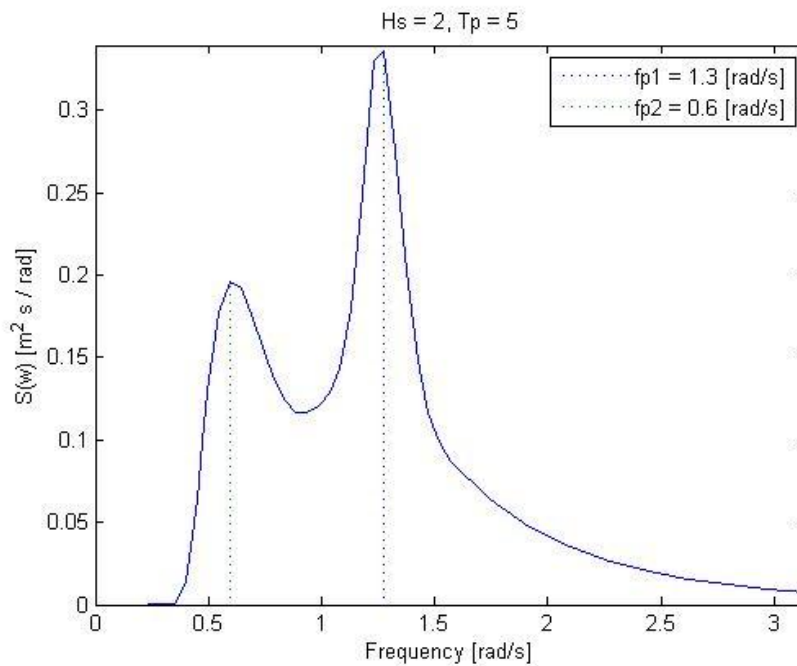
Figure 4.3 - Torsethaugen spectrum. fp1 corresponds to T_p, while fp2 corresponds to T_f.

4.4   Short-crested wave theory

Up until this point, we have only considered long-crested waves. But there is a way to simulate a real sea environment more actually, by adding different directions to the different wave components constituting a wave spectrum. This results in a short-crested wave spectrum which has not only wave frequency, but also wave direction as a parameter. These spectra can be expressed as a product of a long-crested wave spectrum and a directional distribution (21):

$$S_{sc}(\omega, \vartheta) = S_{lc}(\omega)D(\omega, \vartheta) \tag{4.34}$$

where $S_{sc}(\omega, \vartheta)$ is the short-crested wave spectrum, $S_{lc}(\omega)$ is an arbitrary long-crested wave spectrum and $D(\omega, \vartheta)$ is a directional distribution which is not necessarily independent of the wave frequency ω. It must however, satisfy the following condition:

$$\int_0^{2\pi} D(\omega, \vartheta)d\vartheta = 1 \tag{4.35}$$

In our calculations, we assume this distribution to be independent of frequency, and we can thus write:

$$S_{sc}(\omega, \vartheta) = S_{lc}(\omega)D(\vartheta) \tag{4.36}$$

where

$$\int_0^{2\pi} D(\vartheta)d\vartheta = 1 \tag{4.37}$$

There are many examples of directional distributions, and some are included in the WAFO toolbox. The most ordinary form is given as

$$D(\vartheta) = K_{2s}\cos^{2s}\vartheta \tag{4.38}$$

for

$$-\frac{\pi}{2} < \vartheta < \frac{\pi}{2} \tag{4.39}$$

and

$$D(\vartheta) = 0 \tag{4.40}$$

elsewhere. ϑ is a spreading angle variable, and $\vartheta = 0$ corresponds to the main wave propagation direction, and K_{2s} is chosen such that the integration requirement in eq. (4.37) is fulfilled. The variable s is a parameter given by the user which decides the shape of the directional distribution, and thus the level of wave spreading, $s = 1$ giving the highest level. This directional distribution is the one which is used in the program. A visualization of the effect of different spreading levels s is given in Figure 4.4.
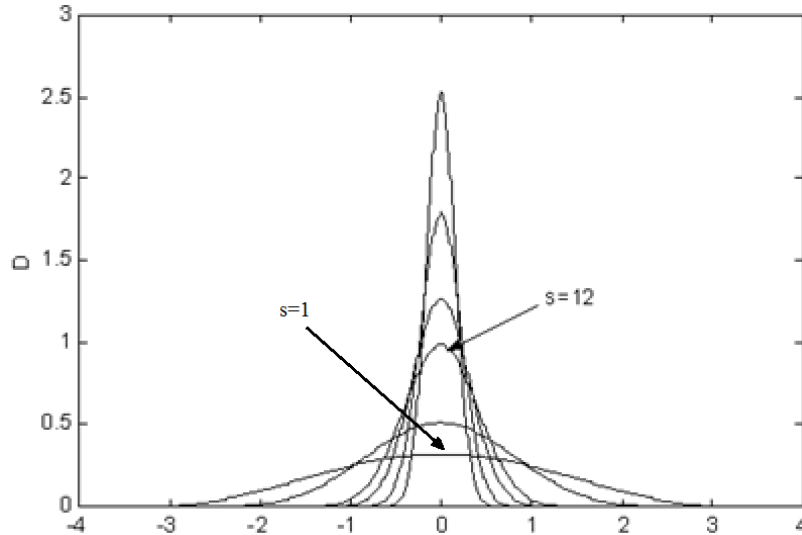
Figure 4.4 - The effect of the parameter s on the directional distribution D(θ)

4.5   Response

At this point, we have derived expressions for the sea state, which represents the wave elevation ζ in the frequency domain. Furthermore, the complex transfer functions for all six degrees of freedom are available, implicitly determining the vessel's motions. We want to link these vessel motions to the wave spectrum to be able to statistically describe the motions in the frequency domain, in the same manner as one would describe a sea spectrum. In other words we want to produce response spectra for the different degrees of freedom, and later also spectra for motion in the specified direction.

4.5.1   Transfer functions

The argument must start in the time-domain. A general method to describe the dynamic characteristics of a linear system is to determine the response to a sine wave input, as shown by Newland (24). If the input $x(t)$ is a sine wave with constant amplitude x_0 and fixed frequency ω

$$x(t) = x_0 \sin \omega t \qquad (4.41)$$

then the steady state output $y(t)$ must also be a sine wave of fixed amplitude y_0, the same frequency ω and a phase difference φ, so that

$$y(t) = y_0 \sin(\omega t - \varphi) \qquad (4.42)$$

Thus, the process can be described by information on the amplitude ratio x_0/y_0 and the phase angle φ. Instead of thinking of these two as separate quantities, it is customary to represent both of them by a single complex number. This is called the complex frequency response function $H(\omega)$ which is defined so that its magnitude equals the amplitude ratio, and the ratio

of its imaginary part to its real part is equal to the tangent of the phase angle. If the transfer function is written as

$$H(\omega) = A(\omega) - jB(\omega) \tag{4.43}$$

where $A(\omega)$ and $B(\omega)$ are real functions of ω an j is the imaginary unit, then these quantities can be expressed by

$$\frac{y_0}{x_0} = |H(\omega)| = \sqrt{A^2 + B^2} \tag{4.44}$$

and

$$\tan \varphi = \frac{Im\{H(\omega)\}}{Re\{H(\omega)\}} = \frac{B}{A} \tag{4.45}$$

In our case the input is the wave elevation ζ, which produces six different outputs η_{1-6}, one for each degree of freedom. We can thus describe the input as

$$\zeta(t) = \zeta_A \sin \omega t \tag{4.46}$$

and the output as

$$\eta_i(t) = \eta_{A,i} \sin(\omega t - \varphi_i), \qquad i = 1 - 6 \tag{4.47}$$

where i represents the different degrees of freedom. The amplitude ratio is given as response amplitude per wave amplitude for the three translations surge, sway and heave, while for the rotations roll, pitch and sway, these ratios are given as response amplitude per wave slope angle. We can write this as

$$H_i(\omega) = \frac{\eta_i}{\zeta}, \qquad i = 1,2,3 \tag{4.48}$$

$$H_i(\omega) = \frac{\eta_i}{k(\omega) \cdot \zeta}, \qquad i = 4,5,6 \tag{4.49}$$

since $k(\omega) \cdot \zeta$ is a common measure of wave slope angle. If we have the input given on the form of a spectrum, we can use the transfer functions to express the response spectra. We have the following relation (Newland, eq. 7.16) (24)

$$S_y(\omega) = |H(\omega)|^2 S_x(\omega) \tag{4.50}$$

where $S_y(\omega)$ is a general response spectrum and $S_x(\omega)$ is an arbitrary input spectrum. We can then write the response spectra for the six degrees of freedom as:

$$S_{\eta_i \eta_i}(\omega) = \left|H_{\zeta \eta_i}(\omega)\right|^2 S_\zeta(\omega), \qquad i = 1,2,3 \tag{4.51}$$

$$S_{\eta_i \eta_i}(\omega) = k^2(\omega)\left|H_{\zeta \eta_i}(\omega)\right|^2 S_\zeta(\omega), \qquad i = 4,5,6 \tag{4.52}$$

4.5.2 Response spectra in the local coordinate system

For an arbitrary point on a floating object, we can calculate the motions in the object's own coordinate system. This system is typically centered in the object's center of gravity or center of roll, and the x-axis points forward, as illustrated in Figure 5.5. The six motions, given as either translations along, or rotations about, their respective axes, are denoted as η_{1-6}. The translations are defined as positive in the direction of the positive axis, and the rotations are given as positive according to the right-hand rule, also shown in the figure. Here, η_1 is surge, η_2 is sway, η_3 is heave, η_4 is roll, η_5 is pitch and η_6 is yaw. If we then denote the point coordinates as (x_p, y_p, z_p) we can express the point motions by the equation of motions as defined by Faltinsen (1990) (25):
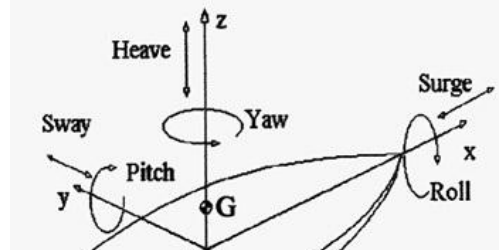
Figure 4.5 - Vessel coordinate system and definition of motions (35)

$$s = (\eta_1 + z_p\eta_5 - y_p\eta_6)i + (\eta_2 - z_p\eta_4 + x_p\eta_6)j + (\eta_3 + y_p\eta_4 - x_p\eta_5)k \tag{4.53}$$

where i, j and k are the unit vectors pointing along the local x-, y- and z-axes respectively. It should be noted that when using this equation, it is assumed that the ship hull is slender, and that the ship motions are small, so the waterplane area does not change much. The assumption of small motions is also made directly in the equation, as the movements from the rotations should strictly speaking be multiplied by the tangent to the angles rather than the angles themselves. These assumptions are widely used, and should be reasonable for most cases.

We see that the motions along each of these axes are built up by three degrees of freedom each, which are not necessarily in phase. Let us consider for example the total motion of the point in z-direction, which is denoted by

$$r_3 = \eta_3(t) + y_p\eta_4(t) - x_p\eta_5(t) \tag{4.54}$$

where each of these three degrees of freedom has different phase angles, but the total motion has an expectation of zero:

$$E[r_3(t)] = 0 \tag{4.55}$$

To find an expression for the total response spectrum in z-direction we need to introduce the concept of correlation functions. The autocorrelation function for motion in z-direction $r_3(t)$ is defined by Newland (2005) (24) as

$$R_{r_3 r_3}(\tau) = E[r_3(t)r_3(t + \tau)] \tag{4.56}$$

and similarly, the cross-correlation function between e.g. heave motion and roll motion is given as

31

$$R_{\eta_3\eta_4}(\tau) = E[\eta_3(t)\eta_4(t+\tau)] \tag{4.57}$$

If we write out the autocorrelation function for motion in z-direction, we end up with the following expression:

$$
\begin{aligned}
R_{r_3 r_3}(\tau) = {} & R_{\eta_3\eta_3}(\tau) + y_p^2 R_{\eta_4\eta_4}(\tau) + x_p^2 R_{\eta_5\eta_5}(\tau) \\
& + y_p[R_{\eta_3\eta_4}(\tau) + R_{\eta_3\eta_4}(-\tau)] \\
& - x_p[R_{\eta_3\eta_5}(\tau) + R_{\eta_3\eta_5}(-\tau)] \\
& - x_p y_p[R_{\eta_4\eta_5}(\tau) + R_{\eta_4\eta_5}(-\tau)]
\end{aligned}
\tag{4.58}
$$

Detailed derivations are provided in appendix B. A spectrum is defined as the Fourier transform of an autocorrelation function:

$$S_x(\omega) = \frac{1}{2\pi} \int_{-\infty}^{\infty} R_x(\tau)\, e^{-i\omega t} d\tau \tag{4.59}$$

By combining these two expressions, we finally obtain the total response spectrum for motion in z-direction:

$$
\begin{aligned}
S_{r_3 r_3}(\omega) = {} & S_{\eta_3\eta_3}(\omega) + y_p^2 S_{\eta_4\eta_4}(\omega) + x_p^2 S_{\eta_5\eta_5}(\omega) \\
& + 2y_p\{Re[S_{\eta_3\eta_4}(\omega)]\} \\
& - 2x_p\{Re[S_{\eta_3\eta_5}(\omega)]\} \\
& - 2x_p y_p\{Re[S_{\eta_4\eta_5}(\omega)]\}
\end{aligned}
\tag{4.60}
$$

To be able to express the cross-correlation spectra, it is necessary to calculate the cross-correlation transfer functions. These are given as:

$$H_{\eta_i\eta_j}(\omega) = \frac{H_{\zeta\eta_j}(\omega)}{H_{\zeta\eta_i}(\omega)}, \qquad i,j = 1,2,3$$

$$H_{\eta_i\eta_j}(\omega) = \frac{H_{\zeta\eta_j}(\omega)}{H_{\zeta\eta_i}(\omega)}, \qquad i,j = 4,5,6$$

$$H_{\eta_i\eta_j}(\omega) = k(\omega)\frac{H_{\zeta\eta_j}(\omega)}{H_{\zeta\eta_i}(\omega)}, \qquad i = 1,2,3 \;\&\; j = 4,5,6 \tag{4.61}$$

$$H_{\eta_i\eta_j}(\omega) = k(\omega)\frac{H_{\zeta\eta_j}(\omega)}{H_{\zeta\eta_i}(\omega)}, \qquad i = 4,5,6 \;\&\; j = 1,2,3$$

Finally, we can express the total response spectrum in z-direction by the wave spectrum:

$$
S_{r_3 r_3}(\omega)
$$
$$
= \Bigg(\left| H_{\zeta \eta_3}(\omega) \right|^2 + y_p^2 k^2(\omega) \left| H_{\zeta \eta_4}(\omega) \right|^2
$$
$$
+ x_p^2 k^2(\omega) \left| H_{\zeta \eta_5}(\omega) \right|^2
$$
$$
+ 2 y_p k(\omega) \left\{ Re \left[\frac{H_{\zeta \eta_4}(\omega)}{H_{\zeta \eta_3}(\omega)} \left| H_{\zeta \eta_3}(\omega) \right|^2 \right] \right\} \tag{4.62}
$$
$$
- 2 x_p k(\omega) \left\{ Re \left[\frac{H_{\zeta \eta_5}(\omega)}{H_{\zeta \eta_3}(\omega)} \left| H_{\zeta \eta_3}(\omega) \right|^2 \right] \right\}
$$
$$
- 2 x_p y_p k^2(\omega) \left\{ Re \left[\frac{H_{\zeta \eta_5}(\omega)}{H_{\zeta \eta_4}(\omega)} \left| H_{\zeta \eta_4}(\omega) \right|^2 \right] \right\} \Bigg) S_\zeta(\omega)
$$

The derivations of the total response spectra in x- and y-direction are analogous and can be found in appendix B.

4.5.3 Global response spectra

Now we have derived the response spectra in the local x-, y- and z-directions, but we need to link these to the global coordinate system. Both the heading and the placement of the origin of the vessel's coordinate system are arbitrary, as is the case with the locations of both the
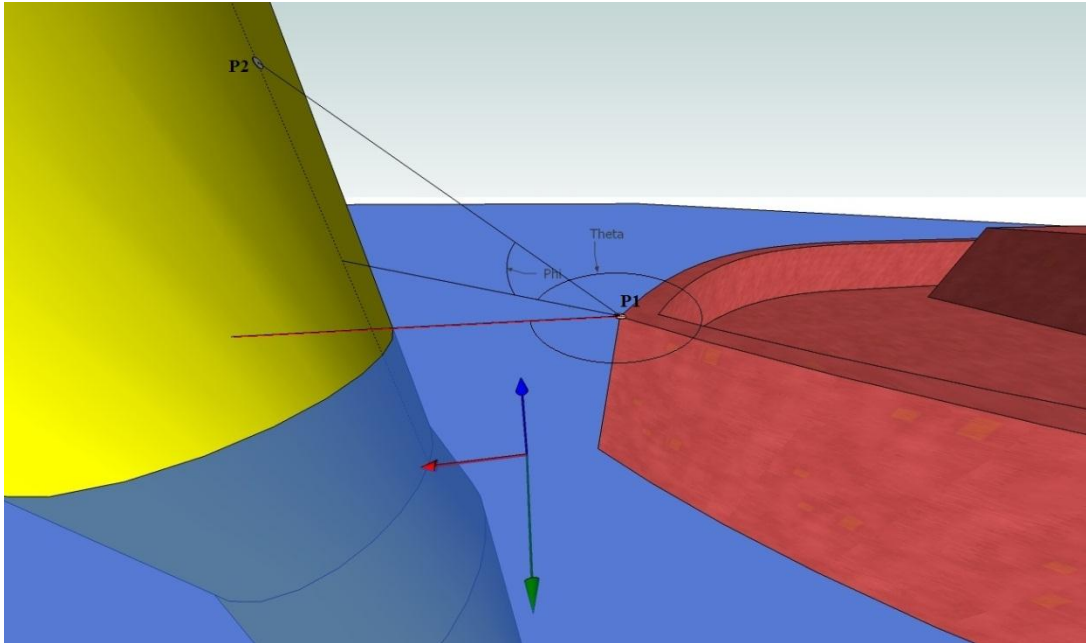
Figure 4.6 – Example of direction of the examined motion

considered point on the vessel, and the considered point on the wind turbine. We want to examine the motion of the vessel point relative to the turbine point, and must therefore look at the motion in the direction pointing towards the turbine point. This direction is automatically calculated by the program, and is given by the angle θ in the xy-plane and the angle ϕ in the vertical plane. The situation is illustrated in Figure 4.6. These angles are calculated from the

mean (zero) position of the vessel, and do not change as the vessel moves. We must now derive the spectrum for the motion along this direction by first finding the spectrum for motion along the angle θ in the xy-plane, and then combining this with the spectrum for motion along the angle ϕ in the vertical plane along θ.

We define the angle θ as the angle between the local x-axis and the projection of the straight line between the points on the xy-plane, measured counterclockwise from the local x-axis, as illustrated in Figure 4.6. The motion in the xy-plane can then be written as

$$r_\theta(t) = r_1(t) \cos \theta + r_2(t) \sin \theta \tag{4.63}$$

By defining the autocorrelation function and using Fourier transform in the same way as before, we obtain an expression for the spectrum for motion in the xy-plane along the angle θ (see appendix B for detailed derivations):

$$
\begin{aligned}
S_{r_\theta r_\theta}(\omega) = {} & S_{r_1 r_1}(\omega) \cos^2 \theta + S_{r_2 r_2}(\omega) \sin^2 \theta \\
& + 2\{Re[S_{r_1 r_2}(\omega)]\} \sin \theta \cos \theta
\end{aligned}
\tag{4.64}
$$

Where $S_{r_1 r_2}(\omega)$ is the cross-correlation spectrum expressed by:

$$
\begin{aligned}
S_{r_1 r_2}(\omega) = {} & S_{\eta_1 \eta_2}(\omega) - z_p S_{\eta_1 \eta_4}(\omega) + x_p S_{\eta_1 \eta_6}(\omega) \\
& + z_p S_{\eta_5 \eta_2}(\omega) - z_p^2 S_{\eta_5 \eta_4}(\omega) \\
& + x_p z_p S_{\eta_5 \eta_6}(\omega) - y_p S_{\eta_6 \eta_2}(\omega) \\
& + y_p z_p S_{\eta_6 \eta_4}(\omega) - x_p y_p S_{\eta_6 \eta_6}(\omega)
\end{aligned}
\tag{4.65}
$$

We define the angle ϕ as zero along the xy-plane, and positive when pointing upwards. Then we have the following expression for motion along the straight line between the points, given by the angles θ and ϕ:

$$r_\phi(t) = r_\theta(t) \cos \phi + r_3(t) \sin \phi \tag{4.66}$$

By following the same procedure, we finally obtain the following spectrum for total response along the straight line between the points:

$$
\begin{aligned}
S_{r_\phi r_\phi}(\omega) = {} & S_{r_\theta r_\theta}(\omega) \cos^2 \phi + S_{r_3 r_3}(\omega) \sin^2 \phi \\
& + 2\{Re[S_{r_\theta r_3}(\omega)]\} \cos \phi \sin \phi
\end{aligned}
\tag{4.67}
$$

where the cross-correlation spectrum is given as

$$
\begin{aligned}
S_{r_\theta r_3}(\omega) = {} & \big[S_{\eta_1\eta_3}(\omega) + y_p S_{\eta_1\eta_4}(\omega) - x_p S_{\eta_1\eta_5}(\omega) \\
& + z_p S_{\eta_5\eta_3}(\omega) + y_p z_p S_{\eta_5\eta_4}(\omega) \\
& - x_p z_p S_{\eta_5\eta_5}(\omega) - y_p S_{\eta_6\eta_3}(\omega) \\
& - y_p^2 S_{\eta_6\eta_4}(\omega) + x_p y_p S_{\eta_6\eta_5}(\omega) \big] \cos\theta \\
& + \big[S_{\eta_2\eta_3}(\omega) + y_p S_{\eta_2\eta_4}(\omega) \\
& - x_p S_{\eta_2\eta_5}(\omega) - z_p S_{\eta_4\eta_3}(\omega) \\
& - y_p z_p S_{\eta_4\eta_4}(\omega) + x_p z_p S_{\eta_4\eta_5}(\omega) \\
& + x_p S_{\eta_6\eta_3}(\omega) + x_p y_p S_{\eta_6\eta_4}(\omega) \\
& - x_p^2 S_{\eta_6\eta_5}(\omega) \big] \sin\theta
\end{aligned} \tag{4.68}
$$

At this point, all unknown are expressed by the known autocorrelation spectra and the cross-correlation spectra found by combining the given transfer functions. Through these equations the program finally computes the total motion spectrum for the straight line between the points.

4.5.4   Velocity and acceleration spectra

To obtain the spectra for the other responses, velocity and acceleration, we use the following relation (Newland, eq. 7.16) (24):

$$
S_{\dot{x}}(\omega) = \omega^2 S_x(\omega) \tag{4.69}
$$

which again imply

$$
S_{\ddot{x}}(\omega) = \omega^2 S_{\dot{x}}(\omega) = \omega^4 S_x(\omega) \tag{4.70}
$$

Using this procedure, we can thus easily find the spectra for velocity and acceleration once the motion spectrum is obtained.

4.6   Statistical analysis

To gain some sensible results out of our obtained spectra, we must look at their extreme values as functions of the time period under observation. In this paper, marine operations in a short time frame are considered. We must therefore analyze our obtained spectra using short term statistics.

4.6.1   Short term statistics

Let us start by looking at the wave spectrum. If we have a real set of wave data, it can be difficult to mathematically express the probability distribution of wave heights, so it is necessary to make some assumptions about the distributions to find a good way to analyze them statistically. We assume that the ocean surface is a stationary narrow-banded stochastic

process (21). In this statement lies that the probability distribution is the same throughout the time period examined, that all the frequencies in the wave spectrum are close to $\omega = 2\pi/T$, that the surface elevations over time are normally distributed around the mean sea surface, and that all wave crests are uncorrelated.

When we apply these assumptions, the probability density distribution of the wave amplitude maxima is given by the Rayleigh distribution, and thus the same is true for the wave height maxima. The Rayleigh cumulative distribution function can be written as

$$F_H(h) = 1 - e^{-\frac{h^2}{8m_0}} \tag{4.71}$$

and the corresponding probability density function is given by

$$f_H(h) = \frac{dF_H(h)}{dh} = \frac{h}{4m_0} e^{-\frac{h^2}{8m_0}} \tag{4.72}$$

Here the quantity m_0 is the zero spectral moment of the wave spectrum $S(\omega)$. The moments are found by

$$m_n = \int_0^\infty \omega^n S(\omega) d\omega \tag{4.73}$$

We use these moments to find the mean zero crossing period, given by

$$T_{m02} = 2\pi \sqrt{\frac{m_0}{m_2}} = T_z \tag{4.74}$$

which again provides us with the total number of waves N in a sea state with duration D:

$$N = \frac{D}{T_z} \tag{4.75}$$

The assumptions that are applied give an approximation of the real situation in a satisfactory manner, although it should be noted that the probability of exceedance is generally estimated too high when using the Rayleigh distribution. This is due to the idealization that the wave process is narrow-banded, and the result is that our extreme values will be conservative estimates.

4.6.2 Extreme value distribution

Classifications of extreme value distributions are made according to the tail behavior of the initial distribution (26). When we have an initial distribution which is exponential such as the Rayleigh distribution, the extreme values are described by the Gumbel distribution. The Gumbel distribution is written as

$$F_y(y) = e^{-\{e^{-\alpha(y-u)}\}} \tag{4.76}$$

where the parameters α and u are found from the initial distribution $F_X(x)$ [28]:

$$F_X(x) = 1 - \frac{1}{n} \tag{4.77}$$

$$\alpha = n \cdot f_X(u) \tag{4.78}$$

If we insert our initial distribution, the Rayleigh distribution, we can calculate values for the Gumbel parameters α and u (detailed derivations are found in appendix C):

$$F_H(u) = 1 - e^{-\frac{u^2}{8m_0}} = 1 - \frac{1}{N} \tag{4.79}$$

$$\Rightarrow -\frac{u^2}{8m_0} = \ln\frac{1}{N} \Rightarrow u = 2\sqrt{2m_0 \ln N} \tag{4.80}$$

$$\alpha = N \cdot f_H(u) = N \cdot \frac{u}{4m_0} e^{-\frac{u^2}{8m_0}} \tag{4.81}$$

$$\Rightarrow \alpha = \sqrt{\frac{\ln N}{2m_0}} \tag{4.82}$$

For a Gumbel distribution, the mean value μ_y and the standard deviation σ_y are given by:

$$\mu_y = u + \frac{0.57722}{\alpha} \tag{4.83}$$

$$\sigma_y = \frac{1.28255}{\alpha} \tag{4.84}$$

The mean value of the Gumbel extreme value distribution gives us the expected extreme value for our initial Rayleigh distribution. By inserting the parameters into eq. (4.83), we obtain the following expression for expected maximum wave height:

$$E[H_{max}] = \mu_y = u + \frac{0.57722}{\alpha}$$

$$= 2\sqrt{2m_0 \ln N} + \frac{0.57722}{\sqrt{\ln N / 2m_0}}$$

$$= \sqrt{2m_0}\left[2\sqrt{\ln N} + \frac{0.57722}{\sqrt{\ln N}}\right] \quad (4.85)$$

$$= 2\sqrt{2m_0}\left[\sqrt{\ln N} + \frac{0.57722/2}{\sqrt{\ln N}}\right]$$

$$= 4\sqrt{m_0}\left[\sqrt{\frac{\ln N}{2}} + \frac{0.28861}{\sqrt{2\ln N}}\right]$$

When the wave elevation is Rayleigh distributed, we have from Myrhaug, 2007 (21) the following commonly used relation:

$$H_s = H_{1/3} = 4\sqrt{m_0} \quad (4.86)$$

which is a good estimate for the mean value of the top 1/3 of the waves. By using this, we can express the expected maximum wave height by the significant wave height H_s:

$$E[H_{max}] = H_s\left[\sqrt{\frac{\ln N}{2}} + \frac{0.28861}{\sqrt{2\ln N}}\right] \quad (4.87)$$

Because all the spectra that are calculated throughout this assignment are direct functions of our initial sea spectrum, they all have the same characteristics and can thus be analyzed in the same way. The formula above is valid for all the spectra, and the different extreme values are only dependent on the significant values calculated from the moments of the relevant spectrum.

5 The program

5.1 Introduction

Relative Motion Calculator is a MATLAB program that calculates motions for a point on a floating system and compares these to a fixed point. The work with the program started in august 2011 after Dr. Rune Yttervik at Statoil had proposed a definite task for me. The object of the assignment was to estimate the magnitudes of the motions between different bodies in marine operations, and therefore to develop

"... a MATLAB application for easily and clearly estimating relative motions between a vessel and points on a wind turbine".

The assignment was split into two parts: The first one, the project thesis, was a limited scope of the assignment which was finished before Christmas. It served as a sort of prequel to the master thesis, which features a more complete solution to the initial problem. The master thesis has been prepared throughout the spring of 2012. The reason that the project thesis is being mentioned is that it plays a part in the validation of the complete program. However the focus is mainly placed on the complete master version of the program (RMC 2.3) in the following.

5.2 Input/output

The program produces certain output when provided with the right input. The most important input is the RAO-file, which has been provided by Dr. Yttervik, and without which the program cannot function at all. Relative Motion Calculator does not produce its own transfer functions, nor does it assess any sea or wave loads whatsoever. It only assesses already existing RAO-files in relation to different wave conditions and different geometries. It should therefore be seen as a sort of statistical analyzing tool for externally generated RAO-files. A brief description of all the different inputs and outputs and their characteristics is provided below.

User provided inputs are:

- RAO-file for the vessel. A transfer function is given by an amplitude and a phase angle (ref. section 4.5.1) for each of the six degrees of freedom. In the current case the RAO-file provides information for every 15 degrees of heading and for 41 frequencies between 0.15 and 4.2 [s^{-1}].
- Sea state data. The sea spectrum is given by the characteristic parameters significant wave height H_s, peak period T_p, type of sea spectrum (JONSWAP or Torsethaugen) and the duration in hours D. Furthermore, a (main) wave propagation direction is given, as well as a wave spreading parameter s in case short-crested waves are being used.

- Geometry. The placement of the fixed wind turbine's origin coincides with the global coordinate system's origin, but as it is fixed, it is not important in any other way than in the visualization of the problem. The only significant parameter in the turbine's geometry is the considered point which can be arbitrary, given by global coordinates. The vessel's origin is given by global coordinates, and should be placed in the vessel's center of rotation. The x-axis is directed by an angle γ which is measured anti-clockwise from the global x-axis, and the considered point on the vessel is given by local coordinates relative to the vessel's origin. The geometry of the problem will be further elaborated in section 5.3.3.
- Criteria. This is the data to which the program compares the calculated values. They are given as minimum distance, maximum distance, maximum velocity and maximum acceleration, all in the direction of the straight line between the considered points, which is automatically computed by the program.

For these inputs the program provides the following output:

- Plots of the transfer functions for the relevant attack angle and plot of the sea spectrum.
- Plots of the spectra for local motions; one plot for each of the six degrees of freedom of the vessel, and one plot for combined motions in x- y- and z-directions for the considered point on the vessel.
- Local motions. Expected maxima of each of the three spectra for combined motions, and for their first- and second order derivatives. Also, the expected maximum wave height of the sea state is provided.
- The angles defining the direction of the vector between the two considered points, θ
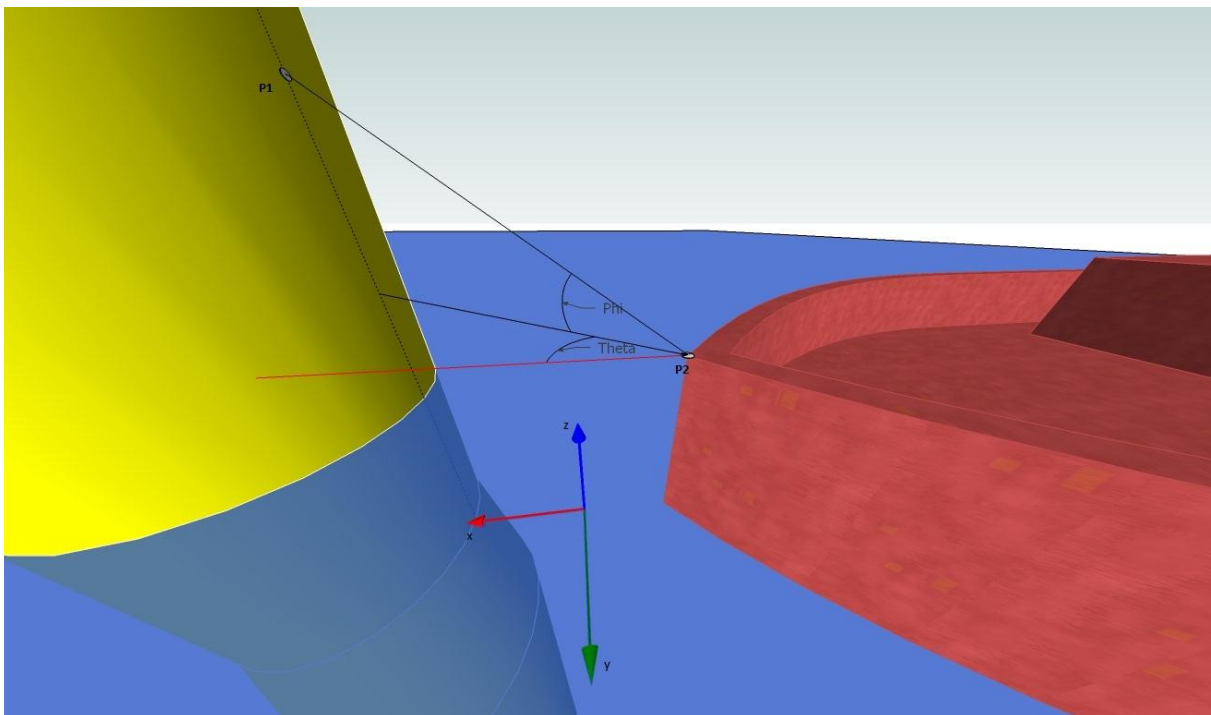
Figure 5.1 - Visualization of the angles θ and ϕ between the considered points

and ϕ as shown in Figure 6.1. This is the vector along which the motions are examined.

- Motions of the vessel point relative to the turbine point, along the given direction. Expected maxima of the motion spectrum and its first- and second-order derivatives in the specified direction.
- Minimum and maximum distance between points, and whether the given criteria have been exceeded or not.

Details in connection with these quantities will be further elaborated on throughout this chapter. First we will review the assumptions and simplifications that the program is based on.

5.3   Assumptions and definitions

Although some definitions have already been made throughout this paper, we will give a systematic overview of which assumptions the program is based on. Then the differences between the project version and the master version of the program are discussed. Furthermore, a visual image of the situation is provided to make clear to the user how the geometry is defined.

5.3.1   Assumptions

Recall that from the theory part (ref. section 5.1) we listed the following assumptions as related to the computations and use of the transfer functions:

- Linear potential theory. We neglect higher order terms in the Bernoulli equation (4.3).
- No hydrodynamic interaction. The effects from the turbine tower changing the waves are not considered. This will cause inaccuracies when the two systems are close.
- No wind loads or current loads are included.
- Large water depth.
- Small vessel motions.
- Slender ship hull (linear sea keeping).

A point that deserves mention is the assumption that there is no hydrodynamic interaction. This is a quite crude simplification, in particular because the moving vessel will often be in very close proximity to the wind turbine. The effects of the wind turbine's presence on the vessel will in many cases be significant, and is something that must be taken into account when planning a marine operation. For example, it is common when boarding a wind turbine to approach it facing the wave propagation direction, thus exploiting the leeward side of the turbine. In this case it is obvious that the hydrodynamic interaction plays a crucial part. However, this interaction is dependent on many factors, such as the geometry of both bodies, distance between them, wave direction and wave frequency. It is therefore difficult or impossible to calculate this effect directly, and should therefore be done by altering the

vessel's transfer function. That means generating a whole new transfer function with the above parameters taken into account. The hydrodynamic interaction-effect is therefore complicated to include without an external program to compute this modified RAO. The simplification is thus crude but necessary.

Furthermore, linear potential theory and large water depth has been assumed when establishing the sea spectra. However, for analyzing the spectra, we had to assume some things about the wave process to establish the equation for the expected extreme values. We assumed that the ocean surface is a stationary narrow-banded stochastic process (21):

- The probability distribution is the same throughout the time period examined (stationary).
- All the frequencies in the wave spectrum are close to $\omega = 2\pi/T$ (narrow-banded).
- The surface elevations over time are normally distributed around the mean sea surface, and all the wave crests are uncorrelated (stochastic process).

Last but not least, another major assumption is made, which is that the wind turbine is considered fixed. The initial idea of the program included relative motions between points on two moving systems, but this was later disregarded in accordance with my supervisors. There were several reasons for this, one being that short-crested waves is equally interesting, and less time consuming to examine. Another is the fact that floating wind turbines, and in particular Hywind, are very large structures, with correspondingly large natural periods for motions. Compared to the quicker motions of the smaller vessel, the situation on the wind turbines can therefore be assumed as a series of stationary positions instead of dynamically moving, without much loss of accuracy. It should be noted however, that for either larger ships or smaller turbines (or other floating objects), this effect becomes increasingly important to include. To make the program as flexible and suitable for use in as many situations as possible, there should of course be two moving systems. But you have to make priorities and choices when you only dispose the limited amount of time that you have for a master thesis.

5.3.2 Project model

The project version of the program, RMC 1.2, was finished before Christmas of 2011, and was the platform on which the master version is founded. It features some further simplifications as the main objective of the project thesis was to establish the basic equations, as well as the programming foundation. The focus was thus not placed on making an applicable program. In RMC 1.2, the geometry is not arbitrary; rather we look at a situation where the boat lies alongside the wind turbine, with waves coming in from the side, as shown in Figure 6.2. On the figure, we see the global coordinate system and the local vessel coordinate system. Both the x-axes point into the paper. We have the two points *A* and *B*, and the distances horizontally and vertically, *dy* and *dz*. This is actually a 2D-representation of the problem, representing i.e. the midship section and thus ignoring the x-coordinate. If we look at the equation of motion, eq. (4.53), while disregarding the terms containing motion in x-direction and setting *x=0*, we can write the following simplified version of the equation:
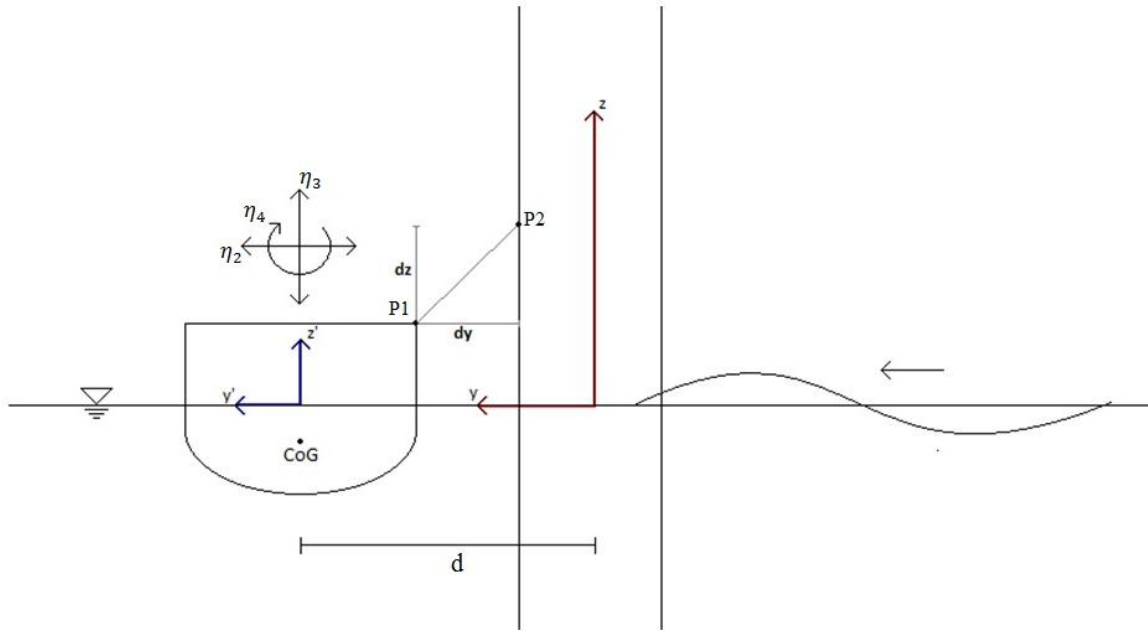
Figure 5.2 - Simplified model

$$\boldsymbol{s} = \left(\eta_2 - z_p\eta_4\right)\boldsymbol{j} + \left(\eta_3 + y_p\eta_4\right)\boldsymbol{k} \tag{5.1}$$

This equation is relatively simple, for example we note that the number of degrees of freedom have been reduced from the initial six to only three, namely sway, heave and roll. Another simplification that has great effect is that the geometry is fixed. Then we only have one situation, and apart from the definitions of directions and coordinates being simple, we also omit the problem of examining the motion along a certain direction, which is complex to determine. In this case it suffices to analyze the local vessel motions almost exclusively. They are only put into a global context when the distances are calculated.

This program, being so simple, provides a good template for us to test our final program up against. It is done by making the same geometrical situation and then setting different degrees of freedom to zero.

5.3.3 Master model

With the beginning of the final semester in January 2012, so began work on the master version of the program, which would eventually end up in version 2.3. The main goal at this point, was to expand the model to include all six degrees of freedom, and thus also include an arbitrary wave heading. Furthermore, an arbitrary heading of the vessel coordinate system was desirable, thus making the program as flexible as possible. Some geometrical definitions had to be made, and visualizing the physical became increasingly important. I spent some

time creating a proper 3D model of the situation for easy reference, and an example of a situation is shown in Figure 5.3.
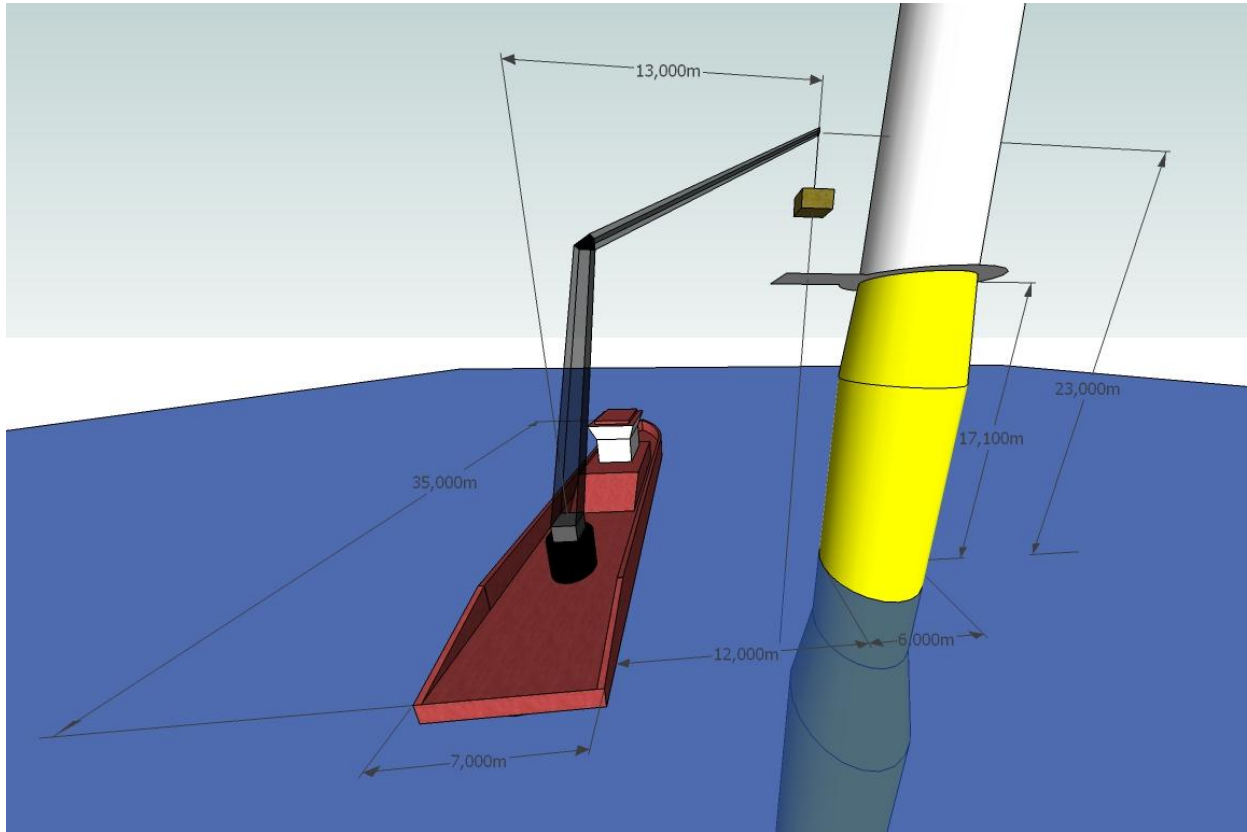
Figure 5.3 - Visualization of the physical problem

The example situation is an imagined crane operation where the ship lies alongside the turbine, and it can be compared to the situation from the project thesis. All measures are shown in the figure.

5.3.3.1 Definition of directions

The best way to define the geometry is to place the global origin in the center of the turbine where it intersects the waterplane. The origin of the vessel's coordinate system is then given by global coordinates, and the direction in which the local x-axis points is given by an angle γ measured counter-clockwise from the global x-axis. Since the local z-axis obviously points upwards, this gives an unique local coordinate system. The same way is used when choosing main wave propagation direction. The angle β is measured counter-clockwise from the global x-axis. The situation is sketched up in Figure 5.4. We observe from the figure that we can write the following relation:

$$\beta - \delta = \gamma \tag{5.2}$$

where δ is the wave propagation direction relative to the local vessel coordinate system.

44
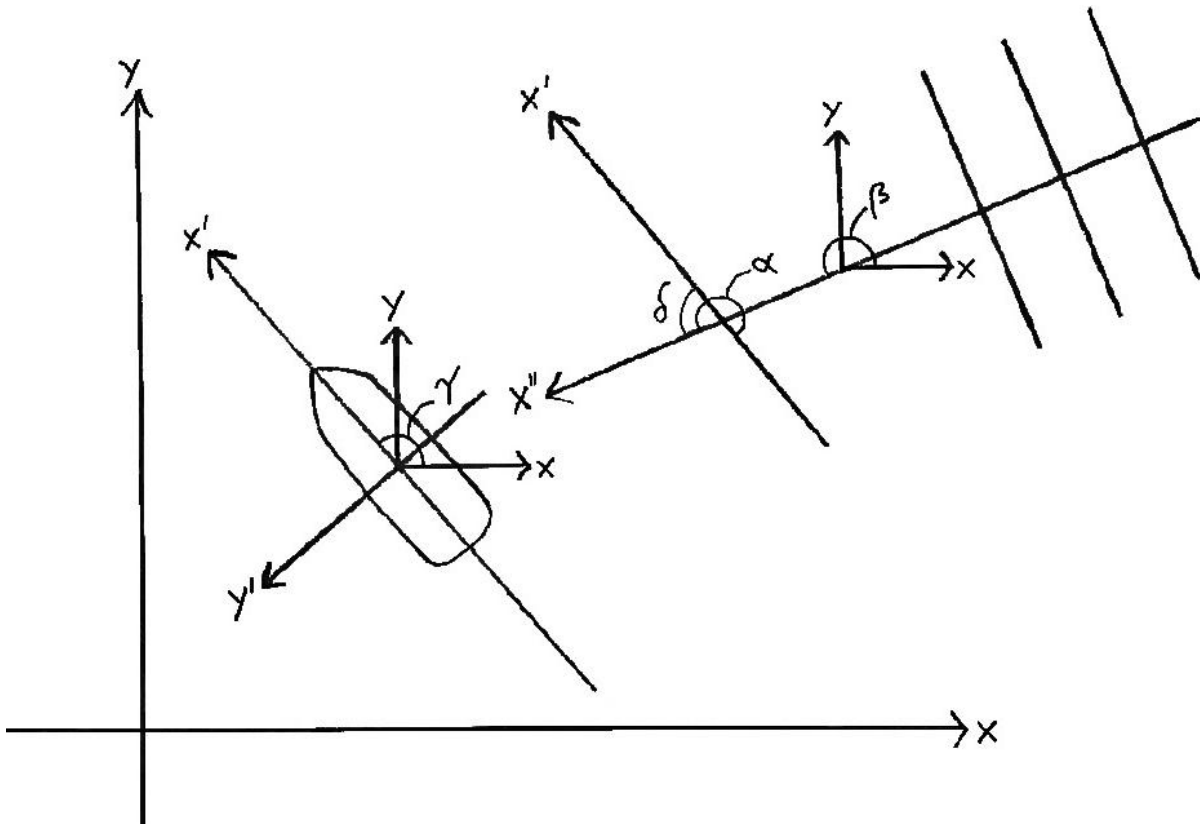
Figure 5.4 - Attack angle of waves on vessel

5.3.3.2 Attack angle

The next step is to determine the attack angle of the wave on the ship. The attack angle is defined from the provided RAO as 0° in head sea, 90° in beam sea and 180° in following sea, which means that the attack angle is zero when facing the opposite direction than that of the ship. If we take the wave propagation angle measured counter-clockwise from the ship's x-axis and call this δ, then we have the attack angle α expressed as

$$\alpha = \delta + 180° \qquad (5.3)$$

which, combined with eq. (5.2) yields

$$\alpha = 180° + \beta - \gamma \qquad (5.4)$$

5.3.3.3 Direction between considered points

When the program was extended to include all degrees of freedom and arbitrary headings and points, an issue emerged related to the motions. When the old version only looked at the local motions, we now had to include direction between the points when examining the motion spectra. Yet another spectrum had to be calculated, taking all the different degrees of freedom and different phase angles into account. Thus the direction of the straight line between the two

considered points had to be defined, as discussed in section 4.5.3. This was done by taking the angle θ as the straight line measured counter-clockwise from the ship's x-axis in the xy-plane, as illustrated in Figure 4.6.

A sketch of the situation from above is provided in Figure 5.5. The angle is a function of the coordinates of the two considered points, as well as the vessel's heading angle γ. The angle ψ is the vector pointing from P1 to P2 measured anti-clockwise from the global x-axis. We see that it can be expressed as

$$\psi = \gamma + \theta = \lambda + 180° \tag{5.5}$$

which can be rewritten for θ into

$$\theta = \lambda + 180° - \gamma \tag{5.6}$$
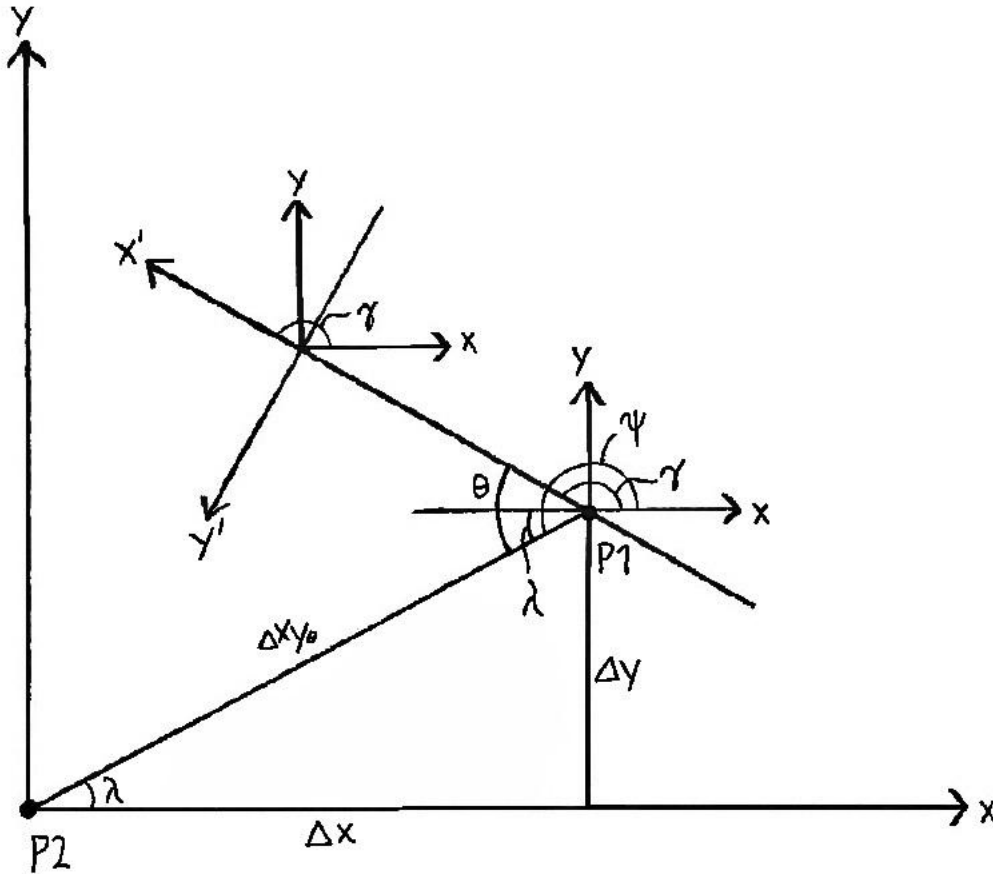
Figure 5.5 - The two considered points and the two coordinate systems seen from above

Now, we have the angle λ easily calculated by

$$\lambda = \tan^{-1}\left(\frac{\Delta y}{\Delta x}\right) = \tan^{-1}\left(\frac{y_1 - y_2}{x_1 - x_2}\right) \tag{5.7}$$

with Δx and Δy being the distances beween the points in global x- and y-directions. Here P1 is defined as the point on the vessel and P2 is the point on the fixed wind turbine. The

problem here is that the *arctan* function by definition produces an angle between -90° and 90°, so it is important to keep track of in which quadrant the point *P1* is located. This is taken care of in the script.

Furthermore, the vector pointing from one point to the other is defined by an angle ϕ in the vertical plane defined by the angle θ. When the latter angle is defined uniquely, it is very easy to find the angle ϕ. A sketch of the two points from the side is given in Figure 6.6. We can write this as

$$
\phi = \tan^{-1}\left(\frac{\Delta z}{\Delta xy_\theta}\right)\tan^{-1}\left(\frac{\Delta z}{\sqrt{(\Delta x^2 + \Delta y^2)}}\right)
$$
$$
= \left(\frac{z_2 - z_1}{\sqrt{((x_1 - x_2)^2 + (y_1 - y_2)^2)}}\right)
$$

(5.8)

Here, the term Δxy_θ is the length of the straight line between the points projected onto the xy-plane, thus along the angle θ. Note that Δz has to be defined oppositely compared to Δx and Δy, that is the coordinate of P1 subtracted from P2, instead of vice versa. That is necessary because the angle ϕ is computed directly from P1, while the angle θ is calculated starting at P2 and then combining with the other angles. Note that since Δxy_θ is always positive, the sign of the term inside the arctan function only depends on Δz. If this is positive i.e. if P2 lies above P1, then ϕ also becomes positive and vice versa. ϕ is thus defined as positive when pointing upwards and negative when pointing downwards.

Figure 5.6 - The two points shown from the side

5.4   Program structure

The master version of the program is built directly on the project version. It has constantly evolved from the foundation featuring the basic equations for three degrees of freedom into the more generalized version with arbitrary geometry and several functions. The approach with initially trying to make a tidy and systematic program has been beneficial, although all the scripts and the total structure have been modified along the way. The most striking difference from the old version is that the distribution of work is more organized. Instead of the main file governing all the processes, it now only calls four function, which in turn call their own functions. The complete buildup of the program is shown in the flow chart in Figure

5.7. Another difference is the implementation of subfunctions, thus reducing the number of files. Some of the old function files have survived into the master version as subfunctions. In total, it is probably not much more code in the final version than it was in the project version; the difference is that more is done using less code. Descriptions of all the script files and subfunctions are now given to illustrate how the program works and how the data is processed. For further details, the reader is advised to refer appendix D.
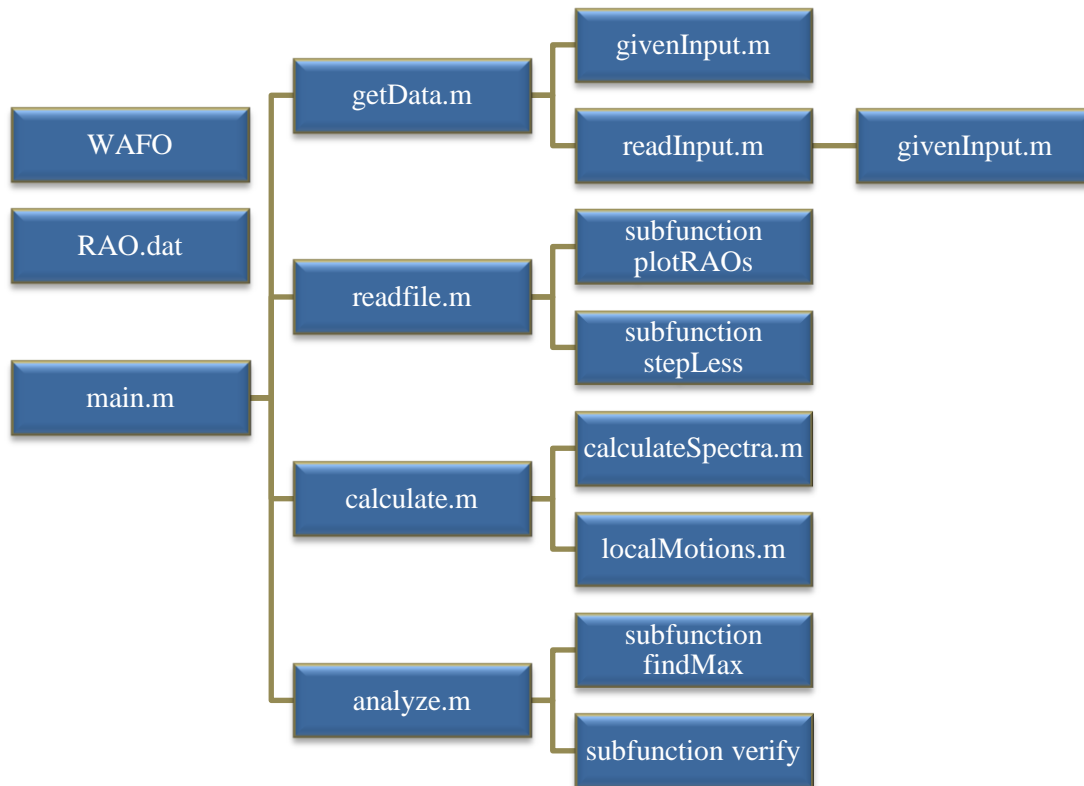
Figure 5.7 - Flow chart

5.4.1 main.m

This is the main file which starts the whole process. It starts by including the WAFO packet (27) for later calculating the wave spectra. Furthermore, it specifies the name of the RAO-file to be used in the *infile* variable, and finally it calls the four subroutines *getData, readFile, calculate* and *analyze*.

5.4.2 getData.m

This is the subroutine which provides the main file with all the user-provided input, and it prints out the welcome screen to the user, as shown in Figure 5.8. It calls on two functions of its own, namely *readInput* and *givenInput*. It gets the default input data from *givenInput* and then it enters a loop prompting the user whether he would like to change the data. In this loop all the default data is printed out to screen, together with some angles which are calculated,

such as Theta, Phi and the attack angle of the wave on the ship α. If the user chooses to alter the default input, he gets a choice between which categories of data he wants to change. This information is then passed on to *readInput*.

Figure 5.8 - Welcome screen

5.4.3 readInput.m

In this function the user can provide whichever input data he wants by typing it at request of the program. First it calls the *givenInput* function to provide basic data which the user then alters all of or part of. The four categories which the data is divided into, is sea data, coordinate system of vessel, considered points and criteria.

5.4.4 givenInput.m

This is actually a data file disguised as a function. For simplicity the default data is stored in this subroutine, which is really nothing more than a list of input variables. The variables are clearly marked with comments to make it easier for the user to understand in case he opens it.

5.4.5 readFile.m

ReadFile is the function that provides the main file with the relevant transfer functions. It gets information on filename, what wave heading to look at, if short crested waves shall be considered, and the corresponding spreading parameter. It calls two subfunctions *plotRAOs* and *stepLess*. *plotRAOs* gives various plots of the RAO's. Since the RAO-file gives transfer functions for every 15 degrees, there is a need to calculate the transfer function for an exact heading. The subfunction *stepLess* takes an exact heading and calculates a transfer function by interpolating the two neighboring transfer functions.

Since the transfer functions are only defined between 0 and 180 degrees, the program must generate the other half. See Figure 6.9. For surge, heave and pitch, the transfer functions are the same regardless of which side of the vessel the wave comes from, so generating the rest of the transfer functions is trivial. For sway, roll and yaw on the other hand, the magnitude of the transfer functions must be inverted to get the right result.

Figure 5.9 - Transfer functions given for one side of the vessel

If long-crested waves are being used, the correct transfer function is easily found from the *stepLess* subfunction, but if short-crested waves are used, the RAO is harder to find. Recall from section 4.4 that a short-crested wave spectrum is found by multiplying a long-crested wave spectrum with a directional distribution. We must therefore include this distribution in our calculations. We can do this by integrating the product of the directional distribution and the transfer function over a sector of π, thus creating a mean transfer function. This can be expressed by:

$$\bar{H}(\omega) = \int_{-\pi/2}^{\pi/2} H(\omega, \vartheta) D(\vartheta) \, d\vartheta \qquad (5.9)$$

This transfer function thus represents the short-crested wave distribution on the vessel. Finally, the function *plotRAOs* is called six times to plot the magnitudes and phases of different transfer functions for different attack angles. Then the six relevant transfer functions, or possibly the six short-crested transfer functions, are plotted.

5.4.6 calculate.m

This subroutine uses the correct transfer functions, the relevant geometry and the key sea parameters to calculate the relevant spectra. It calls two functions *calculateSpectra* and *localMotions*. Before calling these, it also calls WAFO to provide either a JONSWAP or a Torsethaugen sea spectrum, and then plots this. In case a JONSWAP-spectrum is chosen, the

so-called JONSWAP-range is used. This means that the T_p-value must be within certain limits, as given by eq. (4.24). Similarly, if the Torsethaugen-spectrum is chosen, H_s and T_p should be within certain limits. In the WAFO-scripts these are given by:

$$H_s \leq 11$$

$$H_s \leq \left(T_p/3.6\right)^2 \qquad (5.10)$$

$$H_s \leq \left(T_p - 2\right)\frac{12}{11}$$

Note that the second limit corresponds to the JONSWAP-range. Moreover, the significant wave height is only limited upwards, i.e. a Torsethaugen spectrum can be made for whichever low wave heights. The peak period is limited by:

$$3 \leq T_p \leq 20 \qquad (5.11)$$

If these limits are exceeded, a warning message is printed out, informing the user that the limits are exceeded and the results may be inaccurate.

When the subroutine is done generating the wave spectrum, it calls on the two functions to provide all the correlation spectra for the six degrees of freedom, along with the local motion spectra for the vessel. Finally it uses this data to calculate the "Theta-spectrum" in the xy-plane, and in turn the "Phi-spectrum", which is the total motion spectrum along the straight line between the points.

5.4.7 calculateSpectra.m

This function takes the relevant transfer functions for all six degrees of freedom and combines them to make all the cross-correlation transfer function. The expressions for these can be found in eq. (4.61). A matrix is filled with these, as shown in Figure 6.10, and then all the diagonals are substituted for the auto-correlation transfer functions. When this is done, all the corresponding cross-correlation and autocorrelation spectra are put in a similar matrix and returned to *calculate.m*.

$$\begin{bmatrix} H_{11} & H_{12} & H_{13} & H_{14} & H_{15} & H_{16} \\ H_{21} & H_{22} & H_{23} & H_{24} & H_{25} & H_{26} \\ H_{31} & H_{32} & H_{33} & H_{34} & H_{35} & H_{36} \\ H_{41} & H_{42} & H_{43} & H_{44} & H_{45} & H_{46} \\ H_{51} & H_{52} & H_{53} & H_{54} & H_{55} & H_{56} \\ H_{61} & H_{62} & H_{63} & H_{64} & H_{65} & H_{66} \end{bmatrix}$$

Figure 5.10 - Matrix of cross-correlation and autocorrelation transfer functions

5.4.8   localMotions.m

With the matrix containing all the correlations between the different degrees of freedom, the local motions of the vessel is quite easily calculated. After calculating all the local motions for the given point, the function makes two plots; one of the local motions in x-, y- and z-direction together with the sea spectrum, and one with the spectra for each of the six degrees of freedom.

5.4.9   analyze.m

This function analyzes the spectra which have been obtain by using the two subfunctions *findMax* and *verify*. First it finds the spectra for velocity and acceleration by differentiating as discussed in section 4.5.4. This is done for each of the three axes for local motions, as well as for the total motion spectrum along the straight line between the points. Then the expected maxima for each of these spectra are found through the subfunction *findMax,* using eq. (4.85). Then the total distances are calculated, and the program checks if the obtained results are acceptable according to the given criteria, using the subfunction *verify*. Finally, it prints out to screen the relevant results in a table.

5.5   Using the program

To sum up, Relative Motion Calculator is a fairly simple tool for assessing motions on a point on a vessel relative to another point which is fixed. The emphasis has been put on establishing a geometrical model which represents a real physical problem, and making this as general as possible through having as many arbitrary input values as possible. Furthermore, the main target has been establishing the correct equations to provide correct results in any situation. An important point is that for the program to function, a version of MATLAB must be installed on the computer, and the program must lie in the working directory along with a valid RAO-file and the WAFO toolbox.

The program itself is made up of several subroutines and subfunctions, to provide a systematic and flexible buildup of the program. This has been done to give a platform on which further programming can be done, extending the program to include more functions and options. The biggest weakness of the program is the lack of any GUI (Graphical User Interface) which would be very helpful when creating the geometrical situation to be examined. To compensate for this, the user is advised to use a sketch or a 3D-model to aid him when creating the geometry. In general, the user interface in the program is quite cumbersome, and there is much room for enhancement in this field. The user interface is based on the program inquiring the user for input data each time, without any options of saving values or geometries. This is time-consuming, and can be seen as a sort of emergency solution for a user interface.

However, there is a much better way to use the program for analyses, but it requires some basic knowledge of MATLAB programming for the user to be comfortable. That being said, it is very simple. The m-file *givenInput.m* is the script which provides all the "default-data" which is printed out to the welcome screen. The user can manually open this file and provide any data he likes, and the variables in the file are clearly marked. The user needs to be aware of the valid ranges of sea data when altering the input data, and should be careful not to change anything in the script to cause malfunction of the program. When the data has been changed, the program can be run using the default data, and choosing "n" when prompted if the default data should be changed. Additionally, this prompt can be turned off by "commenting out" line 128 in the script file *getData.m*, using the character *%* in front of the line.

The program uses the WAFO-toolbox to generate the sea spectra, and this is a 128 MB packet which must lie in the same directory as the rest of the script files for the program to function. The version used is WAFO 2.5; it is shareware and can be downloaded from http://code.google.com/p/wafo/ (27). In case the WAFO-toolbox should be unavailable, a short script file *spectrum.m* has been provided which creates a JONSWAP spectrum. To use this spectrum, two actions must be taken. First, "comment out" line 10 in *main.m*, which initiates the WAFO toolbox. Then, on line 11 in *calculate.m*, change the variable *WAFO* from *true* to *false*. Now, the program functions as normal, but without the option of using the Torsethaugen two-peaked wave spectrum.

6   Results

6.1   Introduction

Once the program is finished and has the required features, it is necessary to expose it to tests and parameter studies. The tests are performed and carefully documented to assure potential future users that the output from the program is indeed trustworthy. The parameter studies are done to investigate what effect the different input parameters had on the output. The results from the parameter studies are good for discussing features of some marine operations, and running the program many times makes it more reliable.

6.1.1   Crane mode and boarding mode

Before executing the tests and studies, it was useful to define two modes on which the following studies were based. These two modes are based on real marine operations connected to offshore wind turbines, which have been investigated earlier in this report, ref. chapter 2. One mode is based on a crane operation, henceforth referred to as the *crane mode*, while the other mode is based on a boarding operation, henceforth referred to as the *boarding mode*. Both modes are illustrated with measures in Figure 7.1 and Figure 7.2. Sketches where the coordinate systems are shown more clearly are provided in Figure 7.4 and Figure 7.3. In these pictures the x-axes are defined as red, the y-axes are green and the z-axes are blue.

These modes are defined by the local vessel's location and heading and the placements of the considered points on the vessel and the fixed turbine. In these modes we assume that the vessel examined has the dimensions of the reference vessel described in section 2.2. The coordinates of the modes are given schematically in Table 6.1. Even though these modes are used while testing and performing parameter studies, it should be pointed out that the user is free to examine whichever coordinates he chooses, and the program is in no way locked to these two modes. Note that in boarding mode, the two considered points coincide, so this mode is mainly used for assessing local vessel motions. For crane mode, the two points are placed in the same horizontal plane, and this mode is more used for assessing total point motions along a direction.

Table 6.1 - Crane mode and boarding mode

Boarding mode	x	y	z
vessel (origin)	-20.50	0	0
bow tip (local cs)	17.5	0	2.5
platform	-3	0	2.5
Vessel heading: 0 deg			

Crane mode	x	y	z
vessel (origin)	8	18.50	0
crane tip (local cs)	-8	-13	23
platform	0	2.5	17.1
Vessel heading: 0 deg			
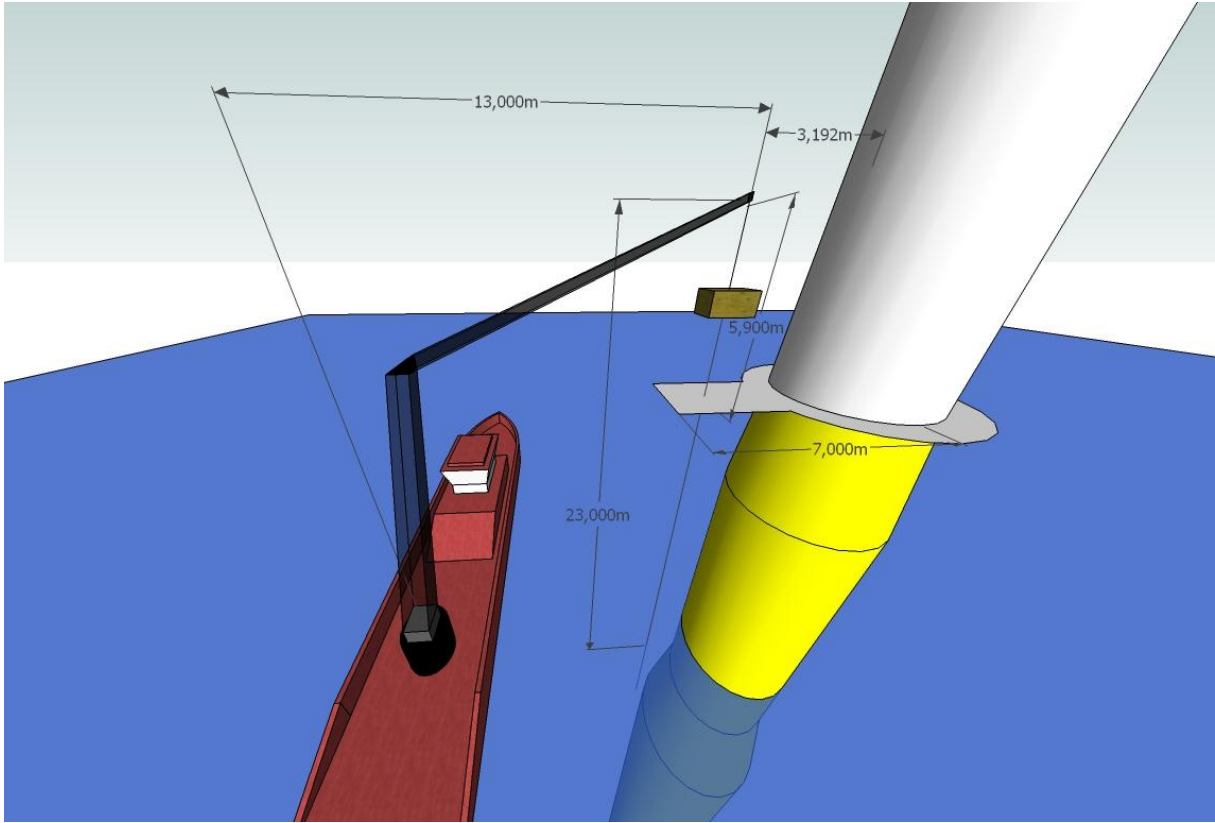
Figure 6.1 - Crane mode
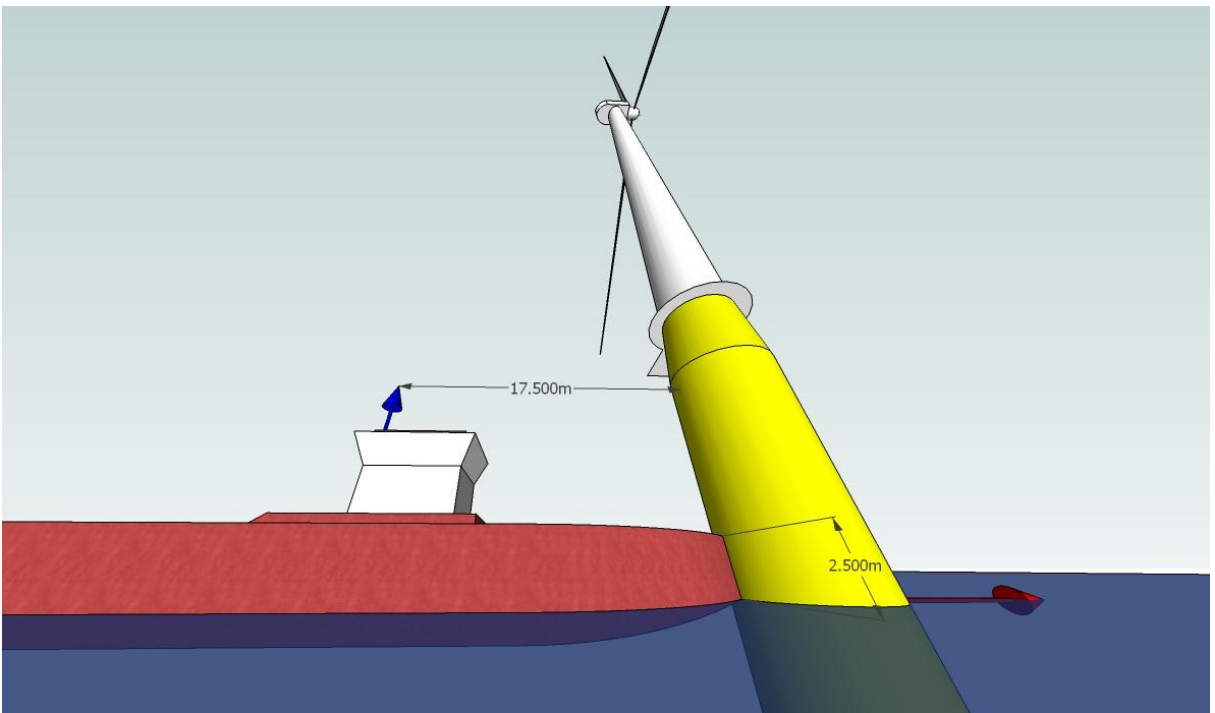
Figure 6.2 - Boarding mode
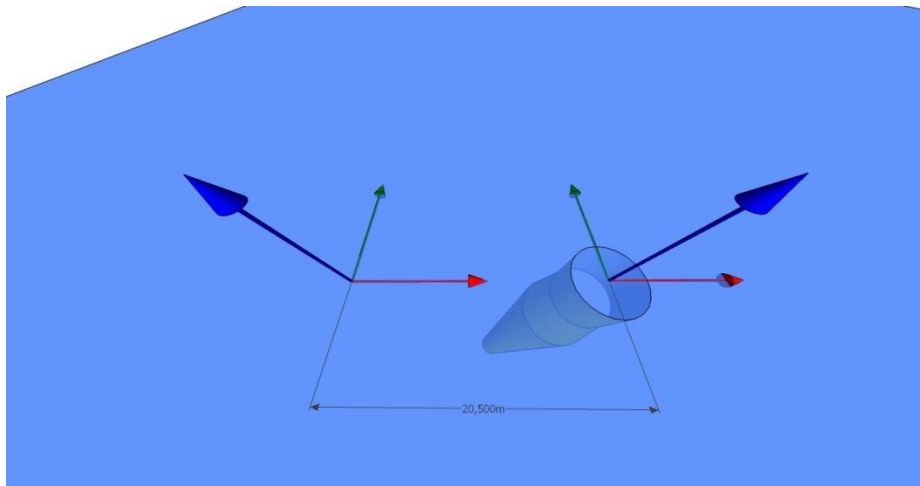
Figure 6.3 - Coordinate systems in boarding mode
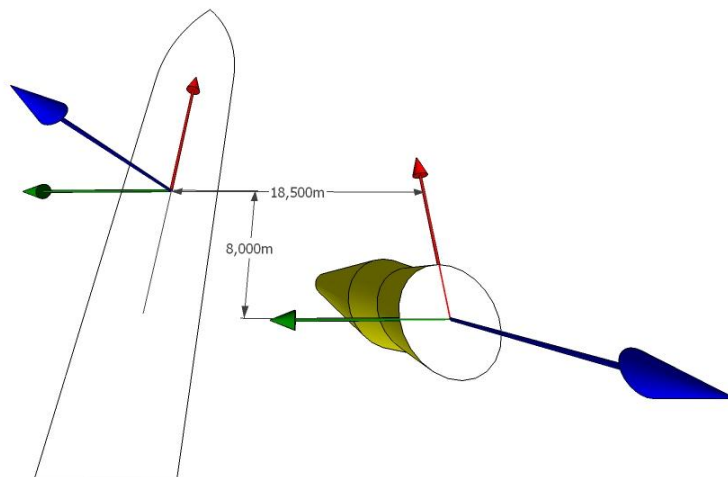
Figure 6.4 - Coordinate systems in crane mode

6.2   Testing

For the program to be useful it obviously needs to provide the correct results according to the assumptions that have been made. To make sure this is the case, it is important to perform thorough tests and carefully assessing the results. In this thesis this is done partly by comparing the results from the master version RMC 2.3 to the results from the project version RMC 1.2, and partly by critically interpreting the results through isolating each degree of freedom and comparing phase angles and magnitudes.

6.2.1   Direct comparison between RMC 1.2 and RMC 2.3

As described in section 5.3.2, RMC 1.2 is a simplified situation in which we have the vessel in a fixed position and with fixed heading, and where the wave attack angle is 90 degrees on the vessel. This model only considers the three most relevant degrees of freedom, namely sway, heave and roll, and it can be regarded as a 2D-problem in the yz-plane. This can be compared directly to RMC 2.3 by reducing the degrees of freedom to three, setting surge, pitch and yaw to zero. By examining the motion in the origin of the vessel the roll rotation can be overlooked, thus further reducing the number of freedom degrees to two, namely sway and heave. To imitate the project model, the vessel heading is set to 0˚, and the wave heading to 90˚ i.e. propagating along the positive y-axis.

For the testing, RMC 1.2 was modified somewhat, for example it was adjusted to include the WAFO-toolbox to base the comparison on identical wave spectra. Also, these tests are performed using an old RAO from the project version of the program which has limited frequency range. These numbers should not be directly compared to the studies which are done later on with an RAO with extended frequency range. The short RAO is only used in the direct comparison between RMC 1.2 and RMC 2.3, and the initial tests of RMC 2.3 with different numbers of degrees of freedom. For the test runs, the significant wave height was set to 2 meters, and three peak periods within the JONSWAP-range were examined. The duration was set to 3 hours, and long-crested wave theory was used. The results for the point (0,0,0) on the vessel, i.e. for two degrees of freedom, are given in Table 6.2.

Table 6.2 - Direct comparison, 2 degrees of freedom

Version used: RMC 1.2 2 dof (sway, heave), in the point (0,0,0)				Version used: RMC 2.3, long crested 2 dof (sway, heave), in the point (0,0,0) Surge, pitch and yaw = 0			
Tp	5.1	6.1	7	Tp	5.1	6.1	7
y-direction				**y-direction**			
max motion	3.03	3.28	3.45	max motion	3.03	3.28	3.45
velocity	3.76	3.59	3.5	velocity	3.76	3.59	3.5
acceleration	4.75	4.15	3.86	acceleration	4.75	4.15	3.86
z-direction				**z-direction**			
max motion	3.49	3.59	3.69	max motion	3.49	3.59	3.69
velocity	4.37	4.02	3.85	velocity	4.37	4.02	3.85
acceleration	5.58	4.75	4.37	acceleration	5.58	4.75	4.37
min combined distance	18.8	18.6	18.4	min combined distance	21.8	21.6	21.4
max wave height	3.64	3.69	3.77	max wave height	3.64	3.69	3.77

We see that the numbers match exactly, which looks promising. The minimum combined distance is calculated in RMC 1.2 simply by Pythagoras, i.e. by assuming that maxima for motions in y- and z-directions could occur at the same time. In RMC 2.3 the phase angles are

taken into consideration when this distance is calculated. The difference is, as we see, significant.

The test was then run again, with the exact same settings, but changing the considered point on the vessel to the original "mode positions". The roll rotation is thus included, increasing the system to three degrees of freedom. The test was run for both modes, and the results are given in Table 6.3. The numbers still match, except for the minimum distance, obviously. With these exactly matching numbers, it is obvious that the equations used in RMC 2.3 are identical to those in RMC 1.2, at least for the degrees of freedom investigated. If we assume that RMC 1.2, which is based on fairly simple equations and derivations, is correct, then these matching numbers imply that also RMC 2.3 is correct for these degrees of freedom. Furthermore, the numbers seem reasonable in magnitude, so we can conclude that so far, the program yields correct results. For the other degrees of freedom, namely surge, pitch and yaw, we cannot validate the results against anything directly, so we need to analyze these in more detail.

Table 6.3 - Direct comparison, 3 degrees of freedom

Version used: RMC 1.2	Version used: RMC 2.3, long crested
3 dof (sway, heave, roll)	3 dof (sway, heave, roll).
	Surge, pitch and yaw = 0

Crane mode

Tp	5.1	6.1	7	Tp	5.1	6.1	7
y-direction				**y-direction**			
max motion	2.76	2.25	2.01	max motion	2.76	2.25	2.01
velocity	3.58	2.83	2.52	velocity	3.58	2.83	2.52
acceleration	4.73	3.7	3.3	acceleration	4.73	3.7	3.3
z-direction				**z-direction**			
max motion	4.53	4.55	4.59	max motion	4.53	4.55	4.59
velocity	5.67	5.13	4.85	velocity	5.67	5.13	4.85
acceleration	7.23	6.08	5.56	acceleration	7.23	6.08	5.56
min combined distance	1.32	1.54	1.61	min combined distance	1.71	1.9	2
max wave height	3.64	3.69	3.77	max wave height	3.64	3.69	3.77

Boarding mode

Tp	5.1	6.1	7	Tp	5.1	6.1	7
y-direction				**y-direction**			
max motion	2.41	2.71	2.91	max motion	2.41	2.71	2.91
velocity	2.97	2.93	2.89	velocity	2.97	2.93	2.89
acceleration	3.74	3.33	3.12	acceleration	3.74	3.33	3.12
z-direction				**z-direction**			
max motion	3.49	3.59	3.69	max motion	3.49	3.59	3.69
velocity	4.37	4.02	3.85	velocity	4.37	4.02	3.85
acceleration	5.58	4.75	4.37	acceleration	5.58	4.75	4.37
max wave height	3.64	3.69	3.77	max wave height	3.64	3.69	3.77

6.2.2   From 3 to 6 degrees of freedom

As we have seen, RMC 1.2 has come in handy in validating results from RMC 2.3, but at this point we will not have to use the simplified version any more. Next, we will extend the program's degrees of freedom to six as is originally intended, and continue to assess the output critically. From here on out, surge, pitch and yaw are thus included in the results. For the current situation with beam sea however, yaw is the dominant of these three motions, as we will see. But before we look at yaw, we will run a test with RMC 2.3 with all degrees of freedom, using (0,0,0) as the considered point, to once again isolate the translations. The results are shown against RMC 1.2 for the same considered point, in Table 6.4. The difference here should thus be the surge motion which is no longer zero.

Table 6.4 - Direct comparison, 3 translations vs. 2 translations

Version used: RMC 2.3, long crested
3 dof, translations in the point (0,0,0)

Version used: RMC 1.2
2 dof (sway, heave), in the point (0,0,0)

Tp	5.1	6.1	7
x-direction			
max motion	0.08	0.07	0.06
velocity	0.11	0.09	0.08
acceleration	0.14	0.11	0.1
y-direction			
max motion	3.03	3.28	3.45
velocity	3.76	3.59	3.5
acceleration	4.75	4.15	3.86
z-direction			
max motion	3.49	3.59	3.69
velocity	4.37	4.02	3.85
acceleration	5.58	4.75	4.37
max wave height	3.64	3.69	3.77

Tp	5.1	6.1	7
x-direction			
max motion	0	0	0
velocity	0	0	0
acceleration	0	0	0
y-direction			
max motion	3.03	3.28	3.45
velocity	3.76	3.59	3.5
acceleration	4.75	4.15	3.86
z-direction			
max motion	3.49	3.59	3.69
velocity	4.37	4.02	3.85
acceleration	5.58	4.75	4.37
max wave height	3.64	3.69	3.77

We see that the numbers still match exactly, even with all six degrees of freedom activated. The only difference in the numbers is the motion along local x-direction, which in this case is only cause by the surge motion. As we would expect for beam sea, this motion is very small. This implies that the program still gives correct results with all degrees of freedom activated, at least when only the translations are considered.

6.2.2.1 Boarding mode

To include the rotations in our discussions, we can start by doing a test for boarding mode, with the considered point on the tip of the bow. The result from this is given along with the

corresponding test for the version where surge, pitch and yaw were removed, in Table 6.5. Now we see some quite interesting results. Motions in x- and z-directions are not very different on the right hand side, but for y-direction we get completely different numbers. To explain this, let us review Faltinsen's equation of motion for a floating body. It is provided once more for simplicity, in eq. (6.1):

$$\boldsymbol{s} = \left(\eta_1 + z_p\eta_5 - y_p\eta_6\right)\boldsymbol{i} + \left(\eta_2 - z_p\eta_4 + x_p\eta_6\right)\boldsymbol{j} \\ + \left(\eta_3 + y_p\eta_4 - x_p\eta_5\right)\boldsymbol{k}$$

(6.1)

Table 6.5 - Boarding mode - 3 vs. 6 degrees of freedom

Version used: RMC 2.3, long crested
3 dof (sway, heave, roll).

Surge, pitch and yaw = 0

Version used: RMC 2.3, long crested
6 dof

Boarding mode

Tp	5.1	6.1	7
x-direction			
max motion	0	0	0
Velocity	0	0	0
acceleration	0	0	0
y-direction			
max motion	2.41	2.71	2.91
Velocity	2.97	2.93	2.89
acceleration	3.74	3.33	3.12
z-direction			
max motion	3.49	3.59	3.69
Velocity	4.37	4.02	3.85
acceleration	5.58	4.75	4.37
max wave height	3.64	3.69	3.77

Tp	5.1	6.1	7
x-direction			
max motion	0.04	0.04	0.03
velocity	0.06	0.04	0.04
acceleration	0.07	0.06	0.05
y-direction			
max motion	0.87	0.86	0.87
velocity	1.09	0.98	0.93
acceleration	1.41	1.18	1.08
z-direction			
max motion	3.77	3.8	3.88
velocity	4.73	4.29	4.09
acceleration	6.07	5.12	4.7
max wave height	3.64	3.69	3.77

We see that the first term, representing motion in x-direction, depends on surge, pitch and yaw. The first two are marginal in magnitude for beam sea, while yaw is negligible when the y-coordinate is zero, as it is in boarding mode, ref. Table 6.1. Thus the small motion in x-direction is as expected. Motion spectra for all degrees of freedom are given in Figure 7.5, and these are produced from the transfer functions and the relevant wave spectrum. It must be noted that the orders of magnitude of the three translations are different from those of the rotations. For the second term, which represents motion in y-direction, sway, roll and yaw are governing degrees of freedom. Since sway and roll are already considered, the difference must be from the yaw motion. We note that x_p is rather large since we look at motion in the bow of the vessel. The third term represents the motion in z-direction, and since the y-coordinate is zero and heave is already accounted for, the difference must come from the pitch motion. From the motion spectra we get the impression that the magnitude of the pitch motion

is very small, but since we look at motion as far ahead as in the bow tip, the pitch motion can be small and still have an impact on the point motion in z-direction.

Let us examine the phase angles for the transfer functions for pitch together with that of heave. The magnitudes and phases of the transfer functions are plotted together in Figure 6.6. We see that the magnitude of the pitch motion is almost zero, while the heave motion is stable at around 1. If we look at the phases, we see that
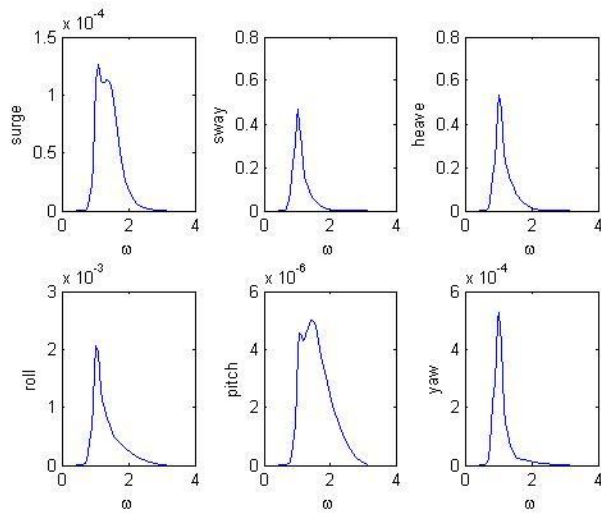
Figure 6.5 - Response spectra for all six degrees of freedom

heave is at about 0˚, while pitch lies around ±180˚, meaning they are in anti-phase to each other. This means that the maximum value of the pitch motion occurs at the same time as the minimum value of the heave motion and vice versa. Furthermore, from the definition of positive direction for the pitch motion, the bow points down when the pitch motion is at its maximum. Thus, the bow points up when the pitch motion reaches its minimum, which occurs at the same time as the heave motion reaches its maximum. We can thus draw the conclusion that the maximum point motion in z-direction should be slightly higher when pitch is included, which fits well with the numbers observed in Table 6.5.
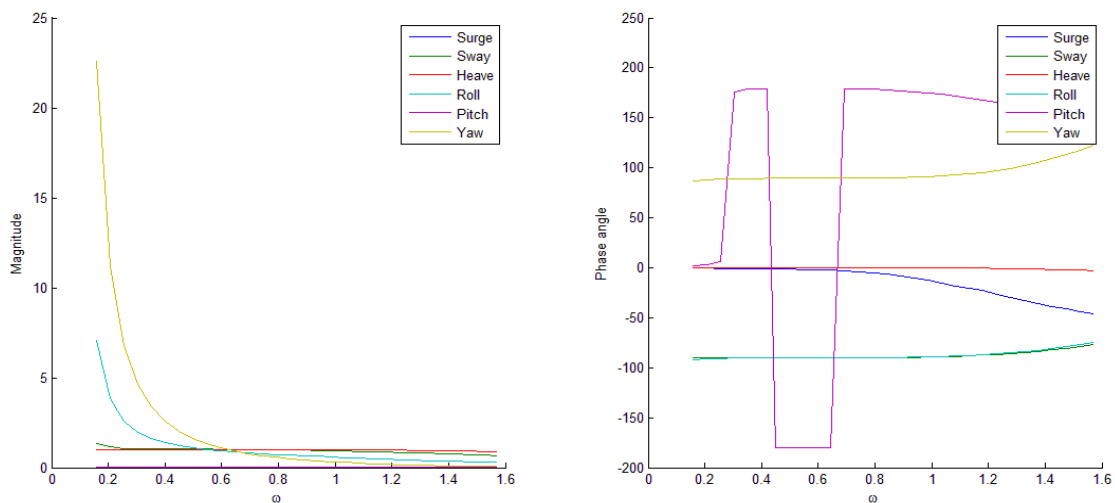
Figure 6.6 - Magnitudes and phase angles for all transfer functions for a 90˚ attack angle

If we go back to considering the point motion in y-direction, we see a difference of over 2 meters expected maximum motion for a peak period of 7 seconds, ref. Table 6.5. Since this difference must come from the yaw motion alone, it must mean that the yaw motion

counteracts the sway/roll motions. Let us examine if this is the case. If we compare the maximum point motion in y-direction on the left hand side in Table 6.5 to the numbers in Table 6.2, we see that the maximum for sway motion alone is actually larger than for sway and roll motion combined, implying that the roll motion counteracts the sway motion slightly. It is thus reasonable to believe that the maximum point motion occurs when the sway motion has its maximum. Thus we need to compare the transfer functions for sway and yaw.

First we note that the magnitude of the yaw motion is much larger than the one for pitch motion, as is implied in Figure 6.6, and we therefore expect larger effect than we saw from the pitch motion. When we look at the phase angles on the right hand side of Figure 6.6, we see that the phase angle for yaw lies around 90˚, while for sway it is about -90˚, which means that also these are in anti-phase to each other. Thus, the maximum of the sway motion occurs simultaneously to the minimum of the yaw motion and vice versa. Because the sway motion is positive along the positive y-axis and the yaw motion is positive according to the right-hand rule, we can conclude that these motions counteract each other exactly. The small numbers on the right hand side of Table 6.5 are therefore reasonable.

6.2.2.2 Crane mode

We proceed with comparing the test run with RMC 2.3 with surge, pitch and yaw set to zero, to RMC 2.3 with all degrees of freedom included, for crane mode. This case is a bit more complex, because the considered point has all three coordinates different from zero, so all rotations do make an impact on the point motion. The coordinates for crane mode are given along with those for boarding mode, in Table 6.1. Compared to boarding mode, which has been discussed so far, we see that the x-coordinate is negative instead of positive, so the effects of both yaw on motion in y-direction, and pitch on motion in z-direction, become reversed, ref. eq. (6.1). Furthermore, the y-coordinate is no longer zero, so yaw has a significant influence on motion in x-direction, as does roll on motion in z-direction. Finally, the z-coordinate is very large, but still positive, so the argument regarding the effect of roll on motion in y-direction is still valid, although amplified. The effect of pitch on motion in x-direction is not negligible, although the magnitude of pitch motion is small. The results from the test for crane mode are given in Table 6.6.

Let us investigate the phase angles once more, as given on the right hand side of Figure 6.6. We start with motion in x-direction, and ignore the small surge motion. From the equation of motion, we then have this motion given by yaw and pitch. We see from the phase angles that these two degrees of freedom are about 90˚ out of phase to each other, which signifies that one is in neutral position when the other one is at its maximum. We can therefore conclude that the expected maximum for motion in x-direction is given by the expected maximum of only one of these degrees of freedom. Recalling that the magnitude of the pitch motion is very small, we can say that the yaw motion produces the expected maximum for motion in x-direction.

If we go back to Table 6.4, which considers only translations, and compare it to Table 6.3, where roll is included, we find that the point motion in y-direction is actually larger for boarding mode than for crane mode, even though the z-coordinate is much larger for crane mode. At first this seems contradictory, but if we analyze it a bit more thoroughly, we find the explanation. If we consider the results for $T_p = 5.1$, we see that the expected maximum for

Table 6.6 - Crane mode - 3 vs. 6 degrees of freedom

Version used: RMC 2.3, long crested
3 dof (sway, heave, roll).
Surge, pitch and yaw = 0

Version used: RMC 2.3, long crested
6 dof

Crane mode

Tp	5.1	6.1	7	Tp	5.1	6.1	7
x-direction				**x-direction**			
max motion	0	0	0	max motion	1.31	1.47	1.59
velocity	0	0	0	velocity	1.62	1.6	1.58
acceleration	0	0	0	acceleration	2.06	1.84	1.73
y-direction				**y-direction**			
max motion	2.76	2.25	2.01	max motion	2.09	1.61	1.51
velocity	3.58	2.83	2.52	velocity	2.76	2.12	1.92
acceleration	4.73	3.7	3.3	acceleration	3.7	2.87	2.57
z-direction				**z-direction**			
max motion	4.53	4.55	4.59	max motion	4.47	4.5	4.54
velocity	5.67	5.13	4.85	velocity	5.59	5.07	4.8
acceleration	7.23	6.08	5.56	acceleration	7.13	6.01	5.5
min combined distance	1.71	1.9	2	min combined distance	1.97	2.19	2.29
max wave height	3.64	3.69	3.77	max wave height	3.64	3.69	3.77

sway only equals 3.03 meters, while for motion including roll, we have an expected maximum of 2.41 meters. The effect of roll is thus about 0.6 meters negatively. Since the z-coordinate for crane mode is almost ten times larger than that for boarding mode, we can expect an effect from roll about ten times more than that from the boarding mode. Thus, the roll effect on the point motion is almost six meters, counteracting the sway motion. So the expected maximum occurs when the roll motion is at its maximum, and the sway is at its minimum, i.e. on the opposite phase from the maximum for boarding mode. The roll motion becomes the dominant term for a z-coordinate of such a large size, and the result is an expected maximum of 2.76 meters as seen in the table. Returning to Table 6.6, we see that the right hand side which includes the yaw motion gives a slightly smaller expected maximum for motion in y-direction. Recall that from our test for boarding mode, we concluded that the yaw motion counteracted the sway motion. In the present case, our considered point lies closer to the aft of the vessel, thus the x-coordinate changes sign. The result is an opposite effect from the boarding mode case, i.e. the yaw motion works in phase with the sway motion. Thus, both of

these degrees of freedom work against the large roll-effect, making the total point motion in y-direction somewhat smaller, as the numbers show. Finally, the only difference for the motion in z-direction is the pitch motion, ref. eq. (6.1). Because the magnitude is so small for pitch, the expected total point motion in z-direction changes only very slightly from the left hand side to the right hand side of Table 6.6.

Having performed these tests, compared RMC 2.3 to RMC 1.2, isolated degrees of freedom and finally carefully investigated the phase angles of the RAOs, we can at last conclude that at least the basic equations describing the local motions of the vessel work as they should. We also have an indication that the total motion spectrum between points works satisfactory from Table 6.2 and Table 6.3, although this will be examined further. Assuming all these reasonable numbers are indeed not merely coincidences, and confirm that our program works well at this point. The next steps will be to perform parameter studies where different input parameters will be adjusted, and the corresponding output will be interpreted in a critical manner.

As a general remark, we see that the derivatives of the motion, i.e. the velocities and accelerations, are larger for small peak periods than for large ones. That is intuitive to anyone who has been on a boat and experienced "choppy" seas, i.e. short, steep waves. Quicker motions cause larger forces, everything becomes difficult to do, and it becomes more uncomfortable to be on board. Needless to say, these conditions would not be favorable when performing marine operations. This aspect will be kept in mind in later parameter studies.

6.3 Parameter studies

We have thus come to the conclusion that our program works well for predicting the local motions of the vessel, and no more detailed investigations of phase angles will be performed. However, results from the parameter studies will be assessed critically and related to the magnitudes of different degrees of freedom and to our experiences from the validation tests which we have just finished. The aim of these parameter studies is to examine whether the different features of the program works as intended, and to see what effect the different parameters have on the expected maximum motions. We will continue using the two established modes (crane and boarding), although not exclusively, throughout these studies.

6.3.1 Attack angles

The first parameter we investigate is the wave heading relative to the vessel heading, i.e. the attack angle α as described in section 5.3.3.2. The focus will still be on the local motions of the ship, so the vessel heading is kept fixed at 0˚ while the wave propagation heading is varied. We will look at both modes, and the boarding mode will make it easier to critically assess the results than the crane mode, as this is still kept in mind. However, we have concluded that the program gives correct result for a given set of RAOs, so if the RAOs vary correctly, we should expect correct results still. As an example, a plot of how the magnitude

64
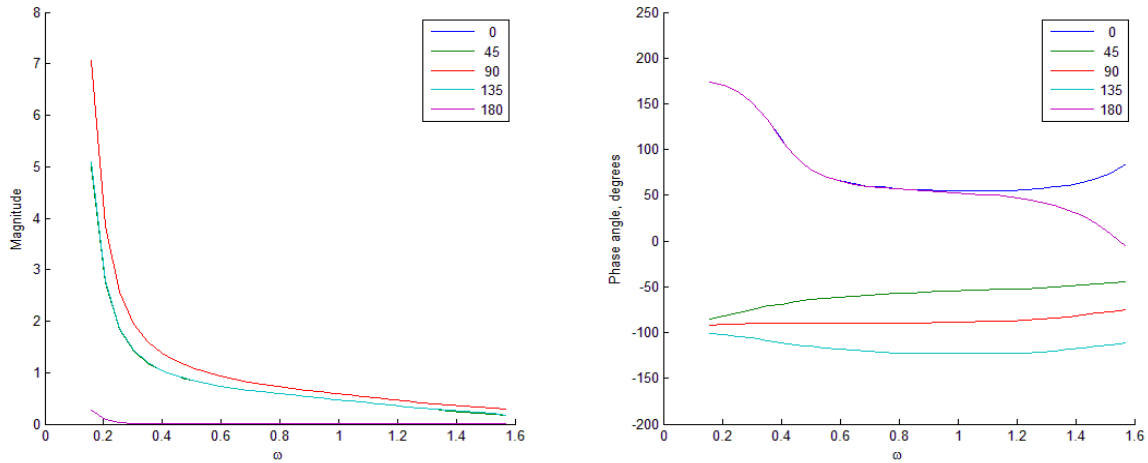
Figure 6.7 - Magnitudes and phase angles for the transfer functions for roll for different wave attack angles

and phase angle of the RAO for roll changes with different attack angles is given in Figure 7.7. We see that it behaves as we would expect, with the magnitude being largest for beam sea, i.e. the attack angle is 90˚. Then it becomes smaller when the attack angle shifts towards the aft or bow, until it almost disappears for head and following sea.

Table 6.7 - Effect of different attack angles

Wave heading: 90 deg		Wave heading: 45 deg		Wave heading: 135 deg		Wave heading: 0 deg		Wave heading: 180 deg	
Crane mode									
x-direction		**x-direction**		**x-direction**		**x-direction**		**x-direction**	
max motion	1.61	max motion	6.64	max motion	7.89	max motion	3.96	max motion	3.96
velocity	2.07	velocity	9.75	velocity	11.54	velocity	5.85	velocity	5.84
acceleration	3.34	acceleration	17.3	acceleration	20.41	acceleration	10.38	acceleration	10.32
y-direction		**y-direction**		**y-direction**		**y-direction**		**y-direction**	
max motion	2.58	max motion	2.31	max motion	2.3	max motion	0.02	max motion	0.02
velocity	4.69	velocity	3.64	velocity	3.64	velocity	0.02	velocity	0.02
acceleration	9.63	acceleration	6.8	acceleration	6.79	acceleration	0.03	acceleration	0.03
z-direction		**z-direction**		**z-direction**		**z-direction**		**z-direction**	
max motion	4.86	max motion	4.34	max motion	4.37	max motion	3.24	max motion	3.22
velocity	6.22	velocity	5.13	velocity	5.88	velocity	3.69	velocity	3.79
acceleration	9.59	acceleration	7.05	acceleration	9.73	acceleration	4.95	acceleration	5.35
min comb distance	1.56	min comb distance	3.28	min comb distance	1.89	min comb distance	3.72	min comb distance	3.75
max wave height	4.06	max wave height	4.06	max wave height	4.06	max wave height	4.06	max wave height	4.06
Boarding mode									
x-direction		**x-direction**		**x-direction**		**x-direction**		**x-direction**	
max motion	0.04	max motion	1.99	max motion	2.02	max motion	2.4	max motion	2.42
velocity	0.06	velocity	2.17	velocity	2.2	velocity	2.48	velocity	2.5
acceleration	0.09	acceleration	2.54	acceleration	2.59	acceleration	2.7	acceleration	2.73
y-direction		**y-direction**		**y-direction**		**y-direction**		**y-direction**	
max motion	0.92	max motion	7.91	max motion	8	max motion	0.04	max motion	0.03
velocity	1.18	velocity	10.8	velocity	10.92	velocity	0.04	velocity	0.04
acceleration	1.89	acceleration	17.9	acceleration	18.05	acceleration	0.06	acceleration	0.06
z-direction		**z-direction**		**z-direction**		**z-direction**		**z-direction**	
max motion	4.05	max motion	5.5	max motion	5.87	max motion	5.95	max motion	5.93
velocity	5	velocity	7.31	velocity	7.93	velocity	7.48	velocity	7.27
acceleration	7.12	acceleration	11.85	acceleration	12.97	acceleration	11.29	acceleration	10.66
max wave height	4.06	max wave height	4.06	max wave height	4.06	max wave height	4.06	max wave height	4.06

Furthermore, we will keep other parameters fixed; Significant wave height is 2 meters, sea state duration is 3 hours, a JONSWAP spectrum is used, only long-crested wave theory is considered, and only one peak period at 6.1 seconds is used. Five attack angles are then examined, namely 0˚, 45˚, 90˚, 135˚ and 180˚. The results are given in Table 6.7.

The reason the results for α=90˚ is not directly comparable to the ones previously obtained, is that new, extended RAOs are used henceforth. The numbers are similar though, even if they are somewhat larger than before. We see from the results that the numbers for α=45˚ and α=135˚ are very close, as is the case with the numbers for α=0˚ and α=180˚. This tells us that the ship hull is very symmetric in the yz-plane, i.e. the after body looks like the bow. We can take a look at the phase angles for different degrees of freedom; all of these are given in appendix D. If we look at α=45˚ and α=135˚ for example, we see that the magnitudes are almost identical, while the phase angles are equally far away from the case where α=90˚. The same is true for α=0˚ and α=180˚, and that is we get so similar values for waves coming from the front and from behind.

For boarding mode, we get high values for motion in y-direction when α=45˚ or α=135˚. It seems that the shifting phase angles for yaw causes the motions from sway, roll and yaw to not cancel each other out to the same extent as before, but work more in the same direction, as can be found from the graphs in appendix D. The result is a high point velocity in y-direction, and an acceleration which is too high, being almost twice the gravitational acceleration. We see that the numbers are large also for motions in z-direction. In general, this wave attack angle is not favorable for boarding mode. The best wave attack angle for the boarding mode actually seems to be beam sea, although it should be noted that in the case with head sea in boarding mode, the hydrodynamic interaction would have a great effect, and reducing pitch motion significantly, so the values here must be interpreted with this in mind.

By looking at the numbers for crane mode, we can draw the same conclusion, that having α=45˚ or α=135˚ should be avoided. The accelerations in x-direction are very large, although the other directions experience more modest motions. It seems that the best attack angle for crane mode is α=0˚ or α=180˚. The acceleration in x-direction is large, but the other ones are more acceptable. For α=90˚ we get an acceleration in z-direction that is more than the gravitational acceleration, which means that there is danger of experiencing snapping loads. In general, we can say that these wave conditions with a significant wave height of 2 meters, which results in an expected maximum of 4.06 meters, is probably too rough for the reference vessel to perform these operations in. Also, this analysis is done with a peak period of 6.1 seconds, which is in the middle of the JONSWAP-range, which means that for developing seas, the peak period could be even shorter, resulting in even higher accelerations.

6.3.2 Short-crested waves

We will now look at the effect of short-crested wave theory on our output. The theory behind this can be referred to in section 4.4, and the way it has been solved in the program is described briefly in section 5.4.5. Since the vessel is quite symmetrical in the after ship and

the bow, we will be looking at different mean attack angles between 0° and 90°. Two studies will be run, one with a wave spreading parameter $s = 1$ and one with $s = 10$. $s = 1$ represents the highest level of wave spreading. Furthermore, the other parameters remain fixed, i.e. $H_s = 2$ meters, $T_p = 6.1$ seconds and $D = 3$ hours, and the JONSWAP spectrum is used. Only crane mode will be considered, as all point coordinates are different from zero. The results from the studies are given in Table 6.8 - Effect of short crested waves.

Table 6.8 - Effect of short crested waves

Wave heading: 90 deg		Wave heading: 75 deg		Wave heading: 45 deg		Wave heading: 15 deg		Wave heading: 0 deg	
s=1									
x-direction		x-direction		x-direction		x-direction		x-direction	
max motion	1.8	max motion	5.5	max motion	6.93	max motion	4.14	max motion	4.21
velocity	2.35	velocity	8.4	velocity	10.06	velocity	6.09	velocity	6.05
acceleration	3.8	acceleration	15.35	acceleration	17.68	acceleration	10.75	acceleration	10.45
y-direction		y-direction		y-direction		y-direction		y-direction	
max motion	2.66	max motion	2.77	max motion	2.15	max motion	0.48	max motion	0.42
velocity	4.83	velocity	4.76	velocity	3.26	velocity	0.66	velocity	0.61
acceleration	9.91	acceleration	9.45	acceleration	5.88	acceleration	1.07	acceleration	1.06
z-direction		z-direction		z-direction		z-direction		z-direction	
max motion	5.01	max motion	5.05	max motion	4.2	max motion	3.27	max motion	3.31
velocity	6.35	velocity	6.3	velocity	4.9	velocity	3.66	velocity	3.82
acceleration	9.61	acceleration	9.25	acceleration	6.65	acceleration	4.75	acceleration	5.23
min comb distance	1.64	min comb distance	2.2	min comb distance	3.51	min comb distance	3.9	min comb distance	3.5
max wave height	4.06	max wave height	4.06	max wave height	4.06	max wave height	4.06	max wave height	4.06
s=10									
x-direction		x-direction		x-direction		x-direction		x-direction	
max motion	1.8	max motion	5.53	max motion	6.96	max motion	4.15	max motion	4.23
velocity	2.35	velocity	8.45	velocity	10.1	velocity	6.1	velocity	6.06
acceleration	3.79	acceleration	15.44	acceleration	17.75	acceleration	10.75	acceleration	10.45
y-direction		y-direction		y-direction		y-direction		y-direction	
max motion	2.67	max motion	2.77	max motion	2.16	max motion	0.48	max motion	0.44
velocity	4.84	velocity	4.77	velocity	3.27	velocity	0.66	velocity	0.64
acceleration	9.93	acceleration	9.47	acceleration	5.89	acceleration	1.08	acceleration	1.1
z-direction		z-direction		z-direction		z-direction		z-direction	
max motion	5.02	max motion	5.06	max motion	4.21	max motion	3.27	max motion	3.29
velocity	6.36	velocity	6.31	velocity	4.91	velocity	3.65	velocity	3.8
acceleration	9.63	acceleration	9.28	acceleration	6.67	acceleration	4.74	acceleration	5.21
min comb distance	1.63	min comb distance	2.19	min comb distance	3.51	min comb distance	3.91	min comb distance	3.51
max wave height	4.06	max wave height	4.06	max wave height	4.06	max wave height	4.06	max wave height	4.06

When we compare these numbers to the ones for long-crested waves, as given in Table 6.7, we see that the long crested waves have a small effect for the most part, making some motions larger and others smaller. But when we look at mean wave attack angle of 0°, we see a significant effect of the short-crested waves, which makes the motions a bit larger. This is intuitive, as the shape of the ship hull changes most dramatically around the bow (and stern). A spread of the waves will thus have a larger effect in this area, especially in amplifying sway, roll and yaw motions. At the same time, surge, pitch and heave do not change much, and the result is larger motions.

The effect of the wave spreading parameter s is small, as we see from the almost identical numbers. When we compare the two wave spreading functions in Figure 7.8, we see that they are significantly different, so this is a bit surprising. When s approaches infinity, we will have
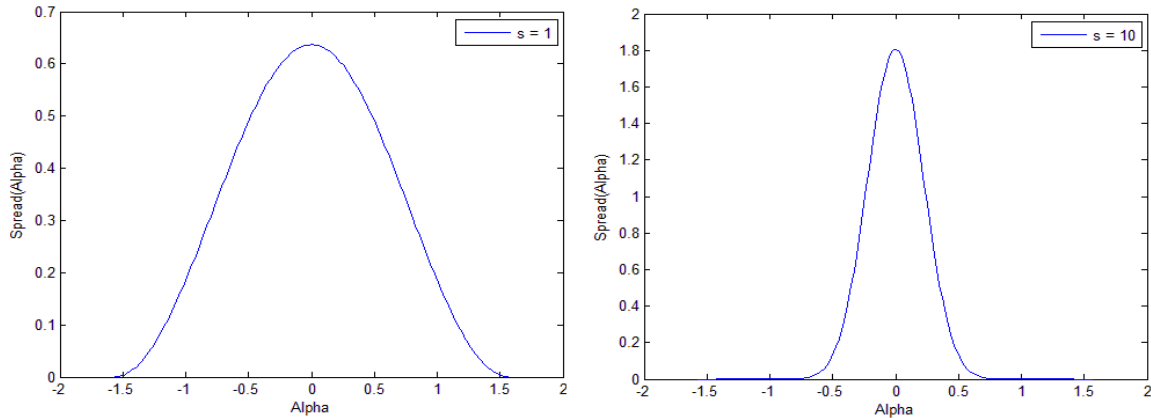
Figure 6.8 - Wave spreading functions

long-crested waves, so it is also noteworthy that $s = 10$ produces slightly larger results than $s = 1$, when both produce larger results than long-crested waves. This might suggest that a moderate wave spreading parameter produces the largest motions, but the differences are too small to conclude with this.

6.3.3 Points and angles

Next, we will do a little study where we change the position of the vessel, the headings of the vessel and the waves, and both the considered points. Then we look at what angles the program gives us as output, and verify that these are valid. We will also look at the expected maximum total motion between the two points and give an interpretation of the results. We will look at the well-known crane mode initially, and then we will choose another four different situations to highlight different features of the program. All these studies are done with significant wave height of 2 meters, peak period of 6.1 seconds, duration of three hours and a JONSWAP spectrum is used. This time short-crested wave theory is considered, and the spreading parameter is set to 10.

6.3.3.1 Mode 1 – Crane mode

In crane mode, we look at the crane tip related to the platform deck of the wind turbine, as is described in Table 6.1. The vessel heading is along the positive x-axis, and the geometry is quite easy to follow. This situation has been investigated before, but this time we pay attention to the angles that are produced and the motion along the straight line between the two considered points, as was described in section 5.3.3.3. We repeat the significance of the different angles:

- Psi is the angle in the horizontal plane of the vector pointing from the vessel point to the fixed point, measured anti-clockwise from the global x-axis.
- Theta is the same angle, but measure anti-clockwise from the local x-axis.

- Phi is the angle of the same vector in the vertical plane. It is positive when pointing upwards and negative when pointing downwards.
- Alpha is the angle of attack of the waves on the ship, 0° being head sea.

The program was run for this situation once more, and yielded the following results:

Table 6.9 - Angles and total motions for mode 1

Mode 1 (crane)					Local motions:	
	x	y	z			
vessel (origin)	8	18.50	0		x-direction	4.23
P1, local cs	-8	-13	23		y-direction	0.44
P1, global cs	0	5.5	23		z-direction	3.29
P2, global cs	0	2.5	17.1			
Vessel heading:	0				Total motions:	
Wave heading:	0				dislocation	3.11
Psi:	270				minimum distance	3.51
Theta:	270				velocity	3.64
Phi:	-63				acceleration	5.1
Alpha:	180					

We see that all the angles are correct for this case. Psi and theta are the same as the vessel heading is 0°, and Phi pointing downwards gives a negative number. Alpha implies following seas. As the vessel lies perfectly alongside the wind turbine, only the motions in y- and z-directions contribute to the total motion. The total dislocation suggests that the local motions in these two directions are more or less in phase.

Table 6.10 - Angles and total motions for mode 2

Mode 2 (crane)					Local motions:	
	x	y	z			
vessel (origin)	-18.5	8.00	0		x-direction	4.23
P1, local cs	-8	-13	23		y-direction	0.44
P1, global cs	-5.5	0	23		z-direction	3.29
P2, global cs	-2.5	0	17.1			
Vessel heading:	90				Total motions:	
Wave heading:	90				dislocation	3.11
					minimum distance	3.51
Psi:	0				velocity	3.64
Theta:	270				acceleration	5.1
Phi:	-63					
Alpha:	180					

6.3.3.2 Mode 2 – displaced crane mode

For this mode the original crane mode has been rotated 90˚ to create an identical situation in different global coordinates. The results are given in Table 6.10. We see that the ship and wave headings, and thus psi changes, but all the motions stay the same nonetheless. This is reassuring because it suggests that the program functions in the same way for different headings.

6.3.3.3 Mode 3 – displaced crane mode with a shifted fixed point

In this mode we will study the same geometry as the previous mode, but the fixed point is altered slightly, by setting the z-coordinate equal to 23. The points are shown in Figure 6.9. This has the effect that we examine motion between the points in the horizontal plane only. Thus we look at the horizontal motion radially between points, which in this case means that it should equal the motion in local y-direction. The wave heading is also altered to produce some new angles and more motions. The results are given in Table 6.11.
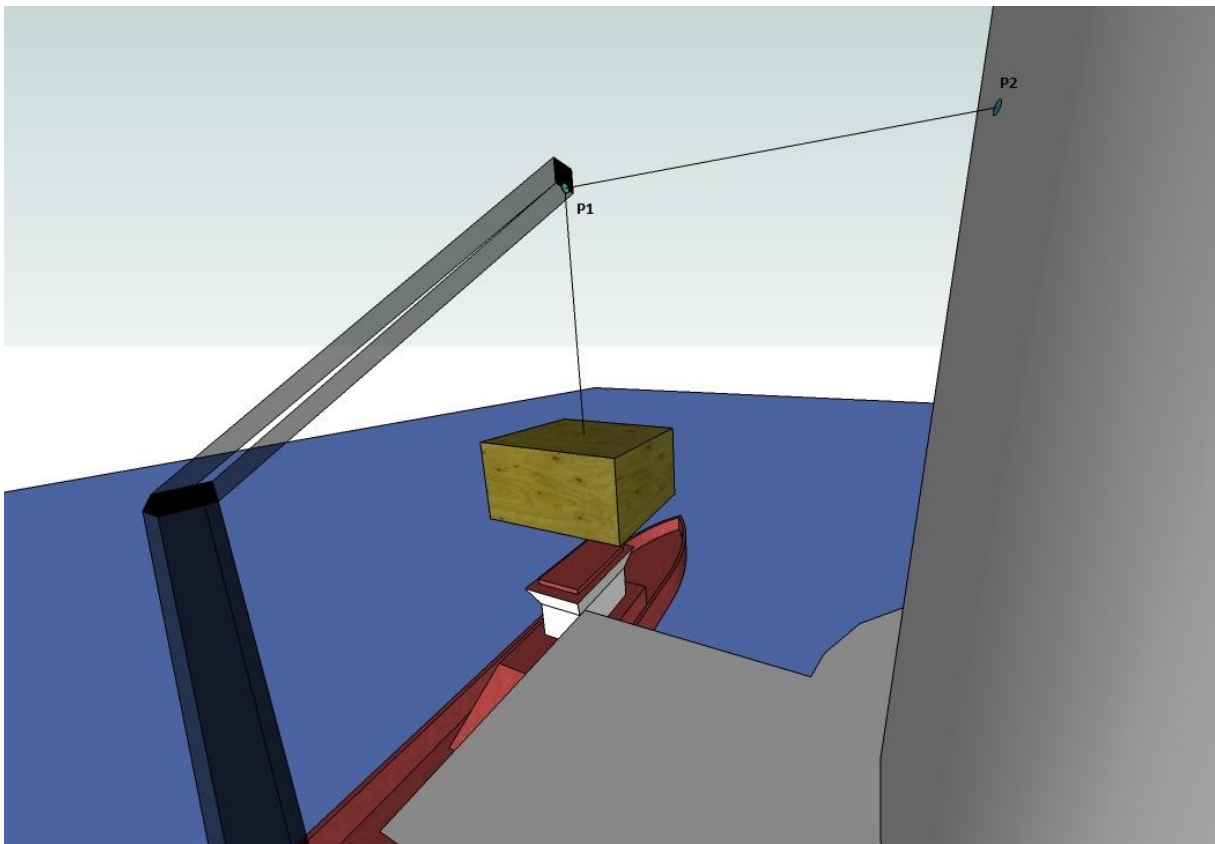
Figure 6.9 - Crane mode with the fixed point shifted

Table 6.11 - Angles and total motions for mode 3

Mode 3 (crane)					Local motions:	
	x	y	z			
vessel (origin)	-18.5	8.00	0		x-direction	8.17
P1, local cs	-8	-13	23		y-direction	2.63
P1, global cs	-5.5	0	23		z-direction	6.43
P2, global cs	-2.5	0	23			
Vessel heading:	90				Total motions:	
Wave heading:	45				dislocation	2.63
Psi:	0				minimum distance	0.37
Theta:	270				velocity	4.21
Phi:	0				acceleration	7.96
Alpha:	225					

We see that psi and theta stays the same as expected, while phi is now 0˚, implying horizontal motions are examined. The altered wave propagation angle gives us a new alpha. The local motions are larger as expected from the wave angle, and we see that the total motion equals the motion in local y-direction as predicted.

6.3.3.4   Mode 4 – displaced boarding mode

This mode is basically the boarding mode with a different origin and heading. We look at the same point in the vessel bow, but the fixed point is moved a bit up, to include more vertical motion in the total motion. Head sea is considered, and the result is given in Table 6.12.

Table 6.12 - Angles and total motions for mode 4

Mode 4 (boarding)					Local motions:	
	x	y	z			
vessel (origin)	16	-16.00	0		x-direction	2.43
P1, local cs	17.5	0	2.5		y-direction	1.55
P1, global cs	3.63	-3.63	2.5		z-direction	5.91
P2, global cs	2.5	-2.5	4			
Vessel heading:	135				Total motions:	
Wave heading:	315				dislocation	5.62
Psi:	135				minimum distance	-3.43
Theta:	360				velocity	6.49
Phi:	43.4				acceleration	8.64
Alpha:	0					

The vessel is placed in the fourth quadrant in the global coordinate system with a heading of 135˚, which is the same as the psi angle. This gives a theta of 360˚, and the fixed point which was shifted upwards gives a larger phi angle. The wave attack angle alpha implies head sea. We note that the rather large local z-motion along with significant local x-motion produce a strong total motion of 5.62 meters, causing collision for the given geometry. We once more experience that head seas are not favorable for boarding operations unless hydrodynamic interaction is considered, or the vessel is somehow fastened to the structure.

6.3.3.5 Mode 5 – alongside

This last mode is a completely new situation, done to illustrate the versatility of the program. The situation is a vessel which lies alongside the structure, and motion is considered for the ship side. The results are given in Table 6.13.

Table 6.13 - Angles and total motions for mode 5

Mode 5 (alongside)					Local motions:	
	x	y	z			
vessel (origin)	-6	-6.00	-1		x-direction	2.44
P1, local cs	2	3.5	4		y-direction	1.63
P1, global cs	-2.52	-3.97	3		z-direction	2.94
P2, global cs	-1.5	-2.5	3			
Vessel heading:	330				Total motions:	
Wave heading:	293				dislocation	1.68
Psi:	55.3				minimum distance	0.11
Theta:	85.3				velocity	1.93
Phi:	0				acceleration	2.71
Alpha:	217					

The vessel lies in the third quadrant of the global coordinate system, and the considered points are chosen such that we get the direction of the total motion close to the radial direction. We see from the total motion being close to the local y-motion, that we came close to this direction. We also see this from the theta angle which is close to 90˚ and phi being 0˚. Also the rest of the angles make sense when related to the given geometry.

6.3.4 Parameter studies

Finally, we will do one more parameter study to see the effect of the Torsethaugen spectrum, and of different peak periods for the same significant wave height. For this purpose, the Torsethaugen is favorable to use, because it is not restricted to such a narrow H_s/T_p-range as is the JONSWAP spectrum. We will use the crane mode for the studies, and long-crested wave theory will be used. Then studies are done for two different significant wave heights and four

different peak periods, and for two different wave headings. The duration will again be set to 3 hours. Initially, we will do a direct comparison between the Torsethaugen and the JONSWAP spectra. The results are given in Table 6.14.

Table 6.14 - Comparison between Torsethaugen and JONSWAP spectra

Wave heading (alpha): 0 deg
Hs=2
Wave spectrum: Torsethaugen
Wave spectrum: JONSWAP

Tp	5	7	5.1	7
x-direction				
max motion	3.89	3.36	4.6	3.5
velocity	6.25	5.15	6.88	5.09
acceleration	11.95	9.65	11.96	8.87
y-direction				
max motion	0.02	0.02	0.02	0.02
velocity	0.02	0.02	0.02	0.02
acceleration	0.03	0.03	0.03	0.03
z-direction				
max motion	3.17	3.42	2.89	3.39
velocity	3.61	3.59	3.88	3.63
acceleration	5.64	4.93	5.92	4.79
Total motion				
max dislocation	2.82	3.04	2.57	3.02
velocity	3.21	3.2	3.45	3.23
acceleration	5.01	4.39	5.27	4.26
min combined distance	3.8	3.58	4.05	3.6
max wave height	4.02	4.02	4.07	4.04

The first thing we notice is that the Torsethaugen spectrum is more stable over the peak periods, i.e. it does not change as rapidly as the JONSWAP spectrum does. Moreover, we see that the numbers are similar all over, and some are bigger and some smaller between the two spectra. If we look at the shapes of the two spectra, which are given in Figure 6.10, we see that their energies are concentrated in different frequency areas. The JONSWAP spectrum has a very steep and narrow top, while in the Torsethaugen spectrum the energy is more evenly distributed, and it has two shorter peaks. This has the effect that different degrees of freedom contribute differently to the motions for the two spectra. If we consider the spectra for different degrees of freedom which are given in appendix E, we see that the significant ones for this wave heading are surge, heave and pitch. We also notice that surge and heave are slightly more dominant in the Torsethaugen sea state, while pitch is more dominant in the JONSWAP sea state. If we in addition compare the phase angles which are given in appendix D, we notice that pitch and surge are in anti-phase to each other. This helps us explain the

difference in the results, as the ship will actually move in different ways for the two sea states, with the pitch motion having different importance.
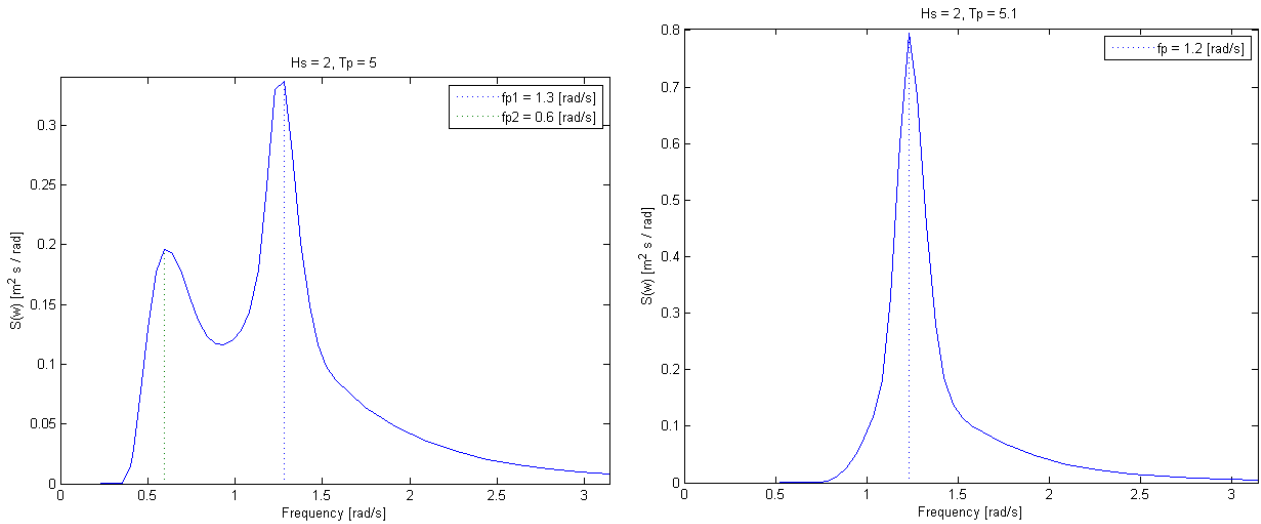
Figure 6.10 - Torsethaugen and JONSWAP spectra

6.3.4.1 H_s=1

Table 6.15 - Different T_p for H_s=1and two different wave headings

Wave heading (alpha): 0 deg
Hs=1

Tp	5	7	9	12
x-direction				
max motion	2.15	1.72	1.38	1.49
velocity	3.55	2.69	2.31	2.34
acceleration	6.9	5.12	4.7	4.68
y-direction				
max motion	0.01	0.01	0.01	0.01
velocity	0.01	0.01	0.01	0.01
acceleration	0.02	0.01	0.01	0.01
z-direction				
max motion	1.45	1.68	1.77	1.75
velocity	1.92	1.83	1.65	1.55
acceleration	3.18	2.58	2.28	2.22
Total motion				
max dislocation	1.29	1.5	1.58	1.56
velocity	1.7	1.63	1.47	1.38
acceleration	2.83	2.29	2.03	1.97
min combined distance	5.32	5.12	5.04	5.06
max wave height	2	2.01	1.99	1.97

Wave heading (alpha): 30 deg
Hs=1

Tp	5	7	9	12
x-direction				
max motion	3.55	3.1	2.56	2.47
velocity	5.77	4.52	3.88	3.85
acceleration	11.1	8.33	7.62	7.58
y-direction				
max motion	0.95	0.77	0.7	0.77
velocity	1.58	1.2	1.07	1.08
acceleration	3.11	2.31	2.13	2.12
z-direction				
max motion	1.9	1.93	1.89	1.87
velocity	2.82	2.39	2.11	2.04
acceleration	5.13	3.94	3.56	3.51
Total motion				
max dislocation	2.01	1.96	1.84	1.82
velocity	3.05	2.52	2.2	2.14
acceleration	5.6	4.26	3.85	3.82
min combined distance	4.6	4.66	4.78	4.8
max wave height	2	2.01	1.99	1.97

In Table 6.15 is given the results from the first study, with significant wave height of 1meter. We start by looking at head sea, and we notice that because of the long-crested wave theory, we have barely any motion at all in y-direction. In x- and z-directions, the numbers are quite small as expected, and we see that the accelerations drop when the peak periods become higher. This is also expected behavior for swell-dominated sea. When the wave attack angle is shifted to 30˚, we see an immediate change in responses. Y-motion becomes significant, and x-, z- and total motion become larger than was the case for head sea. We see the same behavior for the accelerations as the peak periods become larger.

6.3.4.2 $H_s=2$

Table 6.16 - Different Tp for Hs=2and two different wave headings

Wave heading (alpha): 0 deg Hs=2				
Tp	**5**	**7**	**9**	**12**
x-direction				
max motion	3.89	3.36	2.61	2.69
velocity	6.25	5.15	3.97	3.87
acceleration	12	9.65	7.54	7.36
y-direction				
max motion	0.02	0.02	0.02	0.02
velocity	0.02	0.02	0.02	0.02
acceleration	0.03	0.03	0.02	0.02
z-direction				
max motion	3.17	3.42	3.62	3.63
velocity	3.61	3.59	3.24	2.95
acceleration	5.64	4.93	4	3.72
Total motion				
max dislocation	2.82	3.04	3.22	3.23
velocity	3.21	3.2	2.88	2.62
acceleration	5.01	4.39	3.56	3.31
min combined distance	3.8	3.58	3.39	3.39
max wave height	4.02	4.02	3.99	3.95

Wave heading (alpha): 30 deg Hs=2				
Tp	**5**	**7**	**9**	**12**
x-direction				
max motion	6.48	6.05	4.96	4.48
velocity	10.2	8.67	6.78	6.42
acceleration	19.3	15.7	12.3	12
y-direction				
max motion	1.77	1.52	1.34	1.46
velocity	2.79	2.31	1.83	1.8
acceleration	5.38	4.35	3.41	3.33
z-direction				
max motion	3.82	3.86	3.8	3.76
velocity	5.11	4.65	3.93	3.65
acceleration	8.96	7.48	5.92	5.67
Total motion				
max dislocation	3.93	3.9	3.69	3.59
velocity	5.48	4.89	4.04	3.77
acceleration	9.76	8.09	6.37	6.13
min combined distance	2.69	2.72	2.93	3.03
max wave height	4.02	4.02	3.99	3.95

The study was run one last time for significant wave height of 2 meters. The results given in Table 6.16 show numbers that are roughly double the numbers from the previous study. The behavior is similar otherwise, and given the double values for max wave height, the numbers are reasonable. We see again that accelerations are high for short peak periods, and especially in x-direction we get large values. The rotations certainly play a big part in this, as the crane tip is placed far from the origin. For the wave heading angle of 30˚ we see unacceptably high values for acceleration in x-direction, and also in z-direction become too high, approaching close to the gravitational acceleration. Crane operations are not to be recommended for a

significant wave height of as low as 2 meters, at least not for low peak periods. We can also say that the best way to reduce motions is to steer the vessel up against the waves. In this regard, we must keep in mind that these numbers are for long-crested waves, and short-crested waves would cause even larger values.

7 Conclusion

7.1 Discussion

When the assignment was first established, the main target was to develop a MATLAB tool for easy evaluation of ship response as a function of different sea states and geometries. To successfully obtain such a program and have it reflect the real world marine operations, it was necessary to dig in to some areas to get the overview necessary. This is reflected in this thesis, which gives quite extensive introductions to the offshore wind sector and its related marine operations, as well as to some operational criteria. The rest of the thesis is written with the intention of giving the reader the most thorough overview, and the deepest comprehension of the program, as I can possibly provide. This has been done with the aim that perhaps the Relative Motion Calculator program can function as a platform on which a better, more functional program can be developed.

This has been kept in mind also when performing the tests and the parameter studies. That being said, some useful output has been obtained from said studies. The main conclusion is that the functions that have been added in the program all seem to work as intended. This has been found by comparing the latest version of the program, RMC 2.3, with the project version, RMC 1.2. We found that the main equations for calculating local ship motions function as they should. Unless the project version, which is much simpler, is wrong, we can assume that RMC 2.3 gives correct results for the three degrees of freedom of the project version. Then, all six degrees of freedom were included, and found to work properly by assessing the phase angles of the transfer functions.

Moreover, we have examined the effects of different wave attack angles, of short-crested wave theory, the different points and angles in the global coordinate system, and finally the effect of the Torsethaugen spectrum and different peak periods. The studies have provided results that look promising according to what effects were expected, and the conclusion so far is that everything functions as intended. However, the program is large and complex, and the theory behind the output is too complicated for errors to be detected just by looking at the output by itself. There are so many things that can have gone wrong, that one should not be surprised if some errors occur. This is also a good reason to provide a good overview for someone to potentially continuing to develop the program. But, so far the program seems to work very well, and possible errors seem to be of minor importance.

7.2 Ideas for further work

The biggest weakness of the program is, in my opinion, its lack of a proper user interface. Relative Motion Calculator is quite cumbersome to use, as it not only requires the user to be knowledgeable in ship motions and make his own sketches, but the user should preferably be somewhat competent in MATLAB programming in order to be comfortable enough to use the program effectively. A feature that would make the program much more usable is the

inclusion of some kind of graphical user interface. Then the user could see what situation he is examining, instead of just providing digits as coordinates and angles.

This idea could be taken further, and a graphical presentation of the dynamic system in the time-domain could be presented, by modeling irregular waves corresponding to a wave spectrum for a period of time, and then show the ship's motions responding to this. This could be very helpful for the user to understand how the different degrees of freedom affect the ship point's total motions.

An important feature which was originally intended to be included in the program is having two moving systems, acting independently of each other. In this thesis the assumption has been made that the wind turbine is either fixed, or moving so slowly that it can be considered stationary compared to the faster motions of the small support vessel. However, for either faster moving wind turbine concepts, or for larger support- or even construction vessels, the inclusion of two moving systems would definitely provide more accurate results. Also, it would make the program more applicable, as different problems could be modeled, for example an arbitrary buoy floating alongside a vessel.

When the program was developed, a necessary assumption was the exclusion of hydrodynamic interaction between the two systems. This is in fact not completely accurate; as such hydrodynamic effects often do have large effects on the motions, especially on the vessel motions. These effects are actually taken advantage of in real marine operations, as has been discussed in the thesis, so they should be included somehow. The problem is that they cannot be easily modeled, particularly not for arbitrary geometries and headings, so the inclusion of this effect will be complicated. An idea is to have the effect incorporated directly into the transfer functions, by exporting the relevant geometrical situation, e.g. as a 3D model into an external program such as Wadam, which lies under the HydroD software package of DNV Software. New RAO-files would then have to be computed for each situation, and it would be preferable to have the two programs communicating with each other. The picture then becomes very complex, and one should perhaps appreciate the value of having just a small MATLAB tool for quick estimation, and rather account for missing hydrodynamic interaction when interpreting the results.

I have many more ideas for enhancing the program further, such as looking at a pendulum motion of an object in a crane, and setting a point's motion to zero to model mooring or fastening. The more you work with such a program, the more ideas of enhancement you have. The possibilities are virtually endless, but have not been explored very far in this thesis. Rather, the fundamental equations and functionality has been established, and hopefully provide a platform from which Relative Motion Calculator can be developed further.

8   Reference list

1. Offshore Wind Turbines. *University of Strathclyde.* [Online] 1999.
http://www.esru.strath.ac.uk/EandE/Web_sites/98-9/offshore/wind/wintr.htm.

2. **Mary Rock and Laura Parsons.** Offshore Wind Energy. [Online] 2010.
http://www.eesi.org/files/offshore_wind_101310.pdf.

3. **EWEA (The European Wind Energy Association).**
http://ewea.org/fileadmin/ewea_documents/documents/00_POLICY_document/Offshore_Stat
istics/20112707OffshoreStats.pdf. [Online] 2011.
http://ewea.org/fileadmin/ewea_documents/documents/00_POLICY_document/Offshore_Stat
istics/20112707OffshoreStats.pdf.

4. **EWEA.** Wind in our sails - EWEA Offshore Report. [Online] 2011.
http://www.ewea.org/fileadmin/ewea_documents/documents/publications/reports/23420_Offs
hore_report_web.pdf.

5. **Left foot forward.** Britain is the world leader in wind power. [Online] 2011.
http://www.leftfootforward.org/2011/01/britain-leads-world-in-offshore-wind-power/.

6. **Wind energy - The facts.** Offshore Support Structures. [Online] http://www.wind-energy-
the-facts.org/en/part-i-technology/chapter-5-offshore/wind-farm-design-offshore/offshore-
support-structures.html.

7. **Statoil.** Hywind facts. [Online]
http://www.statoil.com/no/TechnologyInnovation/NewEnergy/RenewablePowerProduction/O
ffshore/Hywind/Downloads/Hywind%20Fact%20sheet.pdf.

8. **Lygren, Jon Erik.** *Dynamic Response of a Tension-Leg Wind Turbine.* Trondheim :
NTNU, 2010.

9. **Principle Power.** First WindFloat Successfully Deployed Offshore. [Online] 2011.
http://www.principlepowerinc.com/news/press_PPI_WF_deployment.html.

10. —. [Online]
http://www.principlepowerinc.com/images/PrinciplePowerWindFloatBrochure.pdf.

11. **Blue H Group.** http://www.bluehgroup.com/. [Online] http://www.bluehgroup.com/.

12. **CA-OWEE.** CA-OWEE Technology. *http://www.offshorewindenergy.org.* [Online] 2008.
http://www.offshorewindenergy.org/ca-owee/indexpages/downloads/CA-
OWEE_Technology.pdf.

13. **Odfjell Wind AS.** FOB Trim. *www.odfjellwind.com.* [Online] http://odfjellwind.com/fob-
trim.html.

14. **Maritimt Magasin.** maritimt.com. *FOB SWATH 1*. [Online] 2011.
http://maritimt.com/batomtaler/2011/fob-swath-1.html.

15. *DNV-RP-H103 - Modelling and analysis of marine operations.* **Det Norske Veritas.** 2011.

16. **Nielsen, Finn Gunnar.** *Marine Operations Lecture Notes.* 2004.

17. *Marine Operations.* **NORSOK.** 1997.

18. **Det Norske Veritas.** *DNV-OS-H101 - Marine Operations, General.* 2011.

19. **White, Frank M.** *Fluid Mechanics.* 2003.

20. **Pettersen, Bjørnar.** *Marin Teknikk 3 - Hydrodynamikk.* 2008.

21. **Myrhaug, Dag.** *Marin Dynamikk - Uregelmessig sjø.* 2007.

22. WAFO Homepage. *Centre for Mathematical Sciences, University of Lund.* [Online] http://www.maths.lth.se/matstat/wafo/about.html.

23. **Det Norske Veritas.** *DNV-RP-C205 - Environmental Conditions.* 2010.

24. **Newland, D.E.** *An introduction to random vibrations, spectral and wavelet analysis.* 1993.

25. **Faltinsen, Odd Magnus.** *Sea Loads on Ships and Offshore Structures.* 1990.

26. **Statoil.** www.statoil.com. [Online] http://www.statoil.com/no/NewsAndMedia/News/2008/Downloads/hywind_04.jpg.

27. **Marine Renewable Energy Blog.** Marine Renewable Energy Blog. [Online] http://marinerenewableenergy.blogspot.no/2011/07/floating-wind-turbines-all-systems.html.

28. **Cichon, Meg.** DeepCwind Tirelessly Developing Floating Offshore Wind. *www.RenewableEnergyWorld.com.* [Online] RenewableEnergyWorld.com, 2011. http://www.renewableenergyworld.com/rea/news/article/2011/06/deepcwind-project-tirelessly-developing-floating-offshore-wind.

29. **Statoil.** Offshore Wind in Statoil. *www.norway.org.* [Online] 2011. http://www.norway.org/PageFiles/451518/Eli%20Aamot%20%20Science%20week%20Offshore%20Wind%20in%20Statoil%20for%20web%20final.pdf.

30. **Odfjell Wind AS.** FOB SWATH vessels. *www.odfjellwind.com.* [Online] http://odfjellwind.com/pic/information.fob_swath.2012-05-09.pdf.

31. **Umoe Mandal.** Offshore Service Vessel. *www.um.no.* [Online] http://www.um.no/WEB/um200.nsf/pages/325380656E.

32. **Odfjell Wind AS.** FOB Jr. *odfjellwind.com.* [Online] http://odfjellwind.com/fob-jr.html.

33. **Statoil - Sjur Bratland.** *Hywind – A success story.* 2011.

34. *www.shipspotting.com.* [Online]
http://www.shipspotting.com/gallery/photo.php?lid=728419.

35. SCALE MODEL TESTS OF A FISHING VESSEL IN ROLL MOTION PARAMETRIC
RESONANCE. *http://mingaonline.uach.cl.* [Online]
http://mingaonline.uach.cl/scielo.php?pid=S0718-025X2006000100004&script=sci_arttext.

Appendices

Appendix A: Scatter diagram

Hmo (m)	Tp 0–4	4–5	5–6	6–7	7–8	8–9	9–10	10–11	11–12	12–13	13–14	14–15	15–16	16–17	17–18	18–19	19–20	20 inf	sum	prop	cum
0.0–0.5	25	14	18	14	24	17	8	9	5	0	2	3	1	1	6	2	2	7	156	0.003	0.003
0.5–1.0	79	235	408	539	496	488	426	225	111	46	16	7	6	3	2	0	2	17	3106	0.059	0.062
1.0–1.5	71	466	896	1223	1227	1219	911	626	470	252	108	70	36	12	13	2	2	49	7653	0.146	0.208
1.5–2.0	3	134	768	1342	1443	1288	1143	854	618	404	205	129	44	21	10	3	4	21	8434	0.161	0.370
2.0–2.5		22	292	1013	1328	1359	1056	921	669	431	188	186	56	27	17	5	1	16	7587	0.145	0.514
2.5–3.0	1	2	79	491	1037	1276	1031	795	678	479	208	193	81	35	13	3	2	8	6412	0.122	0.637
3.0–3.5		1	16	189	701	1038	896	729	532	386	235	197	97	40	15	4	1	5	5082	0.097	0.734
3.5–4.0			3	57	318	814	767	562	447	371	193	168	89	50	17	3		3	3862	0.074	0.808
4.0–4.5	1		1	11	130	568	731	500	341	306	146	142	67	29	25	4	3	2	3007	0.057	0.865
4.5–5.0				3	44	329	533	444	337	248	122	95	40	31	20	2	4	1	2253	0.043	0.908
5.0–5.5				1	15	112	339	396	280	195	121	98	31	26	16	5	2		1637	0.031	0.939
5.5–6.0				1	4	46	193	244	224	138	73	70	27	15	15	3			1054	0.020	0.959
6.0–6.5						18	91	177	156	125	65	51	20	15	7	1	2		730	0.014	0.973
6.5–7.0					1	1	34	108	137	106	46	40	14	5	1	1			495	0.009	0.983
7.0–7.5						1	11	53	93	74	50	30	14	7	8				342	0.007	0.989
7.5–8.0								29	61	63	27	19	6	3	1		1		212	0.004	0.993
8.0–8.5						1	1	14	31	43	24	13	6	5					138	0.003	0.996
8.5–9.0								8	19	27	17	8	7	1	1				87	0.002	0.998
9.0–9.5							2		5	18	13	9	2						51	0.001	0.999
9.5–10.0							1		2	7	7	4	3	3					27	0.001	0.999
10.0–10.5									3	3	7	4	4	1	1				22	0.000	1.000
10.5–11.0										3	1	2							6	0.000	1.000
11.0–11.5										4	2	1							7	0.000	1.000
11.5–12.0										1									1	0.000	1.000
12.0–12.5											1		1						2	0.000	1.000
12.5–13.0										1									1	0.000	1.000
13.0–13.5															1				1	0.000	1.000
13.5–14.0																			0	0.000	1.000
																			0	0.000	1.000
sum	180	874	2481	4884	6768	8575	8171	6697	5219	3731	1877	1539	652	331	189	40	24	133			
cum sum	180	1054	3535	8419	15187	23762	31933	38630	43849	47580	49457	50996	51648	51979	52168	52208	52232	52365			
prop	0.003	0.017	0.047	0.093	0.129	0.164	0.156	0.128	0.100	0.071	0.036	0.029	0.012	0.006	0.004	0.001	0.000	0.003			
cum prop	0.003	0.020	0.068	0.161	0.290	0.454	0.610	0.738	0.837	0.909	0.944	0.974	0.986	0.993	0.996	0.997	0.997	1.000			

Total: 52365

Appendix B: Derivations of response spectra

Assuming small motions, the motion on any point on a body can be written as

$$\boldsymbol{s} = (\eta_1 + z\eta_5 - y\eta_6)\boldsymbol{i} + (\eta_2 - z\eta_4 + x\eta_6)\boldsymbol{j} + (\eta_3 + y\eta_4 - x\eta_5)\boldsymbol{k} = r_1\boldsymbol{i} + r_2\boldsymbol{j} + r_3\boldsymbol{k}$$

where

$$r_1 = (\eta_1 + z\eta_5 - y\eta_6)$$

$$r_2 = (\eta_2 - z\eta_4 + x\eta_6)$$

$$r_3 = (\eta_3 + y\eta_4 - x\eta_5)$$

Let us start by assuming the motion of a point in z-direction. The vertical motion in a point $P(x_p, y_p, z_p)$ can be written as

$$r_3(t) = \eta_3(t) + y_p\eta_4(t) - x_p\eta_5(t)$$

where $r_3(t)$ has an expectation of zero:

$$E[r_3(t)] = 0$$

To find an expression for the total response spectrum in z-direction we need to introduce the concept of correlation functions. The autocorrelation function for motion in z-direction $r_3(t)$ is defined as

$$R_{r_3 r_3}(\tau) = E[r_3(t)r_3(t+\tau)]$$

$$= E\left[\left(\eta_3(t) + y_p\eta_4(t) - x_p\eta_5(t)\right)\left(\eta_3(t+\tau) + y_p\eta_4(t+\tau) - x_p\eta_5(t+\tau)\right)\right]$$

$$= E\big[\eta_3(t)\eta_3(t+\tau) + y_p^2\eta_4(t)\eta_4(t+\tau) + x_p^2\eta_5(t)\eta_5(t+\tau)$$
$$+ y_p\eta_3(t)\eta_4(t+\tau) - x_p\eta_3(t)\eta_5(t+\tau) + y_p\eta_4(t)\eta_3(t+\tau)$$
$$- y_p x_p\eta_4(t)\eta_5(t+\tau) - x_p\eta_5(t)\eta_3(t+\tau) - x_p y_p\eta_5(t)\eta_4(t+\tau)\big]$$
$$= E\big[\eta_3(t)\eta_3(t+\tau) + y_p^2\eta_4(t)\eta_4(t+\tau) + x_p^2\eta_5(t)\eta_5(t+\tau)$$
$$+ y_p\big(\eta_3(t)\eta_4(t+\tau) + \eta_4(t)\eta_3(t+\tau)\big)$$
$$- x_p\big(\eta_3(t)\eta_5(t+\tau) + \eta_5(t)\eta_3(t+\tau)\big) - x_p y_p\big(\eta_4(t)\eta_5(t+\tau)$$
$$+ \eta_5(t)\eta_4(t+\tau)\big)\big]$$

$$= R_{\eta_3\eta_3}(\tau) + y_p^2 R_{\eta_4\eta_4}(\tau) + x_p^2 R_{\eta_5\eta_5}(\tau) + y_p[R_{\eta_3\eta_4}(\tau) + R_{\eta_4\eta_3}(\tau)] - x_p[R_{\eta_3\eta_5}(\tau)$$
$$+ R_{\eta_5\eta_3}(\tau)] - x_p y_p[R_{\eta_4\eta_5}(\tau) + R_{\eta_5\eta_4}(\tau)]$$

$$= R_{\eta_3\eta_3}(\tau) + y_p^2 R_{\eta_4\eta_4}(\tau) + x_p^2 R_{\eta_5\eta_5}(\tau) + y_p[R_{\eta_3\eta_4}(\tau) + R_{\eta_3\eta_4}(-\tau)] - x_p[R_{\eta_3\eta_5}(\tau)$$
$$+ R_{\eta_3\eta_5}(-\tau)] - x_p y_p[R_{\eta_4\eta_5}(\tau) + R_{\eta_4\eta_5}(-\tau)]$$

A spectrum is defined as the Fourier transform of an autocorrelation function:

$$S_x(\omega) = \frac{1}{2\pi} \int_{-\infty}^{\infty} R_x(\tau)\, e^{-i\omega t} d\tau$$

We then divide the correlation function by 2π and integrate:

$$\frac{1}{2\pi} \int_{-\infty}^{\infty} R_{r_3 r_3}(\tau)\, e^{-i\omega\tau} d\tau$$

$$= \frac{1}{2\pi} \int_{-\infty}^{\infty} R_{\eta_3 \eta_3}(\tau)\, e^{-i\omega\tau} d\tau + \frac{1}{2\pi} \int_{-\infty}^{\infty} y_p^2 R_{\eta_4 \eta_4}(\tau)\, e^{-i\omega\tau} d\tau$$

$$+ \frac{1}{2\pi} \int_{-\infty}^{\infty} x_p^2 R_{\eta_5 \eta_5}(\tau)\, e^{-i\omega\tau} d\tau + \frac{1}{2\pi} \int_{-\infty}^{\infty} y_p R_{\eta_3 \eta_4}(\tau)\, e^{-i\omega\tau} d\tau$$

$$+ \frac{1}{2\pi} \int_{-\infty}^{\infty} y_p R_{\eta_3 \eta_4}(-\tau)\, e^{-i\omega\tau} d\tau - \frac{1}{2\pi} \int_{-\infty}^{\infty} x_p R_{\eta_3 \eta_5}(\tau)\, e^{-i\omega\tau} d\tau$$

$$- \frac{1}{2\pi} \int_{-\infty}^{\infty} x_p R_{\eta_3 \eta_5}(-\tau)\, e^{-i\omega\tau} d\tau - \frac{1}{2\pi} \int_{-\infty}^{\infty} x_p y_p R_{\eta_4 \eta_5}(\tau)\, e^{-i\omega\tau} d\tau$$

$$- \frac{1}{2\pi} \int_{-\infty}^{\infty} x_p y_p R_{\eta_4 \eta_5}(-\tau)\, e^{-i\omega\tau} d\tau$$

which gives

$$S_{r_3 r_3}(\omega) = S_{\eta_3 \eta_3}(\omega) + y_p^2 S_{\eta_4 \eta_4}(\omega) + x_p^2 S_{\eta_5 \eta_5}(\omega) + y_p \left[S_{\eta_3 \eta_4}(\omega) + S_{\eta_3 \eta_4}^*(\omega) \right]$$
$$- x_p \left[S_{\eta_3 \eta_5}(\omega) + S_{\eta_3 \eta_5}^*(\omega) \right] - x_p y_p \left[S_{\eta_4 \eta_5}(\omega) + S_{\eta_4 \eta_5}^*(\omega) \right]$$

$$= S_{\eta_3 \eta_3}(\omega) + y_p^2 S_{\eta_4 \eta_4}(\omega) + x_p^2 S_{\eta_5 \eta_5}(\omega) + 2 y_p \{ Re[S_{\eta_3 \eta_4}(\omega)] \} - 2 x_p \{ Re[S_{\eta_3 \eta_5}(\omega)] \}$$
$$- 2 x_p y_p \{ Re[S_{\eta_4 \eta_5}(\omega)] \}$$

because

$$z + z^* = (a + ib) + (a - ib) = 2a = 2\{Re(z)\}$$

Now we have obtained the response spectrum for motion in z-direction, expressed by the autocorrelation spectra for heave, roll and pitch, and the cross-spectra between them. Thus, we need to find these spectra by relating them to the wave spectrum via the transfer functions. From the definition of an RAO, we have

$$H_i(\omega) = \frac{\eta_i}{\zeta}, \qquad i = 1,2,3$$

where H is a complex number containing information about both the amplitude and the phase of the output. (Elaborate). Note that in this case, this is true only for the translations (surge, sway and heave), which are given as response amplitude per wave amplitude. By relating the transfer functions to their respective spectra, we have the following relation (From Newland, eq. 7.16) (24):

$$S_y(\omega) = |H(\omega)|^2 S_x(\omega)$$

where the subscripts y denotes the output, and x the input. We can thus express the response spectrum for heave as:

$$S_{\eta_3\eta_3}(\omega) = \left|H_{\zeta\eta_3}(\omega)\right|^2 S_\zeta(\omega)$$

However, the RAOs for the rotations (roll, pitch and yaw) are given as response angle per wave slope angle. A measure for the maximum slope angle of a wave is given as $k_n \cdot \zeta_a$. The transfer functions for the rotation modes then become:

$$H_i(\omega) = \frac{\eta_i}{k \cdot \zeta}, \qquad i = 4,5,6$$

The response spectrum for roll then becomes:

$$S_{\eta_4\eta_4}(\omega) = k^2(\omega)\left|H_{\zeta\eta_4}(\omega)\right|^2 S_\zeta(\omega)$$

and, similarly for pitch:

$$S_{\eta_5\eta_5}(\omega) = k^2(\omega)\left|H_{\zeta\eta_5}(\omega)\right|^2 S_\zeta(\omega)$$

Now, to express the cross-correlation spectra in a similar manner, we must find a way to express the cross-correlation transfer functions by the ordinary transfer functions, linking the relevant output to the corresponding autocorrelation spectra. We use the relation

$$\eta_4 = k(\omega)H_{\zeta\eta_4}(\omega)\zeta = H_{\eta_3\eta_4}(\omega)\eta_3 = H_{\eta_3\eta_4}(\omega)H_{\zeta\eta_3}(\omega)\zeta$$

$$H_{\eta_3\eta_4}(\omega) = k(\omega)\frac{H_{\zeta\eta_4}(\omega)}{H_{\zeta\eta_3}(\omega)}$$

Now that we have found the correct cross-correlation transfer function, we can find the cross-spectrum from the following general expression (From Newland, eq. 7.24) (24):

$$S_{xy}(\omega) = H(\omega)S_x(\omega)$$

where x denotes the input and y the output. Note that the transfer function is a complex entity, so the cross-spectrum also becomes complex. Transferred to our case, this expression becomes

$$S_{\eta_i\eta_j}(\omega) = H_{\eta_i\eta_j}(\omega)S_{\eta_i\eta_i}(\omega)$$

and we can then write the cross-spectrum between roll and heave motion as

$$S_{\eta_3\eta_4}(\omega) = H_{\eta_3\eta_4}(\omega)S_{\eta_3\eta_3}(\omega)$$

$$= k(\omega)\frac{H_{\zeta\eta_4}(\omega)}{H_{\zeta\eta_3}(\omega)}S_{\eta_3\eta_3}(\omega)$$

By following the exact same procedure, we obtain a corresponding result for pitch, namely

$$S_{\eta_3\eta_5}(\omega) = k(\omega)\frac{H_{\zeta\eta_5}(\omega)}{H_{\zeta\eta_3}(\omega)}S_{\eta_3\eta_3}(\omega)$$

When calculating the cross-correlation transfer functions between two rotations, we get a slightly different result, where the wave numbers cancel out:

$$\eta_5 = k(\omega)H_{\zeta\eta_5}(\omega)\zeta = H_{\eta_4\eta_5}(\omega)\eta_4 = H_{\eta_4\eta_5}(\omega)k(\omega)H_{\zeta\eta_4}(\omega)\zeta$$

$$H_{\eta_4\eta_5}(\omega) = \frac{H_{\zeta\eta_5}(\omega)}{H_{\zeta\eta_4}(\omega)}$$

The cross-spectrum between roll and pitch thus becomes

$$S_{\eta_4\eta_5}(\omega) = H_{\eta_4\eta_5}(\omega)S_{\eta_4\eta_4}(\omega) = \frac{H_{\zeta\eta_5}(\omega)}{H_{\zeta\eta_4}(\omega)}S_{\eta_4\eta_4}(\omega)$$

When we calculate the cross-correlations between two translations, we can disregard the wave number altogether. We end up with expressions analogue to the ones for auto-correlation for translations.

To sum up, the cross-correlation transfer functions can generally be expressed as:

$$H_{\eta_i\eta_j}(\omega) = \frac{H_{\zeta\eta_j}(\omega)}{H_{\zeta\eta_i}(\omega)}, \qquad i,j = 1,2,3$$

$$H_{\eta_i\eta_j}(\omega) = \frac{H_{\zeta\eta_j}(\omega)}{H_{\zeta\eta_i}(\omega)}, \qquad i,j = 4,5,6$$

$$H_{\eta_i\eta_j}(\omega) = k(\omega)\frac{H_{\zeta\eta_j}(\omega)}{H_{\zeta\eta_i}(\omega)}, \qquad i = 1,2,3 \ \& \ j = 4,5,6$$

$$H_{\eta_i\eta_j}(\omega) = k(\omega)\frac{H_{\zeta\eta_j}(\omega)}{H_{\zeta\eta_i}(\omega)}, \qquad i = 4,5,6 \ \& \ j = 1,2,3$$

Finally, we obtain a complete expression for our total response spectrum for motion in z-direction:

$$S_{r_3r_3}(\omega) = S_{\eta_3\eta_3}(\omega) + y_p^2 S_{\eta_4\eta_4}(\omega) + x_p^2 S_{\eta_5\eta_5}(\omega) + 2y_p\{Re[S_{\eta_3\eta_4}(\omega)]\}$$
$$- 2x_p\{Re[S_{\eta_3\eta_5}(\omega)]\} - 2x_p y_p\{Re[S_{\eta_4\eta_5}(\omega)]\}$$
$$= S_{\eta_3\eta_3}(\omega) + y_p^2 S_{\eta_4\eta_4}(\omega) + x_p^2 S_{\eta_5\eta_5}(\omega)$$
$$+ 2y_p k(\omega)\left\{Re\left[\frac{H_{\zeta\eta_4}(\omega)}{H_{\zeta\eta_3}(\omega)}S_{\eta_3\eta_3}(\omega)\right]\right\} - 2x_p k(\omega)\left\{Re\left[\frac{H_{\zeta\eta_5}(\omega)}{H_{\zeta\eta_3}(\omega)}S_{\eta_3\eta_3}(\omega)\right]\right\}$$
$$- 2x_p y_p \left\{Re\left[\frac{H_{\zeta\eta_5}(\omega)}{H_{\zeta\eta_4}(\omega)}S_{\eta_4\eta_4}(\omega)\right]\right\}$$

$$= |H_{\zeta\eta_3}(\omega)|^2 S_\zeta(\omega) + y_p^2 k^2(\omega)|H_{\zeta\eta_4}(\omega)|^2 S_\zeta(\omega) + x_p^2 k^2(\omega)|H_{\zeta\eta_5}(\omega)|^2 S_\zeta(\omega)$$
$$+ 2y_p k(\omega)\left\{Re\left[\frac{H_{\zeta\eta_4}(\omega)}{H_{\zeta\eta_3}(\omega)}|H_{\zeta\eta_3}(\omega)|^2 S_\zeta(\omega)\right]\right\}$$
$$- 2x_p k(\omega)\left\{Re\left[\frac{H_{\zeta\eta_5}(\omega)}{H_{\zeta\eta_3}(\omega)}|H_{\zeta\eta_3}(\omega)|^2 S_\zeta(\omega)\right]\right\}$$
$$- 2x_p y_p k^2(\omega)\left\{Re\left[\frac{H_{\zeta\eta_5}(\omega)}{H_{\zeta\eta_4}(\omega)}|H_{\zeta\eta_4}(\omega)|^2 S_\zeta(\omega)\right]\right\}$$

$$= \left(|H_{\zeta\eta_3}(\omega)|^2 + y_p^2 k^2(\omega)|H_{\zeta\eta_4}(\omega)|^2 + x_p^2 k^2(\omega)|H_{\zeta\eta_5}(\omega)|^2\right.$$
$$+ 2y_p k(\omega)\left\{Re\left[\frac{H_{\zeta\eta_4}(\omega)}{H_{\zeta\eta_3}(\omega)}|H_{\zeta\eta_3}(\omega)|^2\right]\right\}$$
$$- 2x_p k(\omega)\left\{Re\left[\frac{H_{\zeta\eta_5}(\omega)}{H_{\zeta\eta_3}(\omega)}|H_{\zeta\eta_3}(\omega)|^2\right]\right\}$$
$$\left.- 2x_p y_p k^2(\omega)\left\{Re\left[\frac{H_{\zeta\eta_5}(\omega)}{H_{\zeta\eta_4}(\omega)}|H_{\zeta\eta_4}(\omega)|^2\right]\right\}\right) S_\zeta(\omega)$$

This equation is based on the expression for motion in z-direction in the equation of motion. By substituting this with the expressions for motions in x- and y-directions, we obtain the response spectra for motions in x- and y-directions in an identical way. These spectra are as follows:

$$S_{r_1r_1}(\omega) = S_{\eta_1\eta_1}(\omega) + z_p^2 S_{\eta_5\eta_5}(\omega) + y_p^2 S_{\eta_6\eta_6}(\omega) + 2z_p\{Re[S_{\eta_1\eta_5}(\omega)]\}$$
$$- 2y_p\{Re[S_{\eta_1\eta_6}(\omega)]\} - 2y_p z_p\{Re[S_{\eta_5\eta_6}(\omega)]\}$$
$$= S_{\eta_1\eta_1}(\omega) + z_p^2 S_{\eta_5\eta_5}(\omega) + y_p^2 S_{\eta_6\eta_6}(\omega)$$
$$+ 2z_p k(\omega)\left\{Re\left[\frac{H_{\zeta\eta_5}(\omega)}{H_{\zeta\eta_1}(\omega)}S_{\eta_1\eta_1}(\omega)\right]\right\} - 2y_p k(\omega)\left\{Re\left[\frac{H_{\zeta\eta_6}(\omega)}{H_{\zeta\eta_1}(\omega)}S_{\eta_1\eta_1}(\omega)\right]\right\}$$
$$- 2y_p z_p \left\{Re\left[\frac{H_{\zeta\eta_6}(\omega)}{H_{\zeta\eta_5}(\omega)}S_{\eta_5\eta_5}(\omega)\right]\right\}$$

and

$$S_{r_2 r_2}(\omega) = S_{\eta_2 \eta_2}(\omega) + z_p^2 S_{\eta_4 \eta_4}(\omega) + x_p^2 S_{\eta_6 \eta_6}(\omega) - 2z_p \{Re[S_{\eta_2 \eta_4}(\omega)]\}$$
$$+ 2x_p \{Re[S_{\eta_2 \eta_6}(\omega)]\} - 2x_p z_p \{Re[S_{\eta_4 \eta_6}(\omega)]\}$$
$$= S_{\eta_2 \eta_2}(\omega) + z_p^2 S_{\eta_4 \eta_4}(\omega) + x_p^2 S_{\eta_6 \eta_6}(\omega)$$
$$- 2z_p k(\omega) \left\{ Re\left[\frac{H_{\zeta \eta_4}(\omega)}{H_{\zeta \eta_2}(\omega)} S_{\eta_2 \eta_2}(\omega) \right] \right\} + 2x_p k(\omega) \left\{ Re\left[\frac{H_{\zeta \eta_6}(\omega)}{H_{\zeta \eta_2}(\omega)} S_{\eta_2 \eta_2}(\omega) \right] \right\}$$
$$- 2x_p z_p \left\{ Re\left[\frac{H_{\zeta \eta_6}(\omega)}{H_{\zeta \eta_4}(\omega)} S_{\eta_4 \eta_4}(\omega) \right] \right\}$$

Spectrum for global motion

We shall now derive the spectrum for the motion along this direction by first finding the spectrum for motion along the angle θ in the xy-plane, and then combining this with the spectrum for motion along the angle ϕ in the vertical plane along θ. The motion in the xy-plane can generally be written as

$$\mathbf{s}_{xy} = r_1 \mathbf{i} + r_2 \mathbf{j}$$

When we have the angle θ given as the angle between the local x-axis and projection of the straight line between the points on the xy-plane, measured counterclockwise from the local x-axis, we can write the motion in the xy-plane along this angle as

$$r_\theta(t) = r_1(t) \cos \theta + r_2(t) \sin \theta$$

From this, we find the autocorrelation function as

$$R_{r_\theta r_\theta}(\tau) = E[r_\theta(t) r_\theta(t + \tau)]$$
$$= E[(r_1(t) \cos \theta + r_2(t) \sin \theta)(r_1(t + \tau) \cos \theta + r_2(t + \tau) \sin \theta)]$$
$$= E[r_1(t) r_1(t + \tau) \cos^2 \theta + r_2(t) r_2(t + \tau) \sin^2 \theta$$
$$+ (r_1(t) r_2(t + \tau) + r_2(t) r_1(t + \tau)) \sin \theta \cos \theta]$$
$$= R_{r_1 r_1}(\tau) \cos^2 \theta + R_{r_2 r_2}(\tau) \sin^2 \theta + (R_{r_1 r_2}(\tau) + R_{r_1 r_2}(-\tau)) \sin \theta \cos \theta$$

By relating this to the definition of a spectrum as before (ref), we get the following expression for the spectrum for motion along θ:

$$S_{r_\theta r_\theta}(\omega) = S_{r_1 r_1}(\omega) \cos^2 \theta + S_{r_2 r_2}(\omega) \sin^2 \theta + \left(S_{r_1 r_2}(\omega) + S_{r_2 r_1}(\omega) \right) \sin \theta \cos \theta$$
$$= S_{r_1 r_1}(\omega) \cos^2 \theta + S_{r_2 r_2}(\omega) \sin^2 \theta + 2\{Re[S_{r_1 r_2}(\omega)]\} \sin \theta \cos \theta$$

We thus need to find the cross-correlation spectrum $S_{r_1 r_2}(\omega)$ through the autocorrelation function $R_{r_1 r_2}(\tau)$. By referring to the equation of motion, we express the autocorrelation function as:

$$R_{r_1 r_2}(\tau) = E[r_1(t)r_2(t+\tau)]$$
$$= E\left[\left(\eta_1(t) + z_p\eta_5(t) - y_p\eta_6(t)\right)\left(\eta_2(t+\tau) - z_p\eta_4(t+\tau) + x_p\eta_6(t+\tau)\right)\right]$$
$$= E[\eta_1(t)\eta_2(t+\tau) - z_p\eta_1(t)\eta_4(t+\tau) + x_p\eta_1(t)\eta_6(t+\tau)$$
$$+ z_p\eta_5(t)\eta_2(t+\tau) - z_p^2\eta_5(t)\eta_4(t+\tau) + x_p z_p\eta_5(t)\eta_6(t+\tau)$$
$$- y_p\eta_6(t)\eta_2(t+\tau) + y_p z_p\eta_6(t)\eta_4(t+\tau) - x_p y_p\eta_6(t)\eta_6(t+\tau)]$$
$$= R_{\eta_1\eta_2}(\tau) - z_p R_{\eta_1\eta_4}(\tau) + x_p R_{\eta_1\eta_6}(\tau) + z_p R_{\eta_5\eta_2}(\tau) - z_p^2 R_{\eta_5\eta_4}(\tau)$$
$$+ x_p z_p R_{\eta_5\eta_6}(\tau) - y_p R_{\eta_6\eta_2}(\tau) + y_p z_p R_{\eta_6\eta_4}(\tau) - x_p y_p R_{\eta_6\eta_6}(\tau)$$

And by Fourier transform we obtain the cross-correlation spectrum:

$$S_{r_1 r_2}(\omega) = S_{\eta_1\eta_2}(\omega) - z_p S_{\eta_1\eta_4}(\omega) + x_p S_{\eta_1\eta_6}(\omega) + z_p S_{\eta_5\eta_2}(\omega) - z_p^2 S_{\eta_5\eta_4}(\omega)$$
$$+ x_p z_p S_{\eta_5\eta_6}(\omega) - y_p S_{\eta_6\eta_2}(\omega) + y_p z_p S_{\eta_6\eta_4}(\omega) - x_p y_p S_{\eta_6\eta_6}(\omega)$$

All these spectra are found through the cross-correlation transfer functions which are already found.

Spectrum for motion in 3D

In a similar manner, we can write the motion along the straight line between the points as

$$r_\phi(t) = r_\theta(t)\cos\phi + r_3(t)\sin\phi$$

which, by following the same steps as above, yields the final spectrum for total response along the straight line between the points:

$$S_{r_\phi r_\phi}(\omega) = S_{r_\theta r_\theta}(\omega)\cos^2\phi + S_{r_3 r_3}(\omega)\sin^2\phi + 2\{Re[S_{r_\theta r_3}(\omega)]\}\cos\phi\sin\phi$$

In this expression the only unknown term is the cross-correlation spectrum $S_{r_\theta r_3}(\omega)$, defined by its cross-correlation function:

$$R_{r_\theta r_3}(\tau) = E[r_\theta(t)r_3(t+\tau)]$$
$$= E\left[\left(\left(\eta_1(t) + z_p\eta_5(t) - y_p\eta_6(t)\right)\cos\theta\right.\right.$$
$$+ \left(\eta_2(t) - z_p\eta_4(t) + x_p\eta_6(t)\right)\sin\theta\right)\left(\eta_3(t+\tau) + y_p\eta_4(t+\tau)\right.$$
$$\left.\left. - x_p\eta_5(t+\tau)\right)\right]$$
$$= \left[R_{\eta_1\eta_3}(\tau) + y_p R_{\eta_1\eta_4}(\tau) - x_p R_{\eta_1\eta_5}(\tau) + z_p R_{\eta_5\eta_3}(\tau) + y_p z_p R_{\eta_5\eta_4}(\tau)\right.$$
$$\left. - x_p z_p R_{\eta_5\eta_5}(\tau) - y_p R_{\eta_6\eta_3}(\tau) - y_p^2 R_{\eta_6\eta_4}(\tau) + x_p y_p R_{\eta_6\eta_5}(\tau)\right]\cos\theta$$
$$+ \left[R_{\eta_2\eta_3}(\tau) + y_p R_{\eta_2\eta_4}(\tau) - x_p R_{\eta_2\eta_5}(\tau) - z_p R_{\eta_4\eta_3}(\tau) - y_p z_p R_{\eta_4\eta_4}(\tau)\right.$$
$$\left. + x_p z_p R_{\eta_4\eta_5}(\tau) + x_p R_{\eta_6\eta_3}(\tau) + x_p y_p R_{\eta_6\eta_4}(\tau) - x_p^2 R_{\eta_6\eta_5}(\tau)\right]\sin\theta$$

And finally, by Fourier transform, we obtain the following cross-correlation spectrum:

$$
\begin{aligned}
S_{r_\theta r_3}(\omega) = {} & \left[S_{\eta_1\eta_3}(\omega) + y_p S_{\eta_1\eta_4}(\omega) - x_p S_{\eta_1\eta_5}(\omega) + z_p S_{\eta_5\eta_3}(\omega) + y_p z_p S_{\eta_5\eta_4}(\omega) \right. \\
& \left. - x_p z_p S_{\eta_5\eta_5}(\omega) - y_p S_{\eta_6\eta_3}(\omega) - y_p^2 S_{\eta_6\eta_4}(\omega) + x_p y_p S_{\eta_6\eta_5}(\omega) \right] \cos\theta \\
& + \left[S_{\eta_2\eta_3}(\omega) + y_p S_{\eta_2\eta_4}(\omega) - x_p S_{\eta_2\eta_5}(\omega) - z_p S_{\eta_4\eta_3}(\omega) - y_p z_p S_{\eta_4\eta_4}(\omega) \right. \\
& \left. + x_p z_p S_{\eta_4\eta_5}(\omega) + x_p S_{\eta_6\eta_3}(\omega) + x_p y_p S_{\eta_6\eta_4}(\omega) - x_p^2 S_{\eta_6\eta_5}(\omega) \right] \sin\theta
\end{aligned}
$$

At This point, all unknown are expressed by the known autocorrelation spectra and the cross-correlation spectra found by combining the given transfer functions. Through these equations the program finally computes the total motion spectrum for the straight line between the points.

Appendix C: Derivation of Gumbel parameters

Derivation of u:

$$F_H(u) = 1 - e^{-\frac{u^2}{8m_0}} = 1 - \frac{1}{N}$$

$$e^{-\frac{u^2}{8m_0}} = \frac{1}{N} \Longrightarrow -\frac{u^2}{8m_0} = \ln\frac{1}{N}$$

$$\Longrightarrow \frac{u^2}{8m_0} = \ln N \Longrightarrow u = 2\sqrt{2m_0 \ln N}$$

Derivation of α:

$$\alpha = n \cdot f_X(u) = N \cdot f_H(u)$$

$$\alpha = N \cdot \frac{u}{4m_0} e^{-\frac{u^2}{8m_0}} = N \cdot \frac{2\sqrt{2m_0 \ln N}}{4m_0} e^{-\frac{\left(2\sqrt{2m_0 \ln N}\right)^2}{8m_0}} = N \cdot \frac{\sqrt{2m_0 \ln N}}{2m_0} e^{-\frac{4 \cdot 2m_0 \ln N}{8m_0}} =$$

$$= N \cdot \sqrt{\frac{\ln N}{2m_0}} e^{-\ln N} = N \cdot \sqrt{\frac{\ln N}{2m_0}} \frac{1}{N}$$

$$\Longrightarrow \alpha = \sqrt{\frac{\ln N}{2m_0}}$$

Appendix D: Magnitudes and phase angles for transfer functions

Wave attack angle = 0˚
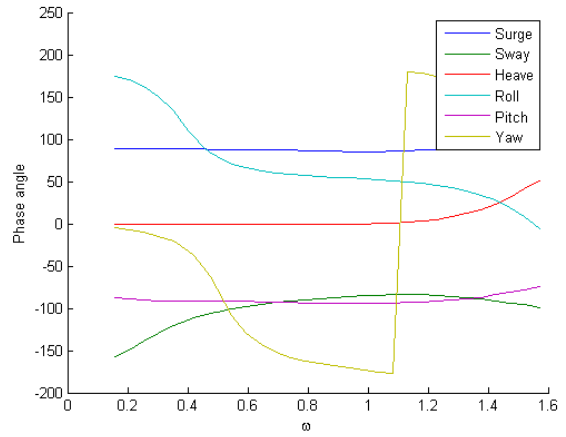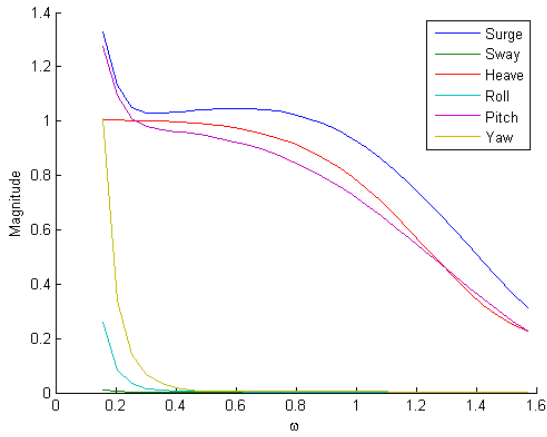
Wave attack angle = 45˚
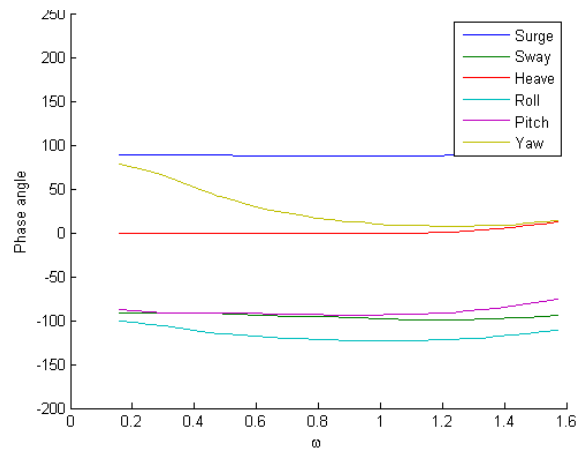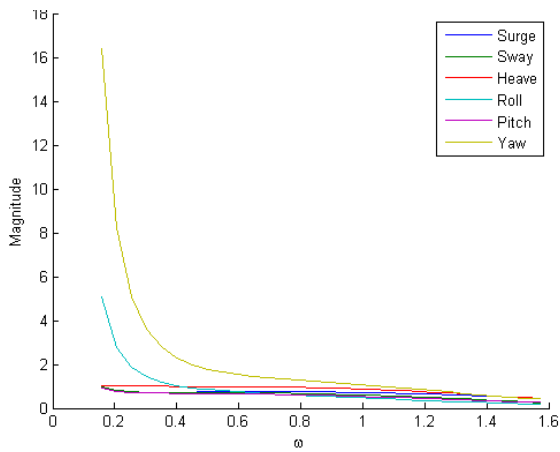
Wave attack angle = 90˚
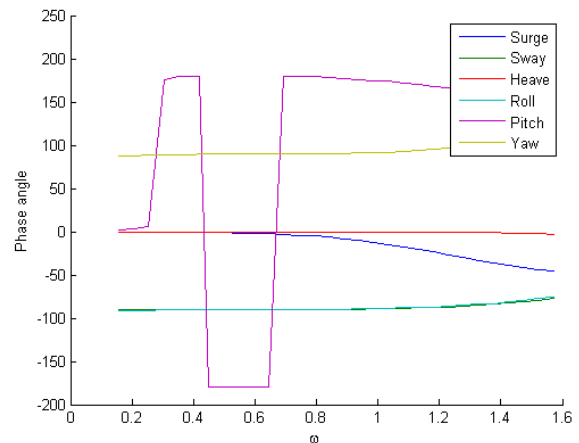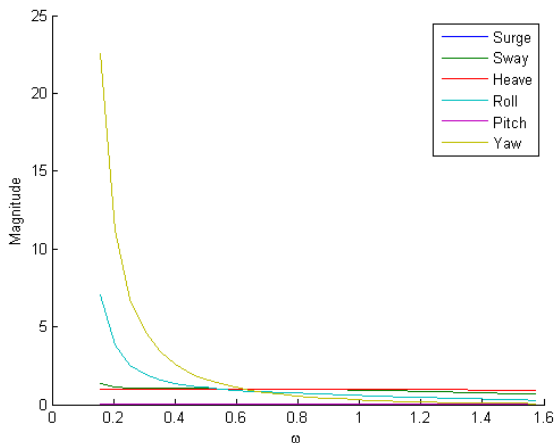
Wave attack angle = 135˚
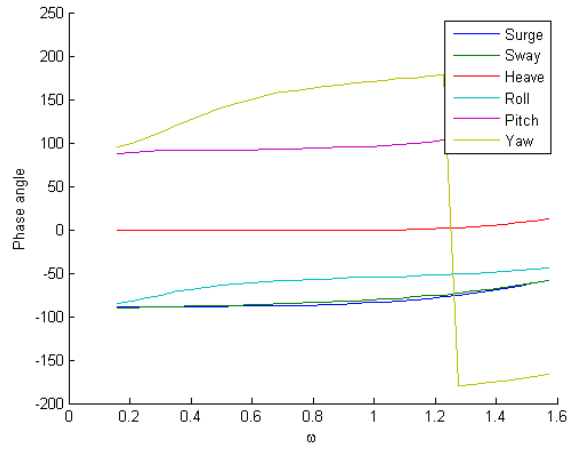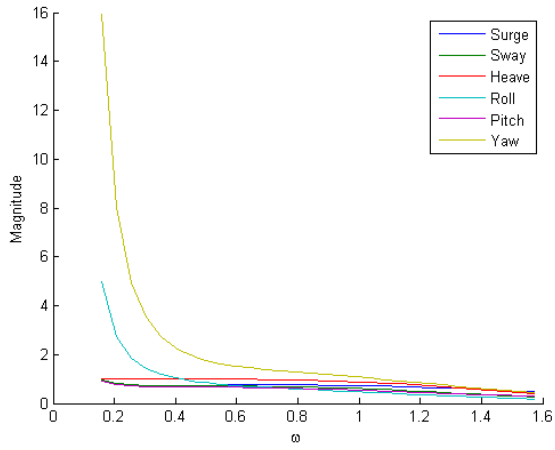
Wave attack angle = 180˚
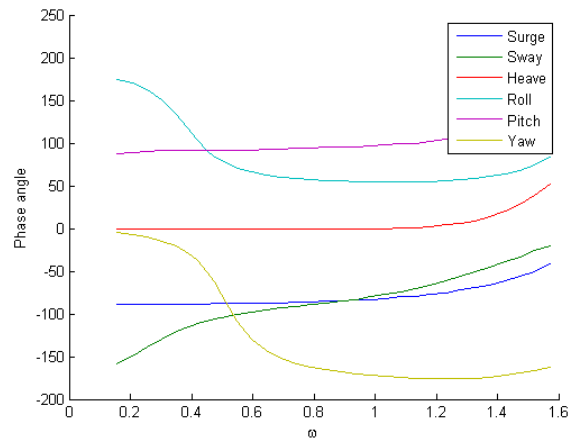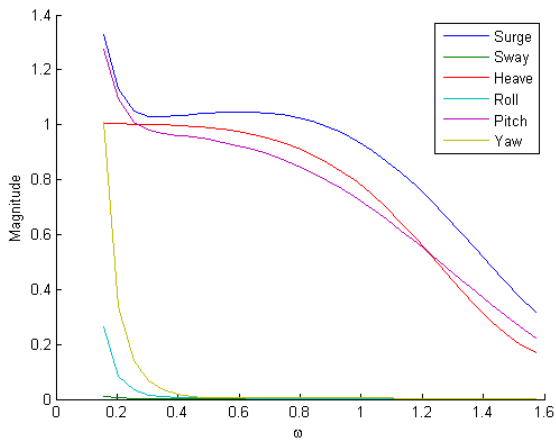
Appendix E: Motion spectra for all the dof for JONSWAP and Torsethaugen spectra

Response spectra for JONSWAP sea state
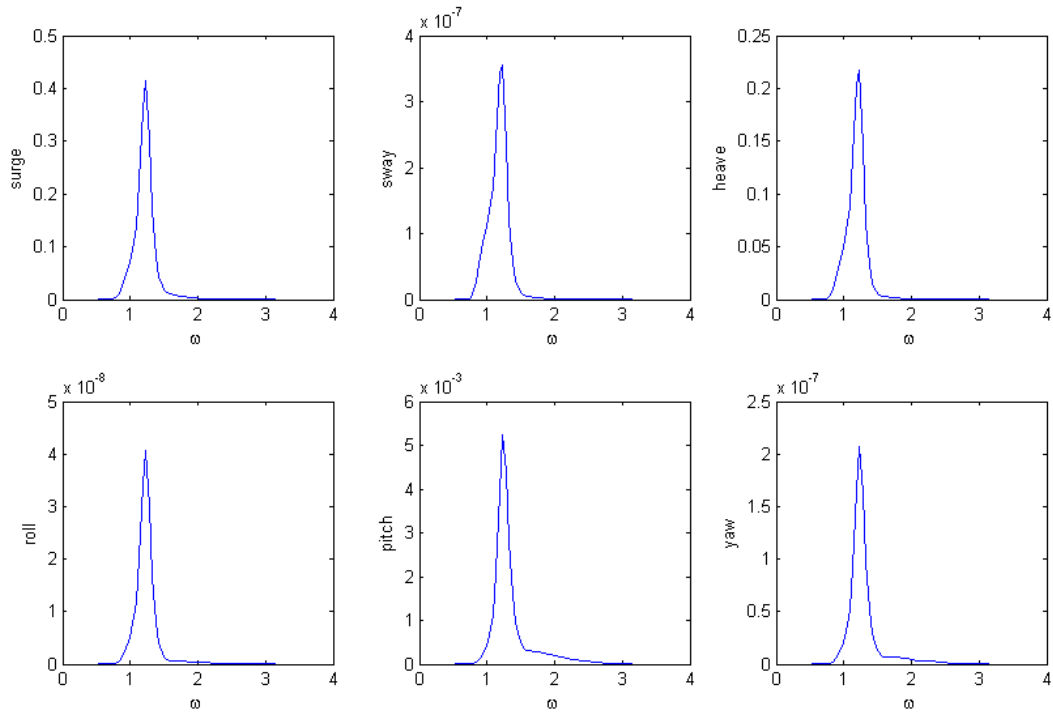
Response spectra for JONSWAP sea state
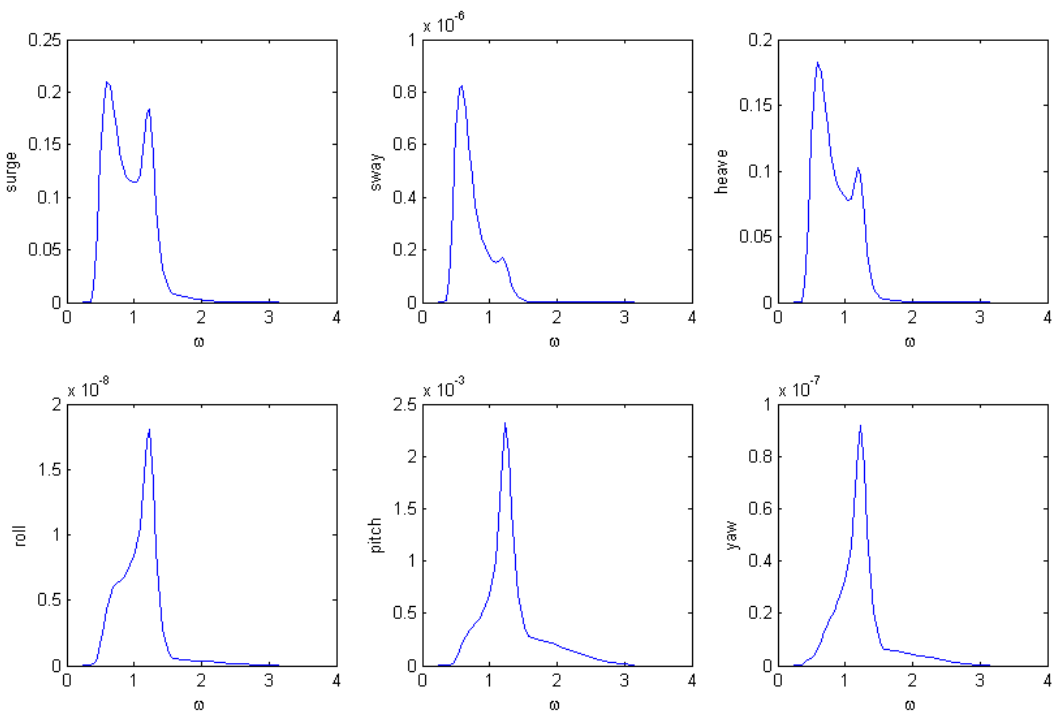
Appendix F: MATLAB scripts

main.m

```
%% Main file.
% Version 2.3 describes motions in 6 dof. Vessel heading and wave heading
% is also taken as input. It gives the local vessel motions as output. It
% also gives the motions in the xy-plane or in 3D relative to the given
% points. The version includes short-crested wave theory as an option.

clear all

addpath(fullfile(pwd,'wafo25'))
initwafo

infile = 'eirik_prosjoppg_rao.dat';
%infile = 'eirik_master_rao.dat';

[Hs,Tp,D,Type,PointPlat,PointVesLoc,PointVesGlob,RelativeHead,CritDistMin,C
ritDistMax,CritAcc,CritVel,Theta,Phi,ShortCrest,s]=getData();
[H_eta,omega]=readFile(infile,RelativeHead,ShortCrest,s);
[S_ThetaPhi,S_Theta,Swave,MotionLoc]=calculate(H_eta,PointVesLoc,Hs,Tp,omeg
a,Type,Theta,Phi);
analyze(Swave,S_ThetaPhi,MotionLoc,omega,D,PointPlat,PointVesGlob,CritDistM
in,CritDistMax,CritAcc,CritVel,RelativeHead);
```

analyze.m

```
function [] =
analyze(Swave,MotionTotal,MotionLoc,omega,D,PointPlat,PointVesGlob,CritDist
Min,CritDistMax,CritAcc,CritVel,RelativeHead)
% Calculates the max values from the spectra, finds extreme values for
% distances, verifies if they are acceptable according to criteria, and
% finally prints out results to screen.

VLoc=zeros(length(Swave),3);
aLoc=zeros(length(Swave),3);

%% Calculating spectra for velocity and acceleration
for i=1:3
    VLoc(:,i)=MotionLoc(:,i).*omega.^2;
    aLoc(:,i)=MotionLoc(:,i).*omega.^4;
end

VTotal=MotionTotal.*omega.^2;
aTotal=MotionTotal.*omega.^4;

%% Finding expected maxima

Smax=findMax(Swave,omega,D);               % Max wave height

for i=1:3
```

```matlab
    MotionLocMax(i)=findMax(MotionLoc(:,i),omega,D);        % Max local
motions
    VLocMax(i)=findMax(VLoc(:,i),omega,D);
    aLocMax(i)=findMax(aLoc(:,i),omega,D);
end


MotionTotalMax=findMax(MotionTotal,omega,D);               % Max total
motions
VTotalMax=findMax(VTotal,omega,D);
aTotalMax=findMax(aTotal,omega,D);



%% Finding distances
MeanDistanceTotal=sqrt((PointVesGlob(1)-PointPlat(1))^2 + (PointVesGlob(2)-
PointPlat(2))^2 + (PointVesGlob(3)-PointPlat(3))^2);      % Mean distance in
3D
DistanceTotalMin=MeanDistanceTotal-MotionTotalMax;
DistanceTotalMax=MeanDistanceTotal+MotionTotalMax;



%% Verify if the values are within acceptable criteria
VerDistTotalMin=verify(DistanceTotalMin,CritDistMin,1);
VerDistTotalMax=verify(DistanceTotalMax,CritDistMax,2);
VerVelTotal=verify(VTotalMax,CritVel,2);
VerAccTotal=verify(aTotalMax,CritAcc,2);



%% Print out results
fprintf('Expected maximum motions on the vessel, in local cs:\n');
fprintf('Direction: \t\t\t x\t\t y\t\t z\n');
fprintf('Motion: \t\t%7.2f %7.2f %7.2f \n' ,MotionLocMax);
fprintf('Velocity: \t\t%7.2f %7.2f %7.2f \n' ,VLocMax);
fprintf('Acceleration: \t%7.2f %7.2f %7.2f \n\n' ,aLocMax);

fprintf('Maximum wave height: %6.2f \n', Smax);
fprintf('Mean wave attack angle on vessel is %6.2f
degrees.\n\n',RelativeHead);

% make table with results
fprintf('Motion examined\t\t\t  value\t\t criterion\t accepted\n');
fprintf('Maximum dislocation \t %6.2f\n',MotionTotalMax);
fprintf('Minimum distance \t\t %6.2f\t\t %6.2f\t\t
%s\n',DistanceTotalMin,CritDistMin,VerDistTotalMin);
fprintf('Maximum distance \t\t %6.2f\t\t %6.2f\t\t
%s\n',DistanceTotalMax,CritDistMax,VerDistTotalMax);
fprintf('Maximum velocity \t\t %6.2f\t\t %6.2f\t\t
%s\n',VTotalMax,CritVel,VerVelTotal);
fprintf('Maximum acceleration \t %6.2f\t\t %6.2f\t\t
%s\n\n',aTotalMax,CritAcc,VerAccTotal);


end



% Subfunction findMax
function [Emax] = findMax(S,omega,D)
% Calculates expected maximum for a spectrum, from spectral values, the
% corresponding frequencies and the duration D
```

```matlab
Som2=S.*omega.^2;
m0=abs(trapz(omega,S));
m2=abs(trapz(omega,Som2));

Tm02=2*pi*sqrt(m0/m2);
N=(D*3600)/Tm02;

Emax=4*sqrt(m0)*(sqrt(log(N)/2)+(0.2886/sqrt(2*log(N))));

end


% Subfunction verify
function [accepted] = verify(value,criteria,type)
% Verifies if the calculated values are acceptable according to given
% criteria

accepted='no';

if type==1              % 1=minimum
    if value>=criteria
        accepted='yes';
    end
elseif type==2          % 2=maximum
    if value<=criteria
        accepted='yes';
    end
end


end
```

calculate.m

```matlab
function[S_ThetaPhi,S_Theta,Swave,MotionLoc] =
calculate(H_eta,PointVesLoc,Hs,Tp,omega,Type,Theta,Phi)
% Calculates the different response spectra and plots them

g=9.81;
k=(omega.^2)./g;        % dispersion relation in deep water

X=PointVesLoc(1);
Y=PointVesLoc(2);
Z=PointVesLoc(3);

WAFO=true;

if WAFO
    %% Calcuate wave spectrum from WAFO!
    if  Type=='j'
        Spec='JONSWAP spectrum';
        % kall jonswap
        S = jonswap(omega,[Hs Tp]);
    else
        Spec='Torsethaugen spectrum';
        % kall torsethaugen
        S = torsethaugen(omega,[Hs Tp]);
```

97

```matlab
        end


    %% Plot the wave spectrum
    figure(3)
    set(figure(3),'name', Spec, 'numbertitle','off')
    plotspec(S);
    title(['Hs = ', num2str(Hs), ', Tp = ', num2str(Tp)]);


    Swave=S.S;

else
    %% If WAFO is unavailable, calculate JONSWAP spectrum from own code
    Spec='JONSWAP spectrum';
    Swave = spectrum(omega,Hs,Tp);
end



%% calculate response spectra
[Svessel]=calculateSpectra(H_eta,Swave,k);                    %
Calculates all auto-correlation and cross-correlation spectra for the
vessel
[MotionLoc]=localMotions(Svessel,omega,PointVesLoc,Swave,Spec);       %
Calculates complete spectra for local motions and derivatives and plots
them

%% horizontal plane (2D)
% calculate cross-spectrum between motions in x- and y-directions
Temp1=Svessel(:,1,2) - Z.*Svessel(:,1,4) + X.*Svessel(:,1,6);
Temp2=Z.*Svessel(:,5,2) - Z^2.*Svessel(:,5,4) + X*Z.*Svessel(:,5,6);
Temp3=-Y.*Svessel(:,6,2) + Y*Z.*Svessel(:,6,4) - X*Y.*Svessel(:,6,6);


Sr1r2=Temp1+Temp2+Temp3;

% calculate Stheta, the response spectrum in the relevant horizontal
direction
S_Theta=(cosd(Theta))^2.*MotionLoc(:,1) + (sind(Theta))^2.*MotionLoc(:,2) +
2*cosd(Theta)*sind(Theta).*real(Sr1r2);

%% including vertical plane (3D)
% calculate cross-spectrum between motions in Theta-direction and in z-
direction
Temp4=Svessel(:,1,3)+Y.*Svessel(:,1,4)-X.*Svessel(:,1,5);
Temp5=Z.*Svessel(:,5,3)+Y*Z.*Svessel(:,5,4)-X*Z.*Svessel(:,5,5);
Temp6=-Y.*Svessel(:,6,3)-Y^2.*Svessel(:,6,4)+X*Y.*Svessel(:,6,5);
Temp7=Svessel(:,2,3)+Y.*Svessel(:,2,4)-X.*Svessel(:,2,5);
Temp8=-Z.*Svessel(:,4,3)-Y*Z.*Svessel(:,4,4)+X*Z.*Svessel(:,4,5);
Temp9=X.*Svessel(:,6,3)+X*Y.*Svessel(:,6,4)-X^2.*Svessel(:,6,5);


S_ThetaR3=(Temp4+Temp5+Temp6)*cosd(Theta)+(Temp7+Temp8+Temp9)*sind(Theta);


% calculate S_ThetaPhi, the response spectrum in the calculated direction,
% i.e. the straight line between the given points in three dimensions.
S_ThetaPhi=(cosd(Phi))^2.*S_Theta + (sind(Phi))^2.*MotionLoc(:,3) +
2*sind(Phi)*cosd(Phi).*real(S_ThetaR3);



end
```

98

localMotions.m

```matlab
function[Motion] = localMotions(Svessel,omega,PointVesLoc,Swave,Spec)
% Calculates complete spectra for local motions and derivatives and plots
them

AutoCorrs1=Svessel(:,1,1)+PointVesLoc(3)^2.*Svessel(:,5,5)+PointVesLoc(2)^2
.*Svessel(:,6,6);          % autocorrelation parts
AutoCorrs2=Svessel(:,2,2)+PointVesLoc(3)^2.*Svessel(:,4,4)+PointVesLoc(1)^2
.*Svessel(:,6,6);          % of the equations
AutoCorrs3=Svessel(:,3,3)+PointVesLoc(2)^2.*Svessel(:,4,4)+PointVesLoc(1)^2
.*Svessel(:,5,5);

S15part=2*PointVesLoc(3).*real(Svessel(:,1,5));
S16part=2*PointVesLoc(2).*real(Svessel(:,1,6));
S56part=2*PointVesLoc(2)*PointVesLoc(3).*real(Svessel(:,5,6));

S24part=2*PointVesLoc(3).*real(Svessel(:,2,4));
S26part=2*PointVesLoc(1).*real(Svessel(:,2,6));
S46part=2*PointVesLoc(1)*PointVesLoc(3).*real(Svessel(:,4,6));

S34part=2*PointVesLoc(2).*real(Svessel(:,3,4));
S35part=2*PointVesLoc(1).*real(Svessel(:,3,5));
S45part=2*PointVesLoc(1)*PointVesLoc(2).*real(Svessel(:,4,5));


Motion(:,1)=AutoCorrs1+S15part-S16part-S56part;
% complete equations
Motion(:,2)=AutoCorrs2-S24part+S26part-S46part;
Motion(:,3)=AutoCorrs3+S34part-S35part-S45part;


%% plotting the spectra for motions in global cs
figure(4)
set(figure(4),'name','Response spectra for total motions in local
coordinate system','numbertitle','off')

subplot(2,2,1)
plot(omega,Swave)
title(['Motion for the point (',num2str(PointVesLoc(1)) ',
',num2str(PointVesLoc(2)) ', ',num2str(PointVesLoc(3)) '), local ship
coordinates.' ])
xlabel('\omega')
ylabel(Spec)
subplot(2,2,2)
plot(omega,Motion(:,1))
xlabel('\omega')
ylabel('Local x-direction')
subplot(2,2,3)
plot(omega,Motion(:,2))
xlabel('\omega')
ylabel('Local y-direction')
subplot(2,2,4)
plot(omega,Motion(:,3))
xlabel('\omega')
ylabel('Local z-direction')

%% plotting spectra for each dof
```

```matlab
figure(5)
set(figure(5),'name','Response spectra for each seperate degree of
freedom','numbertitle','off')

subplot(2,3,1)
plot(omega,Svessel(:,1,1))
xlabel('\omega')
ylabel('surge')
subplot(2,3,2)
plot(omega,Svessel(:,2,2))
xlabel('\omega')
ylabel('sway')
subplot(2,3,3)
plot(omega,Svessel(:,3,3))
xlabel('\omega')
ylabel('heave')
subplot(2,3,4)
plot(omega,Svessel(:,4,4))
xlabel('\omega')
ylabel('roll')
subplot(2,3,5)
plot(omega,Svessel(:,5,5))
xlabel('\omega')
ylabel('pitch')
subplot(2,3,6)
plot(omega,Svessel(:,6,6))
xlabel('\omega')
ylabel('yaw')

end
```

calulateSpectra.m

```matlab
function[Svessel]=calculateSpectra(H_eta,Swave,k)
% Calculates all auto-correlation and cross-correlation spectra

H=zeros(length(H_eta),6,6);
Svessel=zeros(length(H_eta),6,6);

for i=1:6
    for j=1:6
        H(:,i,j)=H_eta(:,j)./H_eta(:,i);               % Fill in all the
cross-correlation transfer functions
    end
end

for i=1:3
    for j=1:3
        H(:,i,j+3)=H(:,i,j+3).*k;                       % Finish the cross-
correlation transfer functions by
        H(:,i+3,j)=H(:,i+3,j)./k;                       % multiplying some
of them by the wave number k
    end
end
```

100

```matlab
for i=1:6
    H(:,i,i)=abs(H_eta(:,i)).^2;                        % Overwrite with
the autocorrelation transfer functions, magnitude squared
    if i>3
        Svessel(:,i,i)=k.^2.*H(:,i,i).*Swave;          % Make the
autocorrelation spectra for rotations
    else
        Svessel(:,i,i)=H(:,i,i).*Swave;                % Make the
autocorrelation spectra for translations
    end
end

for i=1:6
    for j=1:6
        if i~=j
            Svessel(:,i,j)=H(:,i,j).*Svessel(:,i,i);   % Make the cross-
spectra by multiplying with the corresponding autocorrelation spectrum
        end
    end
end

end
```

readFile.m

```matlab
function[H_eta,freq]=readFile(infile,AttackAngle,ShortCrest,s)
% Reads data from .dat-file, interpolates transfer functions according to
% the exact given headings, and finally plots the transfer functions. This
% function also calculates a mean transfer function by integrating transfer
% functions over the spread for short crested waves.

%% Reading the top of the input file and determining key variables
[No_heads,No_freqs,dummy1,dummy2]=textread(infile,'%f\t %f\t %f\t
%f',1,'headerlines',18);

toplines = 23;
space = 4;
preface = toplines+No_heads+space+No_freqs+space;
section = No_heads * No_freqs + space;

[ihead,head]=textread(infile,'%f\t %f',No_heads,'headerlines',toplines);
[ifreq,freq]=textread(infile,'%f\t
%f',No_freqs,'headerlines',toplines+space+No_heads);


%% Reading all the transfer functions and generating for angles between 180
%% and 360 degrees, as described in section 6.4.5. in the report
H=zeros(No_freqs,6,No_heads);
for i=1:2:5                            % For surge, heave, pitch
    for j=1:No_heads
    [idir,ifreq,ampl,phase]=textread(infile,'%f\t %f\t %f\t
%f',No_freqs,'headerlines',preface+(i-1)*section+(j-1)*No_freqs);
    H(:,i,j)=ampl.*exp(1i.*(phase/360)*2*pi);                    % Reading
RAOs for all headings and making a total RAO matrix for 360 degrees
    H(:,i,(2*No_heads-j))=ampl.*exp(1i.*(phase/360)*2*pi);
    head(No_heads-1+j)=head(j)+180;
```

```matlab
        end
end

for i=2:2:6                               % For sway, roll, yaw (dof affected by
the symmetric division of the RAOs)
    for j=1:No_heads
    [idir,ifreq,ampl,phase]=textread(infile,'%f\t %f\t %f\t
%f',No_freqs,'headerlines',preface+(i-1)*section+(j-1)*No_freqs);
    H(:,i,j)=ampl.*exp(1i.*(phase/360)*2*pi);                      % Reading
RAOs for all headings and making a total RAO matrix for 360 degrees
    H(:,i,(2*No_heads-j))=(ampl.*exp(1i.*(-phase/360)*2*pi));      %
Changing signs on the RAOs which are from 180 to 360 degrees
    end
end

%% Calculating the correct transfer function to be used
if ~ShortCrest                                          % Long-crested
waves
    H_eta=stepLess(H,AttackAngle,head);                 % RAO for the
given heading
elseif ShortCrest                                       % Short-crested
waves
    d_Alpha=0.02;                                       % Establishing
the spreading function, with form factor s
    Alpha=(-pi/2:d_Alpha:pi/2);
    K2s=(2^(2*s-1)*factorial(s)*factorial(s-1))/(pi*factorial(2*s-1));
    Spread=K2s*(cos(Alpha)).^(2*s);                     % Spreading
function

    H_eta=0;                                 % Initial value for the "mean"
transfer function
    for i=1:length(Alpha)
        Angle=AttackAngle+Alpha(i);
        if (Angle)<0
            Angle=Angle+360;
        elseif (Angle>=360)
            Angle=Angle-360;
        end
        H_Angle=stepLess(H,Angle,head);
        H_eta=H_eta+(H_Angle.*Spread(i)*d_Alpha);
    end

    figure(1)                        % Plots the spreading function
    set(figure(1),'name','Spreading function','numbertitle','off')
    plot(Alpha,Spread)
    ylabel('Spread(Alpha)')
    xlabel('Alpha')
    legend(['s = ',num2str(s)])
end

%% Plotting all RAO's magnitudes and phases
for i=1:6
    %plotRAOs(H,freq,No_heads,i);
end

%% Plotting magnitudes and phases in same plot
figure(20)
set(figure(20),'name','Magnitude and phase for all transfer
functions','numbertitle','off')
```

```matlab
subplot(1,2,1)
hold all
plot(freq,abs(H_eta))
legend('Surge', 'Sway', 'Heave', 'Roll', 'Pitch', 'Yaw');
ylabel('Magnitude')
xlabel('\omega')

subplot(1,2,2)
hold all
plot(freq,angle(H_eta)*(360/(2*pi)))
legend('Surge', 'Sway', 'Heave', 'Roll', 'Pitch', 'Yaw');
ylabel('Phase angle')
xlabel('\omega')
ylim([-200 250])

%% Extending the range of the "project RAO" for better results
if strcmp(infile,'eirik_prosjoppg_rao.dat')                    % Make the
"project RAO" longer, making it linearly
    for j=1:9                                                  % approach
zero as it approaches double the max frequency.
        for i=1:6
            H_eta(32+j,i)=H_eta(32,i)*(1-j/10);
            freq(32+j)=freq(32)*(1+j/9);
        end
    end
end

%% Plotting the six transfer functions
figure(2)
set(figure(2),'name','Transfer functions for all degrees of
freedom','numbertitle','off')

subplot(3,2,1)
plot(freq,abs(H_eta(:,1)))
title(['Mean attack angle from waves on ship is ',num2str(AttackAngle),'
degrees.'])
ylabel('H surge')
xlabel('\omega')
subplot(3,2,2)
plot(freq,abs(H_eta(:,2)))
ylabel('H sway')
xlabel('\omega')
subplot(3,2,3)
plot(freq,abs(H_eta(:,3)))
ylabel('H heave')
xlabel('\omega')
subplot(3,2,4)
plot(freq,abs(H_eta(:,4)))
ylabel('H roll')
xlabel('\omega')
subplot(3,2,5)
plot(freq,abs(H_eta(:,5)))
ylabel('H pitch')
xlabel('\omega')
subplot(3,2,6)
plot(freq,abs(H_eta(:,6)))
ylabel('H yaw')
xlabel('\omega')
```

103

```matlab
end


% Subfunction stepLess
function[H_return] = stepLess(H,AttackAngle,head)
% Finds the correct interpolation for the given direction, based on the two
% closest directions and the closeness to them, "relation". The subfunction
% thus gives as output an RAO corresponding to an exact angle, using linear
% interpolation.

No_heads=length(head);
H_return=zeros(length(H),6);

for i=1:No_heads-1                                       % pretty scary
variable
    if (head(i)<=AttackAngle)                            % returns the
direction to which RelativeHead
        iHeading=i;                                      % is closest, and
how close it is for interpolation.
        relation=(AttackAngle-head(i))/(180/(No_heads-1));
    end
end

for i=1:6
    H_return(:,i)=H(:,i,iHeading).*(1-
relation)+H(:,i,iHeading+1).*(relation);
end

end

%Subfunction plotRAOs
function [] = plotRAOs(H,freq,No_heads,Dof)
% plots the magnitudes and phases of the different RAOs for different
% headings.

step=3;
RAO=zeros(length(freq),((No_heads-1)/step)+1);
Heads=zeros(((No_heads-1)/step)+1,1);

for j=1:step:No_heads
    RAO(:,(j-1)/step+1)=H(:,Dof,j);
    Heads((j-1)/step+1)=((j-1)*15);
end

Heads=num2str(Heads,3);

if Dof==1
    Freedom='surge';
elseif Dof==2
    Freedom='sway';
elseif Dof==3
    Freedom='heave';
elseif Dof==4
    Freedom='roll';
```

```matlab
elseif Dof==5
    Freedom='pitch';
elseif Dof==6
    Freedom='yaw';
end

String=['Magnitudes and phase angles for the RAO for ',Freedom,];

figure(5+Dof)
set(figure(5+Dof),'name',String,'numbertitle','off')

title('Results are for different attack angles.');
subplot(1,2,1)
hold all
plot(freq,abs(RAO));
legend(Heads,'Location','NorthEast');
ylabel('Magnitude')
xlabel('\omega')

subplot(1,2,2)
hold all
plot(freq,angle(RAO)*(360/(2*pi)));
legend(Heads,'Location','NorthEast');
ylabel('Phase angle, degrees')
xlabel('\omega')
ylim([-200 250])

end
```

getData.m

```matlab
function
[Hs,Tp,D,Type,PointPlat,PointVesLoc,PointVesGlob,RelativeHead,CritDistMin,C
ritDistMax,Critacc,CritV,Theta,Phi,ShortCrest,s] = getData()
% Either takes input data from the user, or provides default data
% Calculates the relative angle between the wave propagation direction and
% the ship heading. Prints out significant data to the welcome screen.

%% Print to screen, calculate relative heading between waves and vessel,
%% and find the vessel point given as global coordinates

[Hs,Tp,D,Type,PointPlat,OriginVes,PointVesLoc,VesselHead,WaveHead,CritDistM
in,CritDistMax,Critacc,CritV,ShortCrest,s]=givenInput();
fprintf('*************************************************************\n
');
fprintf('*                 RELATIVE MOTION CALCULATOR
*\n');
fprintf('*                       Version 2.3
*\n');
fprintf('*************************************************************\n
');
fprintf('*                 Programmed by Eirik Berg
*\n');
fprintf('*                       Spring 2012
*\n');
```

105

```matlab
fprintf('****************************************************************\n
\n');
fprintf('*********************\n');
fprintf('*** Default input ***\n');
fprintf('*********************\n\n');


done=false;
while done==false

    fprintf('*** Sea state ***\n');
    fprintf('Hs = %3.2f m\n', Hs);
    fprintf('Tp = %3.2f s\n', Tp);
    fprintf('Duration = %3.2f hours\n', D);
    fprintf('Wave propagation direction is %3.2f degrees counterclockwise
from the global x-axis.\n',WaveHead);
    fprintf('Sea spectrum type: ');
    if Type=='j'
        fprintf('JONSWAP\n');
    else
        fprintf('Torsethaugen\n');
    end
    if ShortCrest==true
        fprintf('Short ');
    else
        fprintf('Long ');
    end
    fprintf('crested wave theory is being considered.');


    fprintf('\n\n*** Coordinate systems ***\n');
    fprintf('The origin in the platform''s coordinate system coincides with
origo of the global coordinate system.\n');
    fprintf('The origin in the vessel''s coordinate system is (%3.2f %3.2f
%3.2f)\n',OriginVes(1),OriginVes(2),OriginVes(3));
    fprintf('The vessel''s x-axis points %3.2f degrees counterclockwise
from the global x-axis.\n',VesselHead);

    RelativeHead=VesselHead-WaveHead+180;        % Set relative heading
between vessel and wave,
    if RelativeHead>=360                         % such that 0 deg is head
sea, 90 deg is beam sea
        RelativeHead = RelativeHead-360;         % and 180 deg is waves from
behind.
    elseif RelativeHead<0                        % "RelativeHead" is set to
between 0 and 360 degrees.
        RelativeHead = RelativeHead+360;
    end

    fprintf('The angle of attack of the waves on the ship is %3.2f
degrees.\n\n', RelativeHead);
    fprintf('*** Considered points ***\n');
    fprintf('The considered point on the platform is (%3.2f %3.2f
%3.2f)\n',PointPlat(1),PointPlat(2),PointPlat(3));
    fprintf('The considered point on the vessel (in local coordinates) is
(%3.2f %3.2f %3.2f)\n',PointVesLoc(1),PointVesLoc(2),PointVesLoc(3));

    PointVesGlob(1)=OriginVes(1)+(PointVesLoc(1)*cosd(VesselHead)-
PointVesLoc(2)*sind(VesselHead));           % vessel coordinates in global
system
```

106

```matlab
PointVesGlob(2)=OriginVes(2)+(PointVesLoc(2)*cosd(VesselHead)+PointVesLoc(1
)*sind(VesselHead));
    PointVesGlob(3)=OriginVes(3)+PointVesLoc(3);
    fprintf('The considered point on the vessel (in global coordinates) is
(%3.2f %3.2f %3.2f)\n\n',PointVesGlob(1),PointVesGlob(2),PointVesGlob(3));

    fprintf('*** Limiting criteria ***\n');
    fprintf('Minimum distance is %3.2f m\n',CritDistMin);
    fprintf('Maximum distance is %3.2f m\n',CritDistMax);
    fprintf('Maximum velocity is %3.2f m/s\n',CritV);
    fprintf('Maximum acceleration is %3.2f m/s^2\n\n',Critacc);


    %% Calculating angles between given points, and convert these into
    %% angles pointing out from the point on the vessel. Theta is positive
    %% in counter-clockwise direction from local x-axis. Phi is positive
    %% when pointing up, and negative when pointing down. For the theory
    %% behind this, refer to chapter 6.3 in the report.

    deltaY=PointVesGlob(2)-PointPlat(2);
    deltaX=PointVesGlob(1)-PointPlat(1);
    deltaZ=PointPlat(3)-PointVesGlob(3);

    if deltaX==0                                    % To avoid dividing with
zero
        if deltaY>=0
            Lambda = 90;
        else
            Lambda = 270;
        end
    elseif deltaX>0
        if deltaY>=0
            Lambda=atand(deltaY/deltaX);            % First quadrant
        else
            Lambda=360+atand(deltaY/deltaX);        % Fourth quadrant
        end
    elseif deltaX<0
        Lambda=180+atand(deltaY/deltaX);            % Second and third
quadrant
    end

    Psi = Lambda+180;
    if Psi>=360
        Psi = Psi-360;
    end
    Theta = Psi-VesselHead;
    if Theta<0
        Theta = Theta+360;
    end

    deltaXY=sqrt(deltaX^2+deltaY^2);
    if deltaXY==0
        if deltaZ>0
            Phi=90;
        elseif deltaZ<0
            Phi=-90;
        else
            Phi=0;
```

```matlab
        end
    else
        Phi=atand(deltaZ/deltaXY);
    end

    fprintf('Motion is being examined along the straight line between the
points.\n');
    fprintf('The horizontal angle Psi is %4.2f degrees from the global x-
axis.\n',Psi);
    fprintf('This corresponds to an angle Theta of %4.2f degrees relative
from the ship''s x-axis.\n', Theta)
    fprintf('The vertical angle Phi is %4.2f degrees, measured from the
point on the vessel.\n\n',Phi);

    %% Ask user for input

    give='n';
    give=input('Do you want to change these input data? (y/n): ', 's');

    if give=='n'
        done=true;
    end

    if give=='y'
        sea=input('Do you want to alter the sea state data? (y/n): ', 's');
        coord=input('Do you want to alter the coordinate systems? (y/n): ',
's');
        points=input('Do you want to alter the considered points? (y/n): ',
's');
        criteria=input('Do you want to set the limiting criteria? (y/n): ',
's');

[Hs,Tp,D,Type,PointPlat,OriginVes,PointVesLoc,VesselHead,WaveHead,CritDistM
in,CritDistMax,Critacc,CritV,ShortCrest,s]=readInput(sea,coord,points,crite
ria);
    end
end


end
```

readInput.m

```matlab
function[Hs,Tp,D,Type,PointPlat,OriginVes,PointVesLoc,VesselHead,WaveHead,C
ritDistMin,CritDistMax,Maxa,MaxV,ShortCrest,s]=readInput(sea,coord,points,c
riteria)
% Reads input from the user

[Hs,Tp,D,Type,PointPlat,OriginVes,PointVesLoc,VesselHead,WaveHead,CritDistM
in,CritDistMax,Maxa,MaxV,ShortCrest,s]=givenInput();      % default data

%% Take input data for sea state
if sea=='y'
    fprintf('*** Wave spectrum ***\n');
    fprintf('Please give the wanted values for the wave spectrum:\n');
```

```matlab
    Type='x';
    while (Type~='j' && Type~='t')
        Type=input('Would you like to use a JONSWAP or Torsethaugen
spectrum? (j or t): ','s');
    end


    if Type == 'j'
        range=false;
        while range==false
            Hs=input('Hs = ');
            Tp=input('Tp [seconds] = ');
            if (Tp>=3.6*sqrt(Hs))&&(Tp<=5*sqrt(Hs))
                range=true;
            else
                fprintf('Tp must be between 3.6*sqrt(Hs) and 5*sqrt(Hs) to
be in the JONSWAP area.\n')
                input('Consider using another spectrum. Press enter to
continue...');
            end
        end
    else
         Hs=input('Hs = ');
         Tp=input('Tp [seconds] = ');
    end


    D=input('Duration [hours] = ');
    if D>96
        fprintf('Caution: An operation longer than 96 hours is not
classified as weather\n');
        fprintf('restricted according to DNV rules. Sea state calculations
should be performed\n');
        fprintf('using another statistical model. Refer to DNV-OS-H101 for
details.\n');
        input('Press enter to continue...');
    elseif D>=3
    else
        fprintf('Operation time cannot be set lower than 3 hours. Duration
set to 3 hours.\n');
        D=3;
    end
    angle=false;
    while angle==false
        WaveHead=input('Please set wave propagation heading,
counterclockwise from the global x-axis: ');
        if WaveHead>=0 && WaveHead<360
            angle=true;
        else
            disp('Heading angle must be between 0 and 360 degrees.');
        end
    end
    disp('Long-crested wave theory is used by default.');
    short=input('Would you like to deploy short-crested wave theory? (y/n):
','s');
    s=1;
    if short=='y'
        ShortCrest=true;
        s=input('Please give form factor for the spreading function, a non-
negative integer (default s=1): ');
    else
```

109

```matlab
            ShortCrest=false;
    end
end

%% Take input data for coordinate systems
if coord=='y'
    fprintf('\n\n*** Coordinate systems ***\n');
    disp('Please place origin for the vessel''s coordinate system,');
    disp('the z-coordinate will be set as the centre of gravity:');
    OriginVes(1)=input('x = ');
    OriginVes(2)=input('y = ');
    OriginVes(3)=input('z = ');

    angle=false;
    while angle==false
        VesselHead=input('Please set vessel heading, counterclockwise from
the global x-axis: ');
        if VesselHead>=0 && VesselHead<360
            angle=true;
        else
            disp('Heading angle must be between 0 and 360 degrees.');
        end
    end
end

%% Take input data for considered points
if points=='y'
    fprintf('\n*** Considered points ***\n');
    disp('Please place coordinate to be considered on the platform:');
    PointPlat(1)=input('x = ');
    PointPlat(2)=input('y = ');
    PointPlat(3)=input('z = ');
    disp('Please place coordinate to be considered on the vessel, relative
to the local origin: ');
    PointVesLoc(1)=input('x = ');
    PointVesLoc(2)=input('y = ');
    PointVesLoc(3)=input('z = ');
end

%% Take input data for limiting criteria
if criteria=='y'

    fprintf('\n*** Motion criteria ***\n');
    fprintf('The motion is being examined along the straight line between
the points, in 3D.\n');
    disp('Please give limiting criteria for the motions:');
    CritDistMin=input('minimum distance = ');
    CritDistMax=input('maximum distance = ');
    MaxV=input('maximum Velocity [m/s] = ');
    Maxa=input('maximum acceleration [m/s^2] = ');

end


end
```

givenInput.m

```matlab
function[Hs,Tp,D,Type,PointPlat,OriginVes,PointVesLoc,VesselHead,WaveHead,M
inDist,MaxDist,Maxa,MaxV,ShortCrest,s]=givenInput();
% Defines default input data

%% sea state %%
Hs=2;                    % significant waveheight
Tp=6.1;          % top period. NB! Must be between 3.6*sqrt(Hs) and
5*sqrt(Hs) for JONSWAP spectrum
D=3;                     % duration (hours)
Type='j';                % jonswap or torsethaugen spectrum ('j' or 't')
WaveHead=180;             % wave propagation direction, counterclockwise
from the global x-axis
ShortCrest=true;         % long- or shortcrested wave theory
s=10;                    % form-factor for the spreading function, a non-
negative integer
mode=2;                  % mode 1 is custom mode, mode 2 is crane mode and
mode 3 is boarding mode.

if mode==1
    %% coordinate system (custom mode) %%
    VesselHead=90;                        % vessel heading, counterclockwise
from the global x-axis

    OriginVes(1)=-18.5;                     % origin of vessel cs (x,y,z)
    OriginVes(2)=8;
    OriginVes(3)=0;                        % cog of ship

    %% considered points (custom mode) %%
    PointVesLoc(1)=-8;                      % considered point on vessel, local
coordinates (x,y,z)
    PointVesLoc(2)=-13;
    PointVesLoc(3)=23;

    PointPlat(1)=-2.5;                     % considered point on the
platform (x,y,z)
    PointPlat(2)=0;
    PointPlat(3)=23;
elseif mode==2
    %% coordinate system (crane mode) %%
    VesselHead=0;                         % vessel heading, counterclockwise
from the global x-axis

    OriginVes(1)=8;                       % origin of vessel cs (x,y,z)
    OriginVes(2)=18.5;
    OriginVes(3)=0;                       % cog of ship

    %% considered points (crane mode) %%
    PointVesLoc(1)=-8;                      % considered point on vessel, local
coordinates (x,y,z)
    PointVesLoc(2)=-13;
    PointVesLoc(3)=23;

    PointPlat(1)=0;                       % considered point on the platform
(x,y,z)
    PointPlat(2)=2.5;
    PointPlat(3)=17.1;
```

111

```matlab
elseif mode==3
    %% coordinate system (boarding mode) %%
    VesselHead=0;                          % vessel heading, counterclockwise
from the global x-axis

    OriginVes(1)=-20.5;                       % origin of vessel cs (x,y,z)
    OriginVes(2)=0;
    OriginVes(3)=0;                        % cog of ship

    %% considered points (boarding mode) %%
    PointVesLoc(1)=17.5;                   % considered point on vessel,
local coordinates (x,y,z)
    PointVesLoc(2)=0;
    PointVesLoc(3)=2.5;

    PointPlat(1)=-3;                       % considered point on the platform
(x,y,z)
    PointPlat(2)=0;
    PointPlat(3)=2.5;
end

%% criteria %%
% total motions, 3D
MinDist=0;              % min distance
MaxDist=10;             % max distance
MaxV=5;                 % max velocity
Maxa=10;                % max acceleration

end
```

spectrum.m

```matlab
function[Swave] = spectrum(omega,Hs,Tp)
% Creates the JONSWAP spectrum from input data

g=9.81;
omegap=2*pi/Tp;
alfa=0.036-0.0056*(Tp/sqrt(Hs));
gamma=exp(3.484*(1-0.1975*alfa*(Tp^4/Hs^2)));

for i=1:length(omega)
    if (omega(i)>omegap)
        sigma=0.09;
    else
        sigma=0.07;
    end

    S1=exp((-5/4)*(omega(i)/omegap)^-4);
    S2=exp(-(((omega(i)/omegap)-1)^2)/(2*sigma^2));
    S(i)=alfa*g^2*(omega(i)^-5)*S1*gamma^S2;
end

Swave=S.';
end
```

112